

Table of contents

| | |
|---|----|
| Alexander Batkhin, Alexander Petrov On Algorithms of Hamiltonian Normal Form..... | 8 |
| Alexander Batkhin, Cengiz Aydin Network of families of symmetric spatial periodic orbits in the Hill problem via symplectic invariants..... | 13 |
| Shamil Biktimirov, Fatima Alnaqbi Remote Sensing Satellite Constellation Design Based on Repeat Ground Track Orbits Properties..... | 18 |
| Ivan Bizyaev Bifurcation diagram and a qualitative analysis of particle motion in a Kerr metric..... | 24 |
| Sergey Bolotin Chaotic behavior in the generalized n-center problem..... | 28 |
| Alexander Bruno, Alexander Batkhin On Types of Stability in Hamiltonian Systems..... | 32 |
| Pablo Cincotta Chaotic diffusion in a triaxial galactic model: an example of global stable chaos | 37 |
| Victor Edneral On the integrability of dynamical models with quadratic right-hand side..... | 38 |
| Sergey Gutnik Periodic Oscillations of a Two-Body System in the Plane of the Elliptic Orbit | 43 |
| Tomilova I.V., Bordovitsyna T.V., Aleksandrova A.G., Blinkova E.V., Popandopulo N.A. Numerical-analytical approach to the study of resonant structures of nearplanetary orbital spaces..... | 48 |
| Pavel Ivanov A non-dissipative tidal evolution of stellar inclination axis in eccentric inclined close binary systems..... | 53 |

| | |
|--|----|
| Tamara Ivanova | |
| Constructing the Secular System in the Three-Axial Moon's Rotation Theory in the Trigonometrical Form... | 55 |
| Alexey Ivanyukhin | |
| Transit trajectories of ballistic capture near libration points for low-energy transfers... | 56 |
| Nikolai Kirsanov | |
| The case of János Sajnovics as a milestone in history of astronomy, the study of which was inspired by the lectures of Prof. K.V. Kholoshevnikov... | 60 |
| Pavel Krasilnikov, Alexander Dobroslavskiy | |
| On the Evolution of Asteroid Orbit in the Restricted Circular Three-Body Problem: External and Internal Cases, New Results... | 63 |
| Hussein Krayani | |
| On the paper of K.V. Kholoshevnikov about the exactness of epicyclic theory... | 68 |
| Eduard Kuznetsov | |
| Semi-analytical theories of motion for the study of the dynamical evolution of planetary systems... | 69 |
| Lubov Lapshenkova, Mikhail Malykh, and Marina Konyaeva | |
| On the algebraic properties of difference approximations of Hamiltonian systems... | 73 |
| Ivan Mamaev, Ivan Bizyaev | |
| Dynamics of self-gravitating ellipsoids... | 78 |
| Alexander Melnikov, Kristina Lobanova | |
| On perturbations in the rotational dynamics of small asteroids during close approaches to the Earth... | 82 |
| Denis Mikryukov, Ivan Shevchenko | |
| The effect of encounters with interstellar objects of planetary and substellar masses on the Solar system dynamics... | 86 |
| Igor Nikiforov | |
| 4D modeling of the kinematics of a selected subsystem of the Milky Way... | 90 |
| Vasily Nikonov, Alexander Burov | |
| Finite-point approximations of fields of attraction and their verification... | 92 |
| Alexander Petrov | |
| Approximate gyroscope theory and application for the space objects... | 96 |

| | |
|--|-----|
| Nikita Petrov | |
| Dangerous asteroids and the study of their orbits..... | 101 |
| Alexey Rosaev | |
| A new example of stable chaotic orbit in asteroid belt..... | 105 |
| Tatiana Salnikova | |
| Localized trajectories of cosmic particles near libration points... .. | 108 |
| Tatiana Sannikova | |
| Norm of orbit displacement in a problem with perturbing acceleration varying inversely with the square of the heliocentric distance..... | 112 |
| Vakhit Shaidulin | |
| Collocation integrator based on Legendre polynomials..... | 116 |
| Vladislav Sidorenko | |
| Adiabatic approximation in dynamical studies of exoplanetary systems in mean-motion resonance..... | 119 |
| Vladislav Sidorenko | |
| Lerman separatrix map for the problem of satellite attitude motion..... | 122 |
| Evgeny Smirnov | |
| Identifying mean-motion and secular resonances with large language models and classical machine learning..... | 125 |
| Vladimir Titov | |
| General three body problem in the shape space... .. | 126 |
| Vladislav Topinskiy, Roman Baluev | |
| Neural network simulating the Schuster periodogram..... | 130 |
| Irina Tupikova | |
| Towards understanding the astronomical orientation of the Old Kingdom pyramids..... | 134 |
| Nikolay Vassiliev | |
| A natural riemannian metric on the space of Keplerian orbits based on the Hausdorff metric..... | 139 |
| Tamara Vinogradova | |
| Lidov-Kozai mechanism in 3:2 and 1:1 resonances..... | 141 |

| | |
|--|-----|
| Eleonora Yagudina, Margarita Lebedeva | |
| The ephemeris of the Moon in the framework of the numerical theory of Solar system bodies EPM..... | 142 |
| Vyacheslav Ivashkin | |
| K.V. Kholshchevnikov and the Euler-Lambert problem of constructing the orbit of a body based on its two positions..... | 146 |
| Elena Polyakhova, Andrei Vasiliev, Denis Mikryukov, Igor Nikiforov, Boris Eskin | |
| Professor K.V. Kholshchevnikov as a historian of science... .. | 149 |

On Algorithms of Hamiltonian Normal Form

Alexander Petrov and Alexander Batkhin

Abstract. The method of invariant normalization proposed by V.F. Zhuravlev, which is used for autonomous Hamiltonians for normal or symmetrized forms, is discussed. Normalizing canonical transformation is represented by a Lie series using a generating Hamiltonian. This method has a generalization proposed by A.G. Petrov, which normalizes not only autonomous but also non-autonomous Hamiltonians. Normalizing canonical transformation is represented by a series using a parametric function. For autonomous Hamiltonian systems, the first two steps of approximations of both methods coincide, while the remaining steps differ. The normal forms in both methods coincide.

A method for testing normalization software is proposed. For this purpose the Hamiltonian of a strongly nonlinear Hamiltonian system is found for which the normal form is a quadratic Hamiltonian. The normalizing transformation is expressed in elementary functions.

1. Algorithm of invariant normalization

Normalization using Lie series is implemented as follows (see [1, 2, 3]). Let $H(\mathbf{q}, \mathbf{p}) = H_0(\mathbf{q}, \mathbf{p}) + F$ be the initial Hamiltonian, H_0 the principal term and F the perturbation. Its normal form (NF) $h(\mathbf{Q}, \mathbf{P})$ and the generator of the Lie substitution $G(\mathbf{Q}, \mathbf{P})$ are searched in the form of series

$$\begin{aligned} H(\mathbf{q}, \mathbf{p}) &= H_0(\mathbf{q}, \mathbf{p}) + F, & h(\mathbf{Q}, \mathbf{P}) &= H_0(\mathbf{Q}, \mathbf{P}) + f, \\ \%[2ex].F &= \sum_{k=1}^{\infty} \varepsilon^k F_k(\mathbf{q}, \mathbf{p}), & f &= \sum_{k=1}^{\infty} \varepsilon^k f_k(\mathbf{Q}, \mathbf{P}), & G &= \sum_{k=1}^{\infty} \varepsilon^k G_k(\mathbf{Q}, \mathbf{P}). \end{aligned} \quad (1)$$

Then for the NF $h = H_0 + f$ we get the Lie series

$$\begin{aligned} f &= H_0 * G + M, \\ M &= F + F * G + \frac{1}{2!}(H_0 + F) * G^2 + \frac{1}{3!}(H_0 + F) * G^3 + \dots, \end{aligned} \quad (2)$$

where $*$ denotes the Poisson bracket and the expression $Q * G^n$ - n - times Poisson bracket: $Q * G^n = Q * G^{n-1} * G$.

Hence for the coefficients of the series (1) on powers ε of the NF f_k and the generator G_k we obtain a chain of homological equations:

$$H_0 * f_k = 0, \quad f_k = H_0 * G_k + M_k, \quad k = 1, 2, \dots, \quad (3)$$

where the term M_k depends on the values of $H_j, h_j, F_j, f_j, G_j, j < k$ obtained in the previous steps. The structure of M_k for an arbitrary value of k is described in [4]. The solution of the equations (3) in Zhuravlev's method is found using quadrature

$$\int_0^t m_k(\mathbf{Q}, \mathbf{P}) dt = t f_k(\mathbf{Q}, \mathbf{P}) + G_k(\mathbf{Q}, \mathbf{P}) + g(t), \quad (4)$$

where the expression $m_j(t, \mathbf{Q}, \mathbf{P})$ is obtained from M_k by substituting solutions of the unperturbed system with Hamiltonian $H_0(\mathbf{q}, \mathbf{p})$. In the case of semi-simple eigenvalues λ_k of the unperturbed system, the integration of the quadrature (4) is replaced by substitution followed by simplification of exponents of the form $\exp(\lambda_k t)$.

The canonical transformation through the Lie generator is represented by Lie series

$$\mathbf{q} = \mathbf{Q} + \mathbf{Q} * G(\mathbf{Q}, \mathbf{P}) + \frac{1}{2!} \mathbf{Q} * G^2 + \dots, \quad \mathbf{p} = \mathbf{P} + \mathbf{P} * G(\mathbf{Q}, \mathbf{P}) + \frac{1}{2!} \mathbf{P} * G^2 + \dots. \quad (5)$$

2. Normalization Algorithm with Parametric Function

An alternative way of canonical transformation via the parametric function $\Psi(\mathbf{x}, \mathbf{y})$ [5, 3] has the form

$$\begin{cases} \mathbf{q} = \mathbf{x} - \frac{1}{2} \Psi_{\mathbf{y}}, \\ \mathbf{p} = \mathbf{y} + \frac{1}{2} \Psi_{\mathbf{x}}, \end{cases} \quad \begin{cases} \mathbf{Q} = \mathbf{x} + \frac{1}{2} \Psi_{\mathbf{y}}, \\ \mathbf{P} = \mathbf{y} - \frac{1}{2} \Psi_{\mathbf{x}}. \end{cases}$$

Eliminating the parameters \mathbf{x} and \mathbf{y} , we can represent this transformation in the form of series

$$\mathbf{q} = \mathbf{Q} + \mathbf{Q} * \Psi(\mathbf{Q}, \mathbf{P}) + \frac{1}{2!} \mathbf{Q} * \Psi^2 + \dots, \quad \mathbf{p} = \mathbf{P} + \mathbf{P} * \Psi(\mathbf{Q}, \mathbf{P}) + \frac{1}{2!} \mathbf{P} * \Psi^2 + \dots,$$

which have three terms the same as (5) precisely by substituting $G \rightarrow \Psi$. The subsequent expansion coefficients at powers of Ψ^3 and higher will be different.

Instead of the equation (2), we get the following equation:

$$f = H_0 * \Psi + M,$$

$$M = F \left(\mathbf{x} - \frac{1}{2} \Psi_{\mathbf{y}}, \mathbf{y} + \frac{1}{2} \Psi_{\mathbf{x}} \right) - f \left(\mathbf{x} + \frac{1}{2} \Psi_{\mathbf{y}}, \mathbf{y} - \frac{1}{2} \Psi_{\mathbf{x}} \right) + f(\mathbf{x}, \mathbf{y}).$$

Whence we obtain an analogous chain of homological equations. Moreover, for the first two approximations the equations differ only by replacing the coefficients G_1, G_2 by Ψ_1, Ψ_2 .

The algorithm is similar to the Zhuravlev invariant normalization algorithm. Zhuravlev quadrature (4) is replaced by

$$\int_{t_0}^t m_k(\xi, t_0, \mathbf{Q}, \mathbf{P}) d\xi = (t - t_0) f_k(t_0, \mathbf{Q}, \mathbf{P}) + \Psi_k(t_0, \mathbf{Q}, \mathbf{P}) + g(t). \quad (6)$$

In this quadrature, the main property of the NF is preserved: the perturbed part of the Hamiltonian system with Hamiltonian $f(t, \mathbf{Q}, \mathbf{P})$ is the integral of the unperturbed part with Hamiltonian $H_0(t, \mathbf{Q}, \mathbf{P})$. This allows us to find an analytical solution of the problem using the theorem for such a system: the general solution of the Hamiltonian equations with Hamiltonian $h = H_0 + f$ is obtained by substituting into the unperturbed solution the solution of the system with perturbed Hamiltonian $f(0, \mathbf{q}, \mathbf{p})$. This algorithm can be applied to non-autonomous systems.

Example The Mathieu equation $\ddot{x} + x(1 + 3\delta \cos 2t) = 0$ can be written in Hamiltonian form with Hamiltonian

$$H = H_0 + F, \quad H_0 = \frac{1}{2}(x^2 + u^2), \quad F = \delta \frac{3}{2} x^2 \cos 2t$$

Without using the theory of the Mathieu equation, we construct by normalization the asymptotic solution of the first approximation at $\delta \ll 1$.

1. Find the solution to the unperturbed system.

$$x = X \cos(t - t_0) + U \sin(t - t_0), \quad u = -X \sin(t - t_0) + U \cos(t - t_0) \quad (7)$$

2. We define the function $m(t, t_0, Q, P)$ by substituting the solution (7) into the perturbed part of the Hamiltonian

$$m(t, t_0, X, U) = \delta \frac{3}{2} (X \cos(t - t_0) + U \sin(t - t_0))^2 \cos 2t$$

3. Compute the integral within (t_0, t) of the function $m(t', t_0, X, U)$. In this integral, we need to isolate the linear in time $f(t_0, X, U)$, the time-independent summand $\Psi(t_0, X, U)$, and the periodic in time $g(t)$, with period average equal to zero. From the integral (6) we find the functions f, Ψ, φ :

$$f = -3\delta (\cos(2t_0) (U^2 - X^2) + 2XU \sin(2t_0)) / 8,$$

$$\Psi = -3\delta (\sin(2t_0) (5X^2 + 3U^2) - 2XU \cos(2t_0)) / 32,$$

$$g(t) = -\frac{3\delta}{32} ((U^2 - X^2) \sin(4t - 2t_0) + 2XU \cos(4t - 2t_0) - 4(X^2 + U^2) \sin 2t).$$

The first function is a perturbation of the NF, the second term defines a substitution of the variables

$$x = X - \Psi_U(t, X, U) = X + 3\delta(3U \sin 2t - X \cos 2t) / 16,$$

$$u = U + \Psi_X(t, X, U) = 3\delta(-5X \sin 2t + U \cos 2t) / 16,$$

which symmetrizes the Hamiltonian to small orders of δ^2 .

$$h = H_0 + f, \quad H_0 = \frac{1}{2}(X^2 + U^2), \quad f = \frac{3\delta}{8} ((X^2 - U^2) \cos 2t - 2XU \sin 2t).$$

It is easy to see that the perturbed part of f is an integral of the unperturbed part of H_0 . The general solution of the Hamilton equations with Hamiltonian h is obtained by substituting into the unperturbed solution

$$X = q \cos t + p \sin t, \quad U = -q \sin t + p \cos t$$

solutions with perturbed Hamiltonian $f(0, q, p) = 3\delta(-p^2 + q^2)/8$

$$q = A \cosh \tau + B \sinh \tau, \quad p = A \sinh \tau - B \cosh \tau, \quad \tau = \frac{3}{4}\delta t,$$

Here is an example of constructing the asymptotic solution of the Mathieu equation with initial conditions $x(0) = 1, \dot{x}(0) = 0$

$$X = A(\cosh \tau \cos t - \sinh \tau \sin t), \quad U = -A(\cosh \tau \sin t - \sinh \tau \cos t),$$

$$x = X + \frac{3\delta}{16}(3U \sin 2t - X \cos 2t),$$

where $A = (1 - (3/16)\delta)^{-1}, B = 0$.

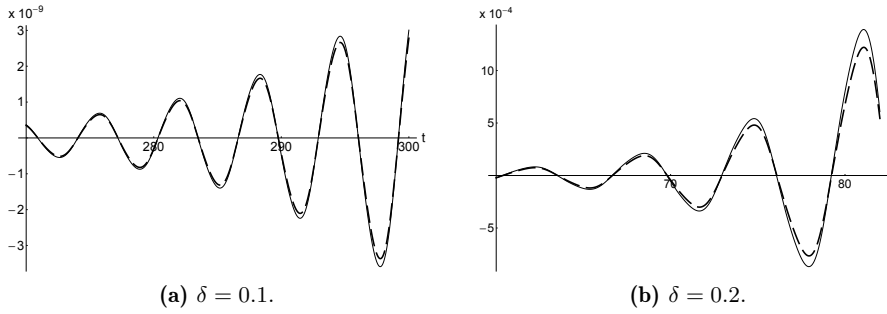


FIGURE 1. Comparison of numerical and asymptotic solutions of the Mathieu equation.

In Fig. 1, the numerical solution of the Mathieu equation (solid line) is compared with the asymptotic solution (dashed line): (a) $\delta = 0.1$ and (b) $\delta = 0.2$. As can be seen, at $\delta = 0.1$ the asymptotic solution begins to differ slightly from the exact solution in the neighborhood of the maximum, when the function $x(t)$ reaches values of the order of 10^9 . For larger values of $\delta = 0.2$ the difference becomes significant, when the function $x(t)$ reaches values of the order of 10^4 .

3. Testing algorithms using tautochronous oscillations

To validate various normalization methods, it is useful to test them on nonlinear systems possessing tautochronous oscillations. For such systems, the NF in the neighborhood of the equilibrium position has the form of the Hamiltonian of a

harmonic oscillator. Applying the invariant normalization method up to some fixed order all terms f_k of the NF should be zero.

An example of a tautochronous system is a system with Hamiltonian is given in [6]:

$$H = \frac{1}{2} \left(p^2 + (1+q)^2 + \frac{1}{(1+q)^2} - 2 \right). \quad (8)$$

It can be shown that substituting the variables

$$q(Q, P) = \sqrt{R(Q, P)/2} - 1, \quad p(Q, P) = \frac{dq}{dt} = P \sqrt{\frac{P^2 + 4Q^2 + 4}{2R(Q, P)}}, \quad (9)$$

where $R(Q, P) = P^2 + 4Q^2 + 2 + 2Q\sqrt{P^2 + 4Q^2 + 4}$, has the following properties:

1. Differential form $PdQ - pdq$ is complete.
2. Substitution into the original Hamiltonian (8) converts it to the NF $h(Q, P) = (Q^2 + 4P^2)/2$.
3. Substitution the solution of the NF equations $Q = Q_0 \cos 2t$, $P = -2Q_0 \sin 2t$ into (9) gives the exact solution of the original Hamiltonian system.

References

- [1] V. F. Zhuravlev. A new algorithm for Birkhoff normalization of Hamiltonian systems. *Journal of Applied Mathematics and Mechanics*, 61(1):9–13, 1997. [https://doi.org/10.1016/S0021-8928\(97\)00002-6](https://doi.org/10.1016/S0021-8928(97)00002-6)
- [2] V. F. Zhuravlev. Invariant normalization of non-autonomous Hamiltonian systems. *Journal of Applied Mathematics and Mechanics*, 66(3):347–355, 2002. URL: [https://doi.org/10.1016/S0021-8928\(02\)00044-8](https://doi.org/10.1016/S0021-8928(02)00044-8)
- [3] V. F. Zhuravlev, A. G. Petrov, and M. M. Shunderyuk. *Selected Problems of Hamiltonian Mechanics*. LENAND, Moscow, 2015. (in Russian).
- [4] A. B. Batkhin. *Computation of homological equations for Hamiltonian normal form*, volume 782 of *Contemporary Mathematics*, pages 7–20. AMS, 2023. <https://doi.org/10.1090/conm/782/15718>
- [5] A. G. Petrov. Invariant normalization of non-autonomous Hamiltonian systems. *Journal of Applied Mathematics and Mechanics*, 68(3):357–367, 2004. URL: [https://doi.org/10.1016/S0021-8928\(04\)00049-8](https://doi.org/10.1016/S0021-8928(04)00049-8)
- [6] A. G. Petrov. About tautochronic movements. *Doklady Mathematics*, 518(4), 2024. (to be published).

Alexander Petrov

Ishlinsky Institute for Problems in Mechanics RAS, Moscow, Russia

e-mail: petrovipmech@gmail.com

Alexander Batkhin

Department of Aerospace Engineering, Technion – Israel Institute of Technology, Haifa, Israel

e-mail: batkhin@technion.ac.il

Network of families of symmetric spatial periodic orbits in the Hill problem via symplectic invariants

Cengiz Aydin and Alexander Batkhin

Abstract. A technique of Conley–Zehnder indices is applied for investigation of interconnections of the basic families of periodic orbits with maximal numbers of symmetries of the well-known Hill problem. These basic families are g , f – families of planar direct and retrograde periodic orbits, and \mathcal{B}_0 – family of rectilinear vertical consecutive collision orbits. The relations among families of periodic orbits are provided by families of spatial symmetric periodic orbits which makes k -covering at the bifurcation points. All the families form a common network and can be represented as well-organized bifurcation graphs of the interconnectedness.

Introduction

1. Circular Hill Problem, its symmetries and basic families

The Hill three-body problem (Hill3BP), a limiting case of the circular restricted three-body problem (RTBP), is a well-known model which provides an approximation of the dynamics of the infinitesimal body in the vicinity of the smaller primary. In its original application, George Hill reformulated the lunar theory and discovered a periodic solution with period equal to the synodic month of the Moon. There are a lot of applications of Hill’s approach such as capturing in the dynamics of natural or artificial satellites, distant moons of asteroids, low-energy escaping trajectories, frozen orbits around planetary satellites. Hill3BP problem’s periodic solution can be continued to RTBP or even into three-body problem solutions and thus can be used in astrodynamical projects.

Hill3BP problem Hamiltonian

$$H(x, y, z, p_x, p_y, p_z) = \frac{1}{2} (p_x^2 + p_y^2 + p_z^2) - \frac{1}{r} + p_x y - p_y x - x^2 + \frac{1}{2} (y^2 + z^2), \quad (1)$$

where $r = \sqrt{x^2 + y^2 + z^2}$, consists of the rotating Kepler problem Hamiltonian with a velocity independent gravitational perturbation produced by the massive

primary (the quadratic form of x, y, z). This difference between the rotating Kepler problem and Hill3BP system gives a dramatic dynamical change. While the rotating Kepler problem is an integrable system, the Hill 3BP is non-integrable. Equations of motion derived from (1) are invariant under discrete group $\mathbb{Z}_2 \times \mathbb{Z}_2 \times \mathbb{Z}_2$ of symplectic (anti-symplectic) symmetries ρ of the extended phase space:

$$\rho(\alpha, \beta, \gamma) : (t, x, y, z, p_x, p_y, p_z) \rightarrow (\alpha t, \beta x, \alpha \beta y, \gamma z, \alpha \beta p_x, \beta p_y, \alpha \gamma p_z), \quad (2)$$

where $\alpha, \beta, \gamma \in \{+1, -1\}$. So all solutions to the Hill3BP can be divided into groups with different number of symmetries (2). The symmetry of a periodic solution plays an essential role, since it allows one to investigate it numerically for only parts of the period.

There are 3 families, called *basic families*, whose orbits are simple and have the largest number of symmetries: g and f are families of planar direct and retrograde satellite orbits [4] and \mathcal{B}_0 is a family of vertical collision orbits [5]. The last one consists of two branches called \mathcal{B}_0^+ and \mathcal{B}_0^- for upper and lower coordinate subspaces correspondingly. Other important families are Lypunov families a and c emanating from the librations points L_1 and L_2 and family g' appeared after symmetry breaking bifurcation of the family g [4]. It was shown in [3] that all these families are connected to each other by families of spatial periodic orbits and form a kind of common network. Current work significantly extends these results by systematically applying the technique of Conley–Zehnder indices.

2. On Conley–Zehnder indices μ_{CZ} of periodic solution

The Conley–Zehnder index μ_{CZ} assigns a mean winding number to non-degenerate periodic orbits, which stays constant until a bifurcation point is achieved. In its formal definition, the index μ_{CZ} is associated with a path of symplectic matrices generated by the linearized flow along the whole orbit. This path starts at the identity and ends at the reduced monodromy matrix whose Floquet multipliers are different from 1 due to the non-degeneracy of the orbit. The index μ_{CZ} measures the twisting of this symplectic path by counting the number of crossing the eigenvalue 1. If the orbit becomes degenerate, i.e., 1 is among its Floquet multipliers, then bifurcation appears and the index jumps according to direction of crossing the eigenvalue 1. For instance, if a pair of elliptic Floquet multipliers in the form $e^{\pm i\theta}$ becomes positive hyperbolic, then the corresponding index jump depends on whether the eigenvalue 1 is crossed from above (i.e., by $e^{i\theta}$) or from below (i.e., by $e^{-i\theta}$). In one case the index jumps down and in the other case the index jumps up. In order to determine this direction of crossing the eigenvalue 1 we consider the Krein signature (especially its version for symmetric periodic orbits) which specifies the direction of the rotation and thereby the index jump.

When working locally near a family of non-degenerate periodic orbits, then there is a fascinating bifurcation-invariant: the local Floer homology and thus its Euler characteristic, the alternating sum of the ranks of the local Floer homology groups. Significantly, the index leads to a grading on local Floer homology and

thus, the index provides important information how different families are related to each other before and after bifurcation.

We use these symplectic invariants to construct bifurcation graphs in the same way as introduced in [2], where networks of families of symmetric spatial periodic orbits associated to g , g' and f , and their multiple cover bifurcations, were demonstrated. A “bifurcation graph” is a labelled graph, whose vertices correspond to bifurcation points and whose edges correspond to families of periodic orbits, labelled with their Conley–Zehnder index (see Figure 1 for an example). This approach provides additional structure to the families of periodic orbits and supports to examine their connections at bifurcation points from a topological point of view. In particular, this allows to check at every bifurcation point the Euler characteristics before and after bifurcation 1. In case the Euler characteristics do not coincide, then there are still undiscovered families at this bifurcation point.

Instead of using the formal definition to determine the indices, we follow the approach developed in [1, 2], in which the indices are known via analytical considerations in view of the origin of the families. For very low energies, the regularized Kepler problem is the source of the families g , f and \mathcal{B}_0^\pm . Notice that planar orbits have planar and spatial indices, μ_{CZ}^p and μ_{CZ}^s . It was shown [1] that their indices are given by

$$\mu_{CZ} = \begin{cases} 6 = \mu_{CZ}^p + \mu_{CZ}^s = 3 + 3 & \text{for family } g \\ 4 & \text{for family } \mathcal{B}_0^\pm \\ 2 = \mu_{CZ}^p + \mu_{CZ}^s = 1 + 1 & \text{for family } f. \end{cases}$$

We start with these indices, continue those families for higher energies, follow their Floquet multipliers together with corresponding Krein signatures, examine the interaction of μ_{CZ} with bifurcation points and construct bifurcation graphs, such as shown in Figure 1.

3. Interconnections between the basic families

The purpose in our study is to provide bifurcation graphs showing rich connections between basic families of periodic orbits and their bifurcations. To be emphasized is that our investigations show the following structures of bifurcation results of families of spatial orbits in each row (in each row the integer n indicates each n -th cover bifurcation of the underlying family in the first row):

| g | g' | \mathcal{B}_0^\pm | f | f_3 | halo |
|-----|------|---------------------|-----|-------|------|
| | 1 | | | | 2 |
| 1 | | 2 | | | |
| 2 | 2 | 3 | | | |
| 3 | 3 | 4 | 5 | 1 | |
| 4 | 4 | 5 | 6 | 2 | |
| 5 | | 6 | 7 | | |

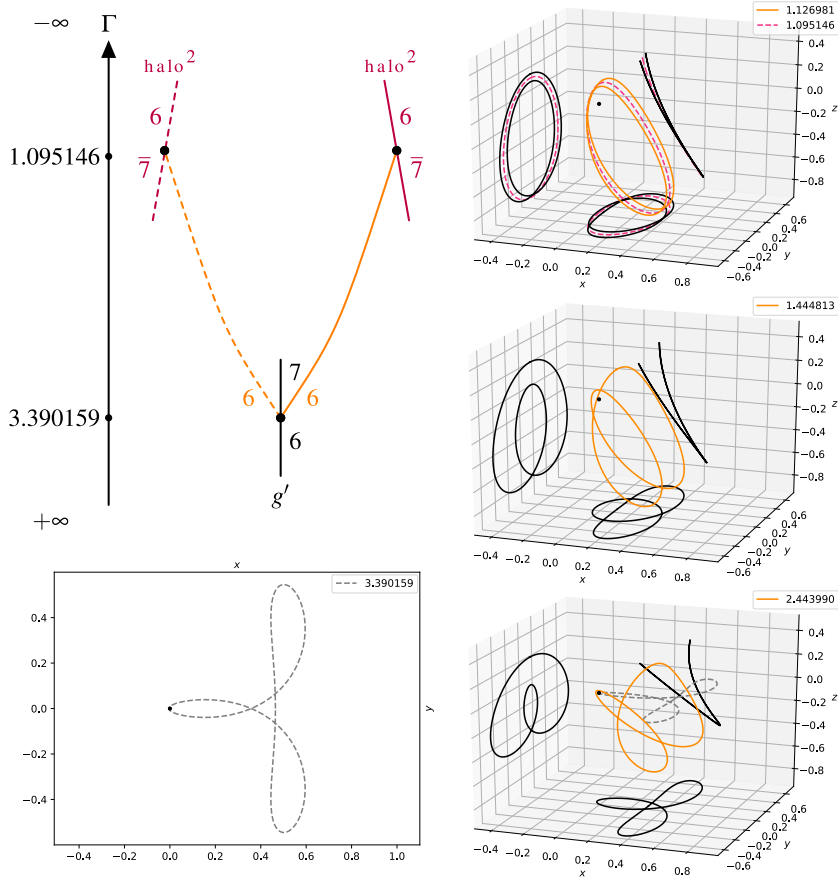


FIGURE 1. Left top: Bifurcation graph associated to connection between g' and double cover of halo orbit (denoted by halo^2). Corresponding orbits start bottom left, then right, then up.

As a consequence, we have discovered connections at bifurcation points between n -th cover of the families g , $n + 1$ -th cover of \mathcal{B}_0^\pm and $n + 2$ -th cover of f , for $n = 3, 4, 5$. Such pattern can be expected in view of their Conley–Zehnder indices, which play a significant role in this paper. In particular, this work aims to demonstrate that the technique of such symplectic invariants supports to deduce such connections at bifurcation points which are hard to see by bare computations.

One example of a bifurcation graph is shown in Figure 1, which shows the connection in the first row from the previous overview, i.e., between g' and double

cover of halo orbits. Let us verify that the corresponding bifurcation points in Figure 1 are in accordance with the Euler characteristics before and after bifurcation. At $\Gamma = 3.390159$ the Euler characteristics before and after bifurcation are

$$(-1)^6 = 1, \quad 2 \cdot (-1)^6 + (-1)^7 = 1.$$

At $\Gamma = 1.095146$ the Euler characteristics are $(-1)^6 = 1$ before and after bifurcation. Notice that the index $\bar{7}$ indicates bad orbits, which are ignored in the local Floer homology and not counted.

References

- [1] Aydin C. From Babylonian lunar observations to Floquet multipliers and Conley–Zehnder Indices. *J. Math. Phys.* **64**(8) (2023) <https://doi.org/10.1063/5.0156959>
- [2] Aydin C. The Conley–Zehnder indices of the spatial Hill three-body problem. *Celest. Mech. Dyn. Astron.* **135**(32) (2023) <https://doi.org/10.1007/s10569-023-10134-7>
- [3] Batkhin A.B. and Batkhina N.V. Hierarchy of periodic solutions families of spatial Hill’s problem. *Solar System Research.* **43**(2) (2009), pp. 178–183. <https://doi.org/10.1134/s0038094609020105>.
- [4] Hénon M. Numerical exploration of the restricted problem V. Hill’s case: periodic orbits and their stability. *Astron. & Astrophys.* **1** (1969), pp. 223–238.
- [5] Lidov M.L. A method of construction of families of spatial periodic orbits in Hill’s problem. *Kosmicheskie Issledovaniia.* **20**(6) (1982), pp. 787–807, (in Russian).

Cengiz Aydin

Institut für Mathematik, Universität Heidelberg, Germany

e-mail: cengiz.aydin@hotmail.de

Alexander Batkhin

Department of Aerospace Engineering, Technion – Israel Institute of Technology, Haifa, Israel

e-mail: batkhin@technion.ac.il

Remote Sensing Satellite Constellation Design Based on Repeat Ground Track Orbits Properties

Shamil Biktimirov and Fatima Alnaqbi

Abstract. The study addresses the problem of Earth remote sensing discontinuous coverage satellite constellation design. An approach is developed to calculate the minimum number of LEO satellites to ensure periodic coverage of entire region of interest on Earth for a given telescope characteristics. It utilizes ground track properties of repeat ground track LEO orbits.

Introduction

Earth remote sensing is one of the key space applications. Remote sensing missions in most cases provide discontinuous Earth coverage and can require single satellite or multiple satellites constellation depending on mission requirements. Remote sensing missions are characterized by sensor ground sample distance (GSD) defining image resolution, instrument swath width S_w , and by various coverage Figures of Merits (FOMs) such as revisit time and response time statistics and percent coverage. Remote sensing space system design necessitates various considerations including coverage geometry, orbit and constellation design, station-keeping, data downlink and others.

The study addresses the Earth remote sensing constellation design problem given the sensor parameters, required image quality, and coverage FOMs. To design a satellite orbit and corresponding orbital configuration in a way guaranteeing certain coverage properties, two general approach can used: multi-objective optimization [1] and analytical consideration of satellite ground track [2]. The paper studies the problem of remote satellite constellation design using ground track properties of repeat ground track (RGT) orbits. An RGT orbit has commensurability of its nodal period T_{sat}^n with nodal period of the Earth self-rotation T_{\oplus}^n and is defined by a number of satellite revolutions to repeat its ground track R within D nodal days. Moreover, taking into account optical observation limitations to daytime imaging we restrict orbits to sun-synchronous to avoid observation of unlit territories.

Problem Statement. Given telescope angular resolution θ_r , find RGT SSO circular orbit radius R and corresponding minimum number of satellites n_{sats} to provide coverage of an area of interest (AOI) with a certain revisit time T_{rev} and a required image quality as per National Image Interpretability Rating Scales NIIRS.

1. Sensor Geometry

Let's consider a constellation containing optical telescopes-equipped satellites. A telescope is defined by its angular resolution θ_r and field of view θ_{fov} for coverage geometry analysis. Figure 1, a) depicts side pointing beam geometry required to calculate GSD for different look angles θ . Look angle defines field of regard (FOR) of a satellite, i.e. a potential area on Earth that can be observed by a steerable sensor and a corresponding sensor swath width $S_w = 2\beta_c$. The relation of ground sample resolution (GSD) with orbit radius R and maximum look angle θ at which a telescope can perform observation is described as follows

$$GSD = (\beta_{out} + \beta_{in}) \cdot R_{\oplus}, \quad (1)$$

$$\beta_{in} = \beta_c - \frac{\pi}{2} - (\theta_l - \frac{\theta_r}{2}) - \arccos\left(\frac{R_s}{R_{\oplus}} \sin(\theta_l - \frac{\theta_r}{2})\right),$$

$$\beta_{out} = \frac{\pi}{2} - (\theta_l + \frac{\theta_r}{2}) - \arccos\left(\frac{R_s}{R_{\oplus}} \sin(\theta_l + \frac{\theta_r}{2})\right) - \beta_c,$$

$$\beta_c = \frac{\pi}{2} - \theta_l - \arccos\left(\frac{R_s}{R_{\oplus}} \sin(\theta_l)\right).$$

Figure 1, b) shows relations of: nadir pointing GSD for different orbit altitudes, and satellite look angle yielding different image qualities according to the NIIRS classes for different orbit altitudes.

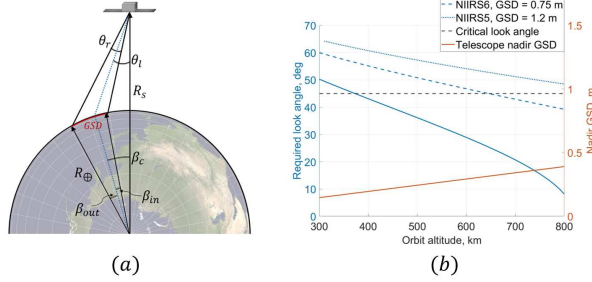


FIGURE 1. a) Sensor geometry, b) Nadir GSD(h) & Required look angle $\theta(h)$ to achieve different GSD or NIIRS classes.

2. Satellite Ground Track

Satellite ground track is a locus of sub-satellite points or points on the Earth surface having the same unit vector \mathbf{e}_{sat}^E as the satellite position vector \mathbf{R}_{sat}^E given in Earth-Centered Earth-Fixed (ECEF) frame. It is common to consider 2D ground track plot (see Fig. 2, a)) where satellite location is defined by a corresponding spherical coordinates or latitude ϕ , and longitude λ .

Figure 2, a) depicts 2D ground track of an RGT SSO orbit that performs 29 revolutions within 2 nodal days. An important parameter for Earth observation mission design is so called fundamental shift S_F . It shows how satellite ground track shifts westward (for LEO satellites) after one nodal period and is calculated as follows

$$S_F = (\omega_{\oplus} - \dot{\Omega}) \cdot T_{sat}^n = 2\pi \cdot \frac{1}{Q}, \quad (2)$$

where ω_{\oplus} is Earth self rotation angular velocity, $\dot{\Omega}$ is secular precession rate of satellite RAAN, $Q = R/D$ is orbit repeating factor describing number of satellite revolutions within one day. It should be noted that Eq. 2 represents fundamental interval at equator while it changes depending on latitude. $S_F(\phi)$ can be found using equations for spherical triangles. Figure 2, b) depicts $S_F(\phi)$ curves for orbits of different altitudes.

Another important property is the maximum latitude of satellite ground track ϕ_{max} that is defined by satellite inclination i is as follows:

$$\sin(\phi_{max}) = \sin(i). \quad (3)$$

It is crucial parameter to ensure coverage of entire area of interest.

3. Constellation Design Approach

The main objective of this study is to identify the minimum required number of satellites n_{sats} to achieve consecutive coverage of all points in a specific region multiple times within a day. Since an optical satellite can only perform imaging during daytime, it has only single opportunity to pass above a certain Earth region within a day for LEO. Therefore, if several access are required, multiple orbital planes should be considered for the satellite constellation.

Let's consider a single plane constellation design yielding a complete coverage of an AOI per day in this study. To get multiple access per day, the configuration of the single plane constellation could be repeated with multiple identical orbital planes shifted by RAAN with respect to each other.

In order to find the required number of satellites n_{sats} , the fundamental shift S_F and swath width S_w at different altitudes h can be considered (refer to Fig. 2, c)). As can be noted from the figure, the swath width S_w of a satellite at LEO with maximum look angle θ of 45° is always smaller than the fundamental shift S_F . Therefore, more than one satellite is needed to ensure the coverage of the entire

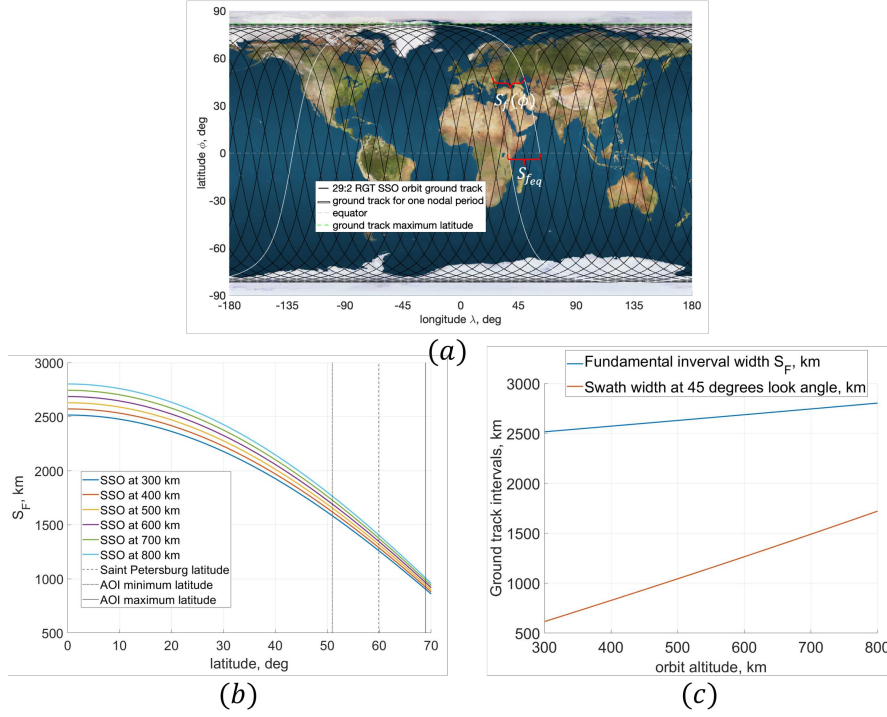


FIGURE 2. a) Ground track Example, b) Fundamental interval S_F versus latitude for sun synchronous orbits of different altitudes, c) Fundamental interval S_F and swath width S_w versus altitude

AOI. The minimum number of satellites to ensure full coverage of the entire area of interest can be found as follows:

$$n_{sats} = \left\lceil \frac{S_F(\phi_{min})}{\tilde{S}_w} \right\rceil, \quad (4)$$

$$\tilde{S}_w = S_w \cdot \frac{1}{\sin(i')}, \quad (5)$$

$$i' = \frac{\sin(i)}{\cos(i) - 1/Q}, \quad (6)$$

where ϕ_{min} is the minimum latitude within an AOI, i' states for apparent inclination.

In order to provide evenly spaced satellites' ground tracks within fundamental interval S_F , the distance between adjacent ground tracks is found as follows

$$\Delta\lambda = \frac{S_F(0)}{n_{sats}},$$

while satellites can pursue the ground track by either RAAN separation or MA separation. The former requires satellite at different planes, i.e. different RAANs, while the latter can be made using single plane. Thus, to yield ground track shift of $\Delta\lambda$ either of the following conditions shall be met:

$$\begin{cases} \Delta\Omega = \Delta\lambda, \\ \Delta MA = \Delta\lambda \cdot Q. \end{cases} \quad (7)$$

4. Constellation Design Example

Let's consider a circumference of Saint Petersburg (latitude $\phi = 59.94^\circ$, longitude $\lambda = 30.31^\circ$) with radius of 1000 km as an area of interest (AOI), yielding minimum latitude $\phi_{min} = 50.95^\circ$. A telescope with diameter $D = 1$ m and angular resolution $\theta_r = 4.88 \cdot 10^{-7}$ rad is considered.

Let's find constellation yielding the entire coverage of the AOI daily with NIIRS 6 (0.75 m GSD) and NIIRS 7 (0.4 m GSD). In this study, 29:2 circular RGT SSO orbit is considered. The orbit altitude is $h = 727.1$ km and inclination $i = 98.27^\circ$.

TABLE 1. Constellation parameters

| Parameters | NIIRS6 | NIIRS7 |
|---|--------|--------|
| Number of satellites | 2 | 4 |
| Swath width S_w , km | 1357.8 | 458.4 |
| Maximum look angle θ , degrees | 41.6 | 17.4 |
| Minimum swathes overlapping, % | 35.98 | 5.19 |
| Mean anomaly separation ΔMA , degrees | 180 | 90 |

Figures 3 a), b) show ground track of the single-plane satellite constellations guaranteeing daily observation of the entire AOI with image quality scales NIIRS6, and NIIRS7, respectively.

Conclusion

The study developed a method for Earth remote sensing constellation design utilizing satellite ground track properties. A coverage geometry model was introduced relating optical telescope parameters, GSD and swath width S_w , and look angle θ for a given LEO orbit. An approach is developed to define the minimum number of satellites to ensure a periodic imaging of the entire AOI for a given LEO orbit

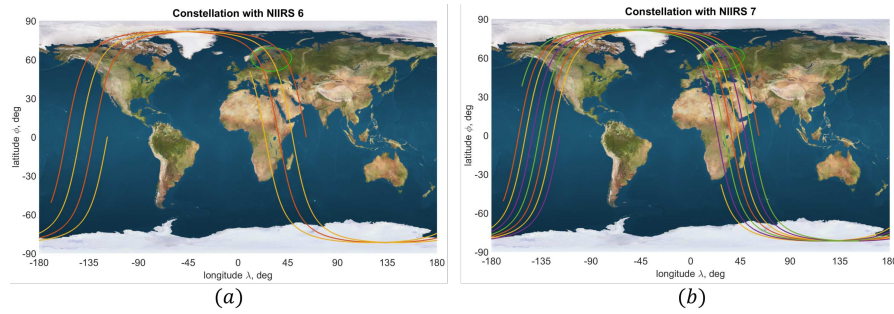


FIGURE 3. a) Satellites ground tracks for NIIRS6: 2 satellites per orbital plane to cover AOI. b) Satellites ground tracks for NIIRS7: 4 satellites per orbital plane to cover AOI.

characterised by its ground track fundamental interval S_f and satellite instrument swath width S_w . An example is presented demonstrating the application of the method for constellation design.

References

- [1] W. Crossley, E. Williams, *Simulated annealing and genetic algorithm approaches for discontinuous coverage satellite constellation design*, Engineering Optimization, 2000
- [2] Ortore Emiliano, Cinelli Marco, Circi Christian, *A ground track-based approach to design satellite constellations*, Aerospace Science and Technology, 2017

Shamil Biktimirov
 Propulsion and Space Research Center
 Technology Innovation Institute
 Abu Dhabi, UAE
 e-mail: biktimirovshamil@gmail.com

Fatima Alnaqbi
 Propulsion and Space Research Center
 Technology Innovation Institute
 Abu Dhabi, UAE
 e-mail: fatima.alnaqbi@tii.ae

Bifurcation diagram of particle motion in a Kerr metric

Ivan Bizyaev and Ivan Mamaev

Abstract. We investigate the dynamics of particles in a Kerr metric which describes the gravitational field in a neighborhood of a rotating black hole. After elimination of cyclic coordinates this problem reduces to investigating a Hamiltonian system with 2 degrees of freedom. This system possesses an additional Carter integral quadratic in momenta and hence is integrable by the Liouville–Arnold theorem. A bifurcation diagram is constructed and a classification of the types of trajectories of the system is carried out according to the values of first integrals.

Introduction

Integrability of the geodesic flow in a Kerr metric was established by Carter [4] in 1968, and a large number of results have been obtained since then in this problem, see, e.g., the reviews [7]. However, a complete bifurcation diagram has been constructed recently in [2]. Using this diagram, an analysis of bifurcations of different types of the system’s trajectories has been carried out for the case where its parameter values are varied. In addition, a graphical representation of possible types of motion depending on the values of the first integrals has been obtained. In what follows, our analysis of the trajectories of a material point will be based on [2].

At the same time, there are a number of particular results in this direction. For example, bifurcation curves for plane orbits have been obtained for the critical value of the Carter integral $Q = 0$ in [1] (in particular, r_{ISCO} (Innermost Stable Circular Orbit) was found for the Kerr metric), and a corresponding diagram was constructed in [8].

There are many other papers describing various special properties of (time-like) geodesics of the Kerr metric. We mention some of them which are related to our analysis. For example, in [3] the motion of particles falling from the state of rest was examined, and the author of [5] found numerically trajectories making a

large number of turns in the neighborhood of a black hole and then receding from it (see also [6], where such orbits are called “zoom-whirl” orbits).

1. The Kerr metric

In the Boyer–Lindquist coordinates $\mathbf{x} = (t, r, \theta, \varphi)$ the Kerr metric is represented in the following form:

$$ds^2 = \frac{\Delta(r)}{\rho^2} (dt - a \sin^2 \theta d\varphi)^2 - \frac{\sin^2 \theta}{\rho^2} ((r^2 + a^2)d\varphi - a dt)^2 - \rho^2 \left(\frac{dr^2}{\Delta(r)} + d\theta^2 \right),$$

$$\rho^2 = r^2 + a^2 \cos^2 \theta, \quad \Delta(r) = r^2 - 2r + a^2, \quad (1)$$

where $\alpha, \beta = 0, 1, 2, 3$, summation is implied over repeated indices, and the signature (1, 3) has been chosen.

The dimensionless parameter a is expressed in terms of the angular momentum of the celestial body M_z relative to the symmetry axis as follows:

$$a = \frac{cM_z}{Gm^2}.$$

If $a = 0$ (i.e., if there is no rotation), the metric (1) becomes a Schwarzschild metric.

As a result, we obtain equations of motion for r and θ in the following form:

$$\left(\frac{dr}{d\tau} \right)^2 = \frac{1}{\rho^4} R(r), \quad \left(\frac{d\theta}{d\tau} \right)^2 = \frac{1}{\rho^4} \Theta(\theta),$$

$$R(r) = (E(r^2 + a^2) - aL)^2 - (Q + (L - aE)^2 + r^2)\Delta(r), \quad (2)$$

$$\Theta(\theta) = Q - \cos^2 \theta \left(a^2(1 - E^2) + \frac{L^2}{\sin^2 \theta} \right).$$

From a physical point of view, E is the energy of the material point, and L is the projection of its angular momentum onto the symmetry axis of the metric, Q is constant Carter integral.

As can be seen, in order to integrate these equations in explicit form, one needs to rescale time as $d\tau = \rho^2(r, \theta) du$.

From the known solutions $r(\tau)$ and $\theta(\tau)$ the evolution of the other variables is defined using the quadratures

$$\rho^2 \frac{d\varphi}{d\tau} = \frac{a}{\Delta(r)} (E(r^2 + a^2) - aL) - aE + \frac{L}{\sin^2 \theta},$$

$$\rho^2 \frac{dt}{d\tau} = \frac{r^2 + a^2}{\Delta(r)} (E(r^2 + a^2) - aL) + aL - a^2 E \sin^2 \theta. \quad (3)$$

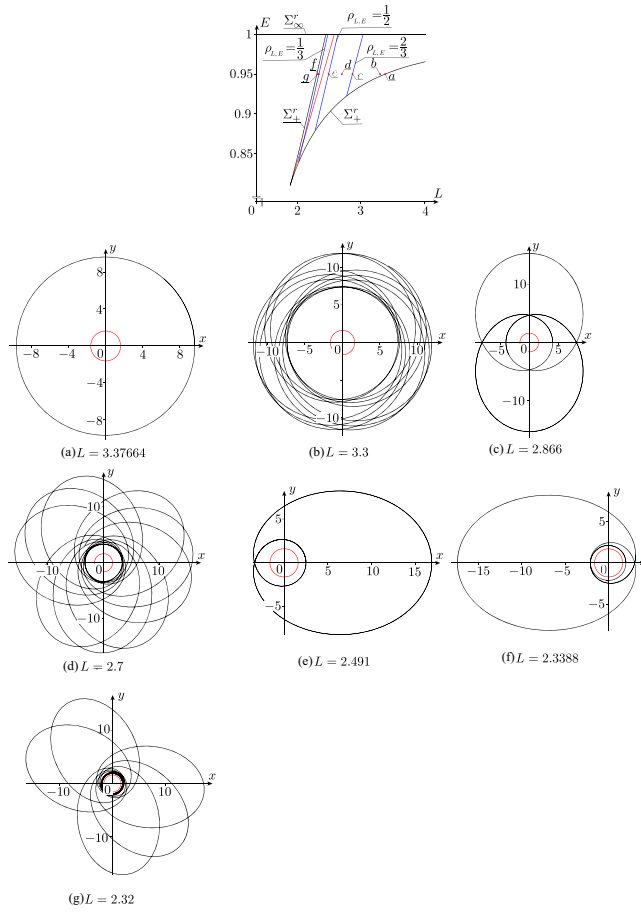


FIGURE 1. Curves for the fixed $a = 0.95$ on the plane L, E which correspond to the rational values of the rotation number $\rho_{\varphi/r}$, and the trajectories in the equatorial plane for the fixed $E = 0.95$ and different L .

2. Trajectories in the equatorial plane

Let the value of the Carter integral be zero, $Q = 0$. Then it follows from the analysis of the latitudinal motion that there exist trajectories lying in the equatorial plane $\theta = \frac{\pi}{2}$, and that all of them are critical (since in this case the latitudinal potential has a critical point).

The system of equations, which governs the evolution of the angles ψ and φ , defines a vector field on the torus \mathbb{T}^2 without fixed points. It is the rotation

number that allows one to classify the trajectories on \mathbb{T}^2 depending on parameters. In this case the rotation number can be represented as

$$\rho_{L,E} = 2\pi d \left[\int_0^{2\pi} \frac{\Phi(\psi) d\psi}{\sqrt{(\Gamma_1 + \cos \psi)(\Gamma_2 + \cos \psi)}} \right]^{-1}.$$

If $\rho_{L,E}$ takes a rational value, then all trajectories on the corresponding invariant torus \mathbb{T}^2 with given values of L and E are periodic. If $\rho_{L,E}$ takes an irrational value, then the trajectories on the torus \mathbb{T}^2 are quasi-periodic. The curves on the plane L, E which correspond to the rational values of the rotation number equal to $\frac{1}{3}, \frac{1}{2}, \frac{2}{3}$ are shown in Fig. 1.

References

- [1] Bardeen J. M., Press W. H., Teukolsky S. A. *Rotating black holes: locally nonrotating frames, energy extraction, and scalar synchrotron radiation*, The Astrophysical Journal, 1972, vol. 178, pp. 347–370.
- [2] Bizyaev I. A., Mamaev I. S. *Bifurcation diagram and a qualitative analysis of particle motion in a Kerr metric*, Physical Review D, 2022, vol. 105, 063003, 28 pp.
- [3] Bicák J., Stuchlik Z. *The fall of the shell of dust on to a rotating black hole*, Monthly Notices of the Royal Astronomical Society, 1976, vol. 175, no. 2, pp. 381–393.
- [4] Carter B. *Global structure of the Kerr family of gravitational fields*, Physical Review, 1968, vol. 174, no. 5, p. 1559.
- [5] Goldstein H. *Numerical calculation of bound geodesics in the Kerr metric*, Zeitschrift für Physik, 1974, vol. 271, no. 3, pp. 275–279.
- [6] Glampedakis K., Kennefick D. *Zoom and whirl: Eccentric equatorial orbits around spinning black holes and their evolution under gravitational radiation reaction*, Physical Review D, 2002, vol. 66, no. 4, p. 044002.
- [7] Sharp N. A. *Geodesics in black hole space-times*, General Relativity and Gravitation, 1979, vol. 10, no. 8, pp. 659–670.
- [8] Stewart J., Walker M. *Black holes: The outside story*, Astrophysics, Springer, Berlin, Heidelberg, 1973, pp. 69–115.

Ivan Bizyaev
 Ural Mathematical Center
 Udmurt State University
 Universitetskaya 1, Izhevsk 426034, Russia
 e-mail: bizyaevtheory@gmail.com

Ivan Mamaev
 Ural Mathematical Center
 Udmurt State University
 Universitetskaya 1, Izhevsk 426034, Russia
 e-mail: mamaev@rcd.ru

Chaotic behavior in the generalized n -center problem

Sergey Bolotin

Abstract. We consider a Hamiltonian system with Hamiltonian $H = \|p\|^2/2 + V(q)$. The configuration space M is a 2-dimensional manifold (for noncompact M certain conditions at infinity are required). It was proved in [2] that if the potential energy V has $n > 2\chi(M)$ Newtonian singularities, then the system is not integrable and has positive topological entropy on energy levels $H = h > \sup V$. We generalize this result to the case when the potential energy has several singular points $\Delta = \{a_1, \dots, a_n\}$ of type $V(q) \sim -\text{dist}(q, a_j)^{-\alpha_j}$. As an application, we consider the generalized n -center problem in \mathbb{R}^2 and discuss possible extensions to the spatial n -center problem.

Our research is motivated by the generalized n -center problem. Let

$$H(q, p) = \frac{1}{2}\|p\|^2 + V(q), \quad V(q) = -\sum_{j=1}^n \frac{m_j}{|q - a_j|^{\alpha_j}} + U(q), \quad q \in \mathbb{R}^2.$$

Then we have:

- $\alpha_j = 1$, $n = 2$, and $U = 0$ – integrable 2 center problem.
- $\alpha_j = 1$ (Newtonian singularities) and $n \geq 3$ – there exists chaotic invariant set on energy levels $H = h > \sup V$ [2, 3].
- $\alpha_j > 2$ (strong singularities) and $n \geq 2$ – chaotic invariant set for $h > \sup V$.

We consider a Hamiltonian system with 2-dimensional configuration space M and Hamiltonian $H = \|p\|^2/2 + V(q)$. The kinetic energy is given by a Riemannian metric (for noncompact M certain conditions at infinity are required). The potential energy V is a smooth function except at a finite number of singular points $\Delta = \{a_1, \dots, a_n\}$. Near a_j ,

$$V(q) = -\frac{f_j(q)}{d(q, a_j)^{\alpha_j}} + U_j(q), \quad f_j(a_j) > 0, \quad \alpha_j > 0.$$

Let $\chi(M)$ be the Euler characteristics of M . For Newtonian singularities we have the following old result.

Theorem 1. [2] *If $n > 2\chi(M)$, the system is non-integrable on energy levels $H = h > \sup V$.*

We may also add a 2-form of gyroscopic forces to the symplectic form $dp \wedge dq$. Our goal is to obtain similar non-integrability conditions for any $\alpha_j > 0$.

Polynomial in p and differentiable in q first integrals on an energy level $\{H = h\}$ are called Birkhoff conditional integrals. Let

$$S(\Delta) = \sum \alpha_j, \quad 1 \leq \alpha_j < 2.$$

Theorem 2. [6] *Let M be a closed manifold and $h > \max V$.*

- *If $S(\Delta) > 2\chi(M)$, there are no nonconstant Birkhoff conditional integrals on the energy level $H = h$.*
- *If $S(\Delta) = 2\chi(M)$, such integrals may exist only when the gyroscopic form is exact.*

To prove chaotic behavior stronger conditions are needed.

Let $A_k = 2 - 2k^{-1}$, $k \in \mathbb{N}$, and let n_k be the number of singular points with $A_k \leq \alpha_j < A_{k+1}$. Set $n_\infty = 2$. Denote

$$A(\Delta) = \sum_{2 \leq k \leq \infty} n_k A_k = n_2 + \frac{4}{3}n_3 + \frac{3}{2}n_4 + \frac{8}{5}n_5 + \cdots + 2n_\infty$$

We have $A(\Delta) \leq S(\Delta)$ and $S(\Delta) = A(\Delta)$ iff all singularities are regularizable.

- If all singularities are weak with $0 < \alpha_j < 1$, then $A(\Delta) = 0$.
- If all singularities are Newtonian with $\alpha_j = 1$, then $A(\Delta) = n$.
- If all singularities are strong with $\alpha_j > 2$, then $A(\Delta) = 2n$.
- Newtonian singularities and Jacobi singularities ($\alpha_j = 2$) are critical.

For simplicity suppose there are no gyroscopic forces.

Theorem 3. [7] *If*

$$A(\Delta) > 2\chi(M),$$

then the system has a compact chaotic invariant set of noncollision trajectories on any energy level $H = h > \sup V$.

For noncompact M certain conditions at infinity are required.

This result is purely topological: almost no analytical properties of the potential, except the presence of singularities, are involved.

Corollary 1. *For the generalized n -center problem in \mathbb{R}^2 , if $A(\Delta) > 2$, the system has a compact chaotic invariant set on any energy level $H = h > \sup V$.*

A weaker result was proved in [5]. For nonintegrability condition $S(\Delta) > 2$ is also sufficient. We do not know if this is enough for chaotic behavior.

Other examples:

- $M = \mathbb{T}^2$, $\chi(\mathbb{T}^2) = 0$. Theorem 3 works if there is a nonweak singularity with $\alpha \geq 1$. We do not know if the existence of a weak singularity on \mathbb{T}^2 always implies chaotic behavior.

- $M = S^2$, $\chi(S^2) = 2$. Theorem 3 works for:
 - $n \geq 5$ singularities with $\alpha_j \geq 1$,
 - $n \geq 4$ singularities with $\alpha_j \geq 4/3$,
 - $n \geq 3$ singularities with $\alpha_j \geq 3/2$.
 - 3 singularities with $\alpha_j \geq 1$ and the 4th with $\alpha_4 \geq 4/3$.

For $n = 4$ Newtonian singularities on S^2 the system may be integrable on an energy level $H = h > \max V$ [2].

The proof of Theorem 3 is based on on the generalized Levi-Civita regularization $q = a_j + z^\beta$, $z \in \mathbb{C}$.

Let

$$\Delta = \Delta_{weak} \cup \Delta_{newt} \cup \Delta_{mod} \cup \Delta_{jac} \cup \Delta_{strong}.$$

The most nontrivial are moderate singularities with $1 < \alpha_j < 2$. Trajectories on $\{H = h\}$ are geodesics of the Jacobi metric

$$g_h(q, \dot{q}) = \sqrt{2(h - V(q))} \|\dot{q}\|.$$

The Jacobi distance to the strong singularities is infinite, so they may be removed replacing M by $M \setminus \Delta_{strong}$.

Theorem 4. *There exists a surface \hat{M} , a K -sheet covering $\phi : \hat{M} \rightarrow M \setminus (\Delta_{jac} \cup \Delta_{strong})$ branched over the set $\Delta_{newt} \cup \Delta_{mod}$, and a smooth Riemannian metric on \hat{M} such that:*

- *Projections to M of minimal geodesics on the universal covering of \hat{M} are trajectories with energy $H = h$ having no collisions with Δ , except maybe with regularizable singularities Δ_{reg} .*
- *The Euler characteristics*

$$\chi(\hat{M}) = K(\chi(M) - \frac{1}{2}A(\Delta)) < 0.$$

Since $\chi(\hat{M}) < 0$, a modification of old results of Kozlov [1] may be applied to prove Theorem 3.

Our results can be partly extended to the spatial generalized n -center problem. For $n \geq 3$ Newtonian singularities in \mathbb{R}^3 the existence of a chaotic invariant set may be proved using global KS regularization [4]. It replaces the configuration space $M = \mathbb{R}^3$ by the 4-dimensional manifold

$$\hat{M} = (S^2 \times \mathbb{R}^2) \# (S^2 \times S^2) \# \dots \# (S^2 \times S^2).$$

Then Gromov's theorem may be used to prove positive topological entropy. If there is a generalized n -center problem in \mathbb{R}^3 with $n \geq 3$ singularities of order $1 < \alpha_j < 2$, global KS regularization gives a system with configuration space \hat{M} and weak singularities of order $0 < \tilde{\alpha}_j < \alpha_j$ [8]. Then we hope that a modification of Gromov's theorem can be applied to obtain a chaotic invariant set. The problem is that, contrary to the 2-dimensional case, we can't exclude that chaotic trajectories enter weak singularities. Nevertheless, we have:

Conjecture. Let

$$B_k = 2 - 2^{k-1}, \quad m_k = \#\{a_k : B_k \leq \alpha_j < B_{k+1}\}.$$

If

$$B(\Delta) = \sum_{1 \leq k \leq \infty} m_k B_k > 2,$$

then the generalized n center problem in \mathbb{R}^3 has positive topological entropy on energy levels $H = h > \sup V$.

References

- [1] V.V. Kozlov, Topological obstructions to the integrability of natural mechanical systems, *Sov. Math. Dokl.*, **20** (1979).
- [2] S. Bolotin, The effect of singularities of the potential energy on the integrability of mechanical systems, *J. Appl. Math. Mech.*, **48** (1984).
- [3] A. Knauf, Ergodic and topological properties of Coulombic periodic potentials, *Commun. Math. Phys.* **110** (1987).
- [4] S. Bolotin and P. Negrini, Regularization and topological entropy for the spatial n -center problem. *Ergodic Theory Dynam. Systems*, **21** (2001).
- [5] R. Castelli, Topologically distinct collision-free periodic solutions for the N -center problem. *ARMA*, **223** (2017).
- [6] S. Bolotin and V. Kozlov, Topology, singularities and integrability in Hamiltonian systems with two degrees of freedom. *Izvestiya RAN*, **81** (2017).
- [7] S. Bolotin and V. Kozlov, Topological approach to the generalized n -center problem. *Uspekhi Mat. Nauk*, **72** (2017).
- [8] S. Bolotin, Generalized n -center problem in \mathbb{R}^3 . In preparation.

Sergey Bolotin
 Moscow Steklov Mathematical Institute of RAS
 Moscow, Russia
 e-mail: bolotin@mi-ras.ru

On Types of Stability in Hamiltonian Systems

Alexander Bruno and Alexander Batkhin

Abstract. We consider conditions of three types of stability: Lyapunov, formal and weak of a stationary solution in a Hamiltonian system with a finite number of degrees of freedom. The conditions contain restrictions on the order of resonances and some inequalities for coefficients of the normal forms of the Hamiltonian functions. We also estimate the orders of solutions' divergence from the stationary ones under lack of formal stability.

1. Resonant normal form

Consider a Hamiltonian system

$$\dot{\xi}_j = \frac{\partial \gamma}{\partial \eta_j}, \quad \dot{\eta}_j = -\frac{\partial \gamma}{\partial \xi_j}, \quad j = 1, \dots, n \quad (1)$$

with n degrees of freedom in the neighborhood of a stationary point at the origin

$$\zeta \stackrel{\text{def}}{=} (\xi, \eta) = 0. \quad (2)$$

If the Hamilton function $\gamma(\zeta)$ is analytic at this point, then it expands into a convergent power series

$$\gamma(\zeta) = \sum \gamma_{\mathbf{p}\mathbf{q}} \xi^{\mathbf{p}} \eta^{\mathbf{q}}, \quad (3)$$

where $\mathbf{p}, \mathbf{q} \in \mathbb{Z}^n$, $\mathbf{p}, \mathbf{q} \geq 0$, $\xi^{\mathbf{p}} = \xi_1^{p_1} \dots \xi_n^{p_n}$, $\gamma_{\mathbf{p}\mathbf{q}}$ are constant coefficients. Since the point (2) is stationary, the expansion (3) starts with quadratic terms. They correspond to the linear part of the system (1). The eigenvalues of its matrix are divided into pairs $\lambda_{j+n} = -\lambda_j$, $j = 1, \dots, n$. Denote by vector $\boldsymbol{\lambda} = (\lambda_1, \dots, \lambda_n)$ the set of *basic eigenvalues*. As known, canonical coordinate substitutions $\xi, \eta \rightarrow \mathbf{x}, \mathbf{y}$ preserve the Hamiltonian nature of the system.

Theorem 1 ([1, §12]). *There is a canonical formal transformation $\xi, \eta \leftrightarrow \mathbf{x}, \mathbf{y}$ that reduces the Hamiltonian (3) to the normal form*

$$g(\mathbf{x}, \mathbf{y}) = \sum g_{\mathbf{p}\mathbf{q}} \mathbf{x}^{\mathbf{p}} \mathbf{y}^{\mathbf{q}}, \quad (4)$$

where the series g contains only resonant terms satisfying **resonant equation** $\langle \mathbf{p} - \mathbf{q}, \boldsymbol{\lambda} \rangle = 0$. Here $\langle \cdot, \cdot \rangle$ means the scalar product.

Condition A_k^n for system with n DOF takes place if the resonant equation has no integer solutions $\mathbf{p} \in \mathbb{Z}^n$ with $\|\mathbf{p}\| \leq k$.

This condition means that there are no resonances up to and including the order k . If it is satisfied, then in the normal form (4) is $g = \sum_{l=1}^{\lfloor k/2 \rfloor} g_l(\boldsymbol{\rho}) + \tilde{g}^{(k)}(\mathbf{z}, \bar{\mathbf{z}})$, where $g_l(\boldsymbol{\rho})$ are homogeneous polynomials from $\rho_j = iz_j \bar{z}_j$, $j = 1, \dots, n$, of degree l , and $\tilde{g}^{(k)}$ is a series from $\mathbf{z}, \bar{\mathbf{z}}$ starting with powers above k . In particular, under the condition A_2^n we have

$$g = \langle \boldsymbol{\rho}, \boldsymbol{\lambda} \rangle + \tilde{g}^{(3)}(\mathbf{z}, \bar{\mathbf{z}}),$$

and under the condition A_4^n we have

$$g = \langle \boldsymbol{\rho}, \boldsymbol{\lambda} \rangle + \langle C\boldsymbol{\rho}, \boldsymbol{\rho} \rangle + \tilde{g}^{(5)}(\mathbf{z}, \bar{\mathbf{z}}), \quad (5)$$

where C is $n \times n$ matrix.

2. Lyapunov and formal stabilities of stationary point

2.1. Lyapunov stability

Definition 1. A stationary point (SP) $\zeta = 0$ of a real Hamiltonian system (1) is *stable by Lyapunov* if for every $\varepsilon > 0$ in “cube” $\|\zeta\| < \varepsilon$ there exists a closed integral $(2n - 1)$ -dimensional manifold \mathcal{L} surrounding the point $\zeta = 0$ from all sides, where $\|\zeta\| = \sum_{j=1}^{2n} |\zeta_j|$.

Lemma 1. A SP $\zeta = 0$ is *Lyapunov stable* if there exists a sign-definite real integral

$$f(\zeta) = f_l(\zeta) + \tilde{f}^{(l)}(\zeta) \quad (6)$$

of the system (1), where $f_l(\zeta)$ is a homogeneous form of degree l . In other words,

$$\{f, \gamma\} = 0, \quad (7)$$

where $\{\cdot, \cdot\}$ is the Poisson bracket, and $f_l(\zeta)$ does not equal to zero at any ζ except the point $\zeta = 0$.

Stability is possible only if $\text{Re } \boldsymbol{\lambda} = 0$.

Theorem 2 (Dirichlet). Suppose $\lambda_j = i\alpha_j$, $\alpha_j \in \mathbb{R}$, $j = 1, \dots, n$. If the condition A_2^n is satisfied and the numbers $\alpha_1, \dots, \alpha_n$ are of the same sign, then the SP $\zeta = 0$ is stable according to Lyapunov.

Here the role of the integral f is played by the Hamiltonian γ itself.

2.2. Formal stability

By *formal* we will mean power series, about the convergence of which nothing is known.

Definition 2 ([2]). A SP (2) of a real Hamiltonian system (1) is *formally stable* if there exists a formal real sign-defined integral (6) of the system (1), i.e., the formal identity (7) is satisfied and the homogeneous form f_l is null only at $\zeta = 0$.

Formal stability means that the departure of solutions from the SP, if anything, is very slow: slower than any finite degree of t .

Definition 3 ([3, Ch. 4, § 4]). A SP (2) of a real Hamiltonian system (1) is *formally stable* if there exists a formal real integral

$$f(\zeta) = f_l(\zeta) + f_{l+1}(\zeta) + \dots + f_m(\zeta) + \tilde{f}^{(m)}(\zeta)$$

of system (1), where $f_k(\zeta)$ are homogeneous forms of degree k and the sum

$$f^*(\zeta) = f_l + f_{l+1} + \dots + f_m \quad (8)$$

does not equal to zero in some neighborhood of the point $\zeta = 0$ besides it.

Let $K \subset \mathbb{R}^n$ be a linear shell of integers \mathbf{q} satisfying the equation $\langle \alpha, \mathbf{q} \rangle = 0$, and $Q = \{\mathbf{q} \geq 0, \mathbf{q} \neq 0\} \subset \mathbb{R}^n$ is a non-negative orthant without origin.

Theorem 3 (Formal Stability Theorem [4]). *If Condition A_4^n is satisfied and in (5)*

$$\langle C\mathbf{q}, \mathbf{q} \rangle \neq 0 \text{ for } \mathbf{q} \in K \cap Q, \quad (9)$$

then the point $\zeta = 0$ is formally stable in the sense of Definition 2

Here, the normal form of the Hamiltonian (4) from Theorem 1 is used to construct the formal integral.

In the situation when any resonance of multiplicity 1 takes place, there exists the only integral vector $k\mathbf{p}$, $k \in \mathbb{Z} \setminus \{0\}$, $\mathbf{p} \in \mathbb{Z}^n$, satisfying the resonant equation. Let ω_j , $j = 1, \dots, n-1$, be the basis of the orthogonal complement to the one-dimensional solution space, then $\langle \omega_j, \rho \rangle$ is the first integral of the normalized system with Hamiltonian $g(\mathbf{z}, \bar{\mathbf{z}})$ [5, Ch. I, Sect. 3].

Lemma 2. *If there exists only one resonant vector $k\mathbf{p}$, $k \in \mathbb{Z}$, which does not belong to the positive orthant Q , than SP $\zeta = 0$ is formally stable.*

2.3. Method of formal stability investigation in a generic case with 3DOF

Consider a Hamiltonian system in the vicinity of the SP for which the following conditions are satisfied:

- the number of degrees of freedom of the system is greater than two;
- the quadratic form γ_2 in expansion (3) is nondegenerate and is not definite;
- the Hamiltonian function γ smoothly depends of the vector of parameters \mathbf{P} from a domain $\Pi \subset \mathbb{R}^m$.

Corollary 1 (of Formal Stability Theorem 3). *If under the condition of Theorem 3 in \mathbb{R}^3 the intersection of the plane $\langle \boldsymbol{\lambda}, \mathbf{q} \rangle = 0$ and the cone $\langle C\mathbf{q}, \mathbf{q} \rangle$ either does not belong to \mathcal{Q} , or belongs to $\mathcal{Q} = \mathbb{R}_+^3$, but does not contain the integral vector \mathbf{q} , then the SP is formally stable.*

Definition 4. A resonant variety $\mathcal{R}_n^{\mathbf{p}}$ in the space K of coefficients a_1, \dots, a_n of the semi-characteristic polynomial $\chi_n(\mu)$ of degree n is an algebraic variety, on which the vector of basis eigenvalues $\boldsymbol{\lambda}$ is a nontrivial solution to the resonant equation $\langle \mathbf{p}, \boldsymbol{\lambda} \rangle = 0$ for a fixed integer vector $\mathbf{p}^* \in \mathbb{Z}^n \setminus \{0\}$. An analytical representation of the variety $\mathcal{R}_n^{\mathbf{p}^*}$ in an implicit or parametric form is denoted by $R_n^{\mathbf{p}^*}$.

To examine the formal stability of a SP of a Hamiltonian system (1), we should [6]:

- find in the space of parameters Π the stability set Σ of the linear system;
- find such domains, in which the quadratic form $\gamma_2(\mathbf{z})$ is not sign definite;
- find parts S_k in these domains that do not contain strong resonances;
- normalize the Hamiltonian in each of these parts S_k up to order four, and
- apply Formal Stability Theorem 3.

To do this, it is sufficient to select a point in each S_k in the space of parameters and use one of the normalization algorithms for the Hamiltonian function. Since all eigenvalues λ_k ($k = 1, \dots, n$) are simple at each interior point of S_k , the invariant normalization algorithm can be easily applied.

Remark. Most of presented above statements are applicable for stability of a periodic solution.

3. Scattering order of solution

Let the function $f(t)$ be defined at real $t \rightarrow -\infty$. It is said to have *order* $\delta = \delta(t)$ if $\delta = \inf \varepsilon$ such that $f(t)/(-t)^\varepsilon \rightarrow 0$ at $t \rightarrow -\infty$. If $\delta > 0$, then $f(t)$ is unbounded, if $\delta < 0$, then $f(t) \rightarrow 0$ at $t \rightarrow -\infty$. In the latter case $\delta(f) < 0$, the larger δ is, the slower $f(t)$ approaches zero.

Definition 5. Let the solution $\zeta(t)$ of the Hamiltonian system (1) tends to a SP (2) at $t \rightarrow -\infty$. On this solution *order of scattering* $\Delta = \min \{\delta \|\zeta\|\}$.

Definition 6. The *scattering order* $\tilde{\Delta}$ of solutions of the system (1) from the SP (2) is the lower bound of the scatter order Δ over all solutions $\zeta(t)$ that tend to the point (2) at $t \rightarrow -\infty$.

The smaller $\tilde{\Delta} < 0$, the faster the solutions are scattered from the SP. At formal stability the order of scattering of solutions from the SP is zero. Let us estimate the order of scattering $\tilde{\Delta}$ in the absence of formal stability. The cases $-10^{-10} < \tilde{\Delta} < 0$ can be considered as *weak stable*.

Conjecture. Let the condition A_2^n and $\varkappa = \min \|\mathbf{p} + \mathbf{q}\| > 2$ by integer solutions $\mathbf{p} \geq 0$, $\mathbf{q} \geq 0$ of equation $\langle \boldsymbol{\alpha}, \mathbf{p} - \mathbf{q} \rangle = 0$ be satisfied, then the order of scatter of the system solutions (1) from the SP $\tilde{\Delta} \geq (2 - \varkappa)^{-1}$.

4. Conclusion

These results were published in [7] together with:

1. more details, with examples;
2. number-theoretical approach simplifying the proofs of formal stability;
3. computing of formal stability in a complicated case;
4. similar theory for a neighborhood of a periodic solution.

References

- [1] A. D. Bruno. Analytical form of differential equations (II). *Trans. Moscow Math. Soc.*, 26:199–239, 1972. = Trudy Moskov. Mat. Obsc. 25 (1971) 119–262 (in Russian).
- [2] J. K. Moser. New aspects in the theory of stability in hamiltonian systems. *Comm. Pure Appl. Math.*, 11(1):81–114, 1958.
- [3] A. P. Markeev. *Libration Points in Celestial Mechanics and Cosmodynamics*. Nauka, Moscow, 1978. (in Russian).
- [4] A. D. Bruno. Formal stability of Hamiltonian systems. *Mathematical Notes of the Academy of Sciences of the USSR*, 1:216–219, 1967. <https://doi.org/10.1007/BF01098887>
- [5] A. D. Bruno. *The Restricted 3-body Problem: Plane Periodic Orbits*. Walter de Gruyter, Berlin, 1994. = Nauka, Moscow, 1990. 296 p. (in Russian).
- [6] A. B. Batkhin and Z. Kh. Khaydarov. Calculation of a strong resonance condition in a Hamiltonian system. *Computational Mathematics and Mathematical Physics*, 63(5):687–703, 2023. <https://doi.org/10.1134/S0965542523050068>
- [7] A. D. Bruno and A. B. Batkhin. On types of stability in hamiltonian systems. *Mathematics and Systems Science*, 1(1):2269, 2023. <https://doi.org/10.54517/mss.v1i1.2269>

Alexander Bruno
Keldysh Institute of Applied Mathematics of RAS, Moscow, Russia
e-mail: abruno@keldysh.com

Alexander Batkhin
Department of Aerospace Engineering, Technion – Israel Institute of Technology, Haifa, Israel
e-mail: batkhin@technion.ac.il

Chaotic diffusion in a triaxial galactic model: an example of global stable chaos

Pablo M. Cincotta and Claudia M. Giordano

In this work we focus on the chaotic diffusion in the phase space of a triaxial potential resembling an elliptical galaxy. The transport process is studied in two different action-like starting spaces in order to cope with circulating and non-circulating orbits. Estimates of the diffusion rate obtained by means of the variance approach are discussed in detail and their limitations are exposed. After revisiting the Shannon-entropy-based method from a conceptual point of view in the framework of simple arguments taken from the information theory, we apply it to measure changes in the unperturbed actions or integrals of motion of the system for different sets of small ensembles of random initial conditions. For such sets of ensembles, estimates of the Lyapunov times are also provided. The results show that, within the chaotic component of the phase space, the Lyapunov times are shorter than any physical time-scale as the Hubble time, but the diffusion times are much larger than the latter. Thus we conclude that stable chaos dominates the dynamics of realistic galactic models.

Pablo M. Cincotta

Grupo de Caos en Sistemas Hamiltonianos, Facultad de Ciencias Astronómicas y Geofísicas, Universidad Nacional de La Plata and Instituto de Astrofísica de La Plata (CONICET), Paseo del Bosque S/N, B1900FWA, La Plata, Argentina
e-mail: pmc@fcaglp.unlp.edu.ar

Claudia M. Giordano

Grupo de Caos en Sistemas Hamiltonianos, Facultad de Ciencias Astronómicas y Geofísicas, Universidad Nacional de La Plata and Instituto de Astrofísica de La Plata (CONICET), Paseo del Bosque S/N, B1900FWA, La Plata, Argentina
e-mail: giordano@fcaglp.unlp.edu.ar

On the integrability of dynamical models with quadratic right-hand side

Victor F. Edneral

Abstract. We use a heuristic method that allows us to determine in advance the cases of integrability of autonomous dynamical systems with a polynomial right-hand side. The capabilities of the method are demonstrated using examples of two- and three-dimensional systems with quadratic nonlinearity on the right side. Application of the discussed approach allows us to find many integrable cases of such systems, which can be used in the study of mathematical models.

Introduction

In previous works [1, 2] a technique was described for constructing some systems of algebraic equations for the parameters of an ODE system with resonance in the linear part. It was experimentally shown that using relations on the parameters obtained as a result of solving such systems, one can find explicit expressions for the first integrals or solutions of ODEs in quadratures. It was also discovered that by considering integrability conditions simultaneously for several resonances, it is possible to obtain integrability conditions for general (non-resonant) cases.

The talk discusses the use of this method for finding first integrals of two- and three-dimensional systems with quadratic nonlinearity and possible applications of these results in modeling.

1. Two-dimensional case

First we considered a two-dimensional system in the case of a center. In this situation, the only possible resonance is for purely imaginary and opposite-sign eigenvalues of the linear part

$$\begin{aligned}\dot{x} &= y + a_1x^2 + a_2xy + a_3y^2, \\ \dot{y} &= -x + b_1x^2 + b_2xy + b_3y^2,\end{aligned}\tag{1}$$

where we found 13 sets of parameters for which the system is integrable [3].

For the saddle case there are many resonances $\alpha : 1$ for natural values of α

$$\begin{aligned}\dot{x} &= \alpha x + a_1 x^2 + a_2 x y + a_3 y^2, \\ \dot{y} &= -y + b_1 x^2 + b_2 x y + b_3 y^2.\end{aligned}\tag{2}$$

At the resonance 1:1, i.e. at $\alpha = 1$ we got 7 cases of the integrability, and for $\alpha = 2$ also 7 sets of parameters for which the system is integrable [3].

The above results were obtained by solving algebraic systems for the parameters of the system. Each of these systems was created for a specific resonance, i.e. for a fixed natural parameter α . But the form of all these equations and their variables are the same, so the idea arises to look for a general solution to the combined system for several resonances. We created such a system by combining systems for 1:1, 2:1 and 3:1 resonances. For all sets of parameters obtained as a result of solving such a unified system, it was possible to calculate the first integrals of the system (2) for an arbitrary (symbolic) α . We found 11 sets of parameters under which the system integrates with an arbitrary α .

The first integrals for the systems discussed above were calculated using the DSolv procedure of the MATHEMATICA-11 system or manually using the Darboux method.

2. Three dimension case

First we again considered resonant cases of the system

$$\begin{aligned}\dot{x} &= \alpha x + a_2 x y + a_4 x z + a_5 y z, \\ \dot{y} &= -\beta y + b_2 x y + b_4 x z + b_5 y z, \\ \dot{z} &= -z + c_2 x y + c_4 x z + c_5 y z,\end{aligned}\tag{3}$$

with natural α, β on the square table $\{1, 2, 3\} \times \{1, 2, 3\}$. In the two-dimensional case, we struggled to evaluate each integral. But here we limited ourselves to calculations only using the DSolve procedure of the MATHEMATICA 13.3.1.0 system. The results are in table 1.

| N | α | β | Algebraic solutions | Integrals |
|----|----------|---------|---------------------|-----------|
| 8 | 1 | 1 | 23 | 19 |
| 8 | 1 | 2 | 16 | 12 |
| 8 | 1 | 3 | 25 | 19 |
| 8 | 2 | 1 | 57 | 49 |
| 8 | 2 | 2 | 34 | 29 |
| 8 | 2 | 3 | 43 | 35 |
| 9 | 3 | 1 | 60 | 51 |
| 9 | 3 | 2 | 63 | 58 |
| 10 | 3 | 3 | 43 | 38 |

TABLE 1

“N” here is the normal form order, “Algebraic solutions” is a number of rational solutions of the corresponding algebraic system and the “Integrals” is a number of success solutions by the MATHEMATICA.

Then we solved the unied algebraic system from these 9 systems above (329 equations), found its 10 solutions, and opened that system MATHEMATICA-13.3.1.0 solves all corresponding systems of ODEs of the form (3) except one, but the dsolve procedure of the Maple 17 calculated solutions for the 9-th case. The integrable systems for arbitrary α and β are:

- 1 $\dot{x} = \alpha x + a_2 x \cdot y + a_4 x \cdot z + a_5 y \cdot z,$
 $\dot{y} = -\beta y + b_5 y \cdot z,$
 $\dot{z} = -z + c_5 y \cdot z;$
- 2 $\dot{x} = \alpha x,$
 $\dot{y} = -\beta y + b_2 x \cdot y + b_4 x \cdot z,$
 $\dot{z} = -z + c_4 x \cdot z;$
- 3 $\dot{x} = \alpha x + a_2 x \cdot y + a_4 x \cdot z + a_5 y \cdot z,$
 $\dot{y} = -\beta y + a_4 y \cdot z,$
 $\dot{z} = -z - a_2 y \cdot z;$
- 4 $\dot{x} = \alpha x,$
 $\dot{y} = -\beta y + b_2 x \cdot y,$
 $\dot{z} = -z + c_4 x \cdot z;$
- 5 $\dot{x} = \alpha x,$
 $\dot{y} = -\beta y + b_4 x \cdot z,$
 $\dot{z} = -z + c_4 x \cdot z;$
- 6 $\dot{x} = \alpha x,$
 $\dot{y} = -\beta y,$
 $\dot{z} = -z + c_4 x \cdot z + c_5 y \cdot z;$
- 7 $\dot{x} = \alpha x,$
 $\dot{y} = -\beta y + b_2 x \cdot y + b_5 y \cdot z,$
 $\dot{z} = -z;$
- 8 $\dot{x} = \alpha x + a_4 x \cdot z,$
 $\dot{y} = -\beta y + b_4 x \cdot z + a_4 y \cdot z,$
 $\dot{z} = -z;$
- 9 $\dot{x} = \alpha x + a_5 y \cdot z,$
 $\dot{y} = -\beta y + b_2 x \cdot y,$
 $\dot{z} = -z - b_2 x \cdot z;$
- 10 $\dot{x} = \alpha x,$
 $\dot{y} = -\beta y,$
 $\dot{z} = -z + c_4 x \cdot z.$

Please note that a_i, b_j, c_k are free, unrelated parameters; they are arbitrary for each case separately.

3. The general three-dimension system

Finally, we considered the general case of a three-dimensional system with 20 parameters

$$\begin{aligned}\dot{x} &= \alpha x + a_1 x^2 + a_2 x \cdot y + a_3 y^2 + a_4 x \cdot z + a_5 y \cdot z + a_6 z^2, \\ \dot{y} &= -\beta y + b_1 x^2 + b_2 x \cdot y + b_3 y^2 + b_4 x \cdot z + b_5 y \cdot z + b_6 z^2, \\ \dot{z} &= -z + c_1 x^2 + c_2 x \cdot y + c_3 y^2 + c_4 x \cdot z + c_5 y \cdot z + c_6 z^2.\end{aligned}\quad (4)$$

Calculating the normal form up to 6th order for 4 pairs $\{\alpha, \beta\}$, i.e. for $\{1, 1\}$, $\{1, 2\}$, $\{2, 1\}$ and $\{2, 2\}$, we got a system of 121 equations with 18 parameters. We received 174 of its solutions. For 109 of them the MATHEMATICA system calculated solutions of the corresponding ODEs.

4. Chemical Kinetics Models

There are many cases of integrability of three-dimension systems, and the corresponding exact solutions can be useful in applications, for example, in problems of chemical kinetics. The explicit form of solutions allows one to study bifurcation behavior depending on the parameters of the system. This will make it possible to discover new effects in simulated systems. See, for example, the Jabotinsky-Korzukhin model [4].

$$\begin{aligned}\dot{x} &= k_1 x(C - y) - k_0 x z, \\ \dot{y} &= k_1 x(C - y) - k_2 y, \\ \dot{z} &= k_2 y - k_3 z.\end{aligned}\quad (5)$$

The eigenvalues of the linear part the system above are $\{C \cdot k_1, -k_2, -k_3\}$.

After diagonalizing the linear part of equation (5) takes the form (4). The question arises: under what additional conditions does the diagonalized equation (gensyst) appear among the exactly solvable cases? We found that system (5) has 5 integrable in quadratures cases if the below relations are satisfied

$$k_0 = \frac{Ck_1 + 1}{C}, \quad k_2 = -Ck_1, \quad k_3 = 1.\quad (6)$$

Unfortunately, the coefficients in the model (5) must be positive, so requirement (6) is not feasible in reality. But this example illustrates the possibility of discovering integrable cases of dynamical models.

References

- [1] Edneral V.F., *Integrable Cases of the Polynomial Liénard-type Equation with Resonance in the Linear Part* // Mathematics in Computer Science **17** 19 (2023). <https://doi.org/10.1007/s11786-023-00567-6>
- [2] Bruno A. D., Edneral V. F., *Integration of a degenerate system of odes*. Programming and Computer Software **50**, no. 2 (2024) 128–137.

- [3] Edneral V.F., *On the integrability of two- and three-dimensional dynamical systems with a quadratic right-hand side in cases of resonances in linear parts and in cases of general position*. International Conference on Polynomial Computer Algebra PCA-2024, VVM publishing, St. Petersburg, ISBN 978-5-9651-1566-2 (2024) 46–49.
- [4] Korzukhin M. D., Zhabotinsky A. M. *Mathematical modeling of chemical and environmental self-oscillating systems* // M.: Nauka (1965). (Russian).

Victor F. Edneral

Skobeltsyn Institute of Nuclear Physics of Lomonosov Moscow State University

1(2) Leninskie gory, Moscow, 119991, Russian Federation

e-mail: edneral@theory.sinp.msu.ru

Periodic Oscillations of a Two-Body System in the Plane of the Elliptic Orbit

Sergey A. Gutnik

Abstract. The planar oscillations of a system of two bodies connected by a spherical joint that moves along an elliptic orbit under the action of gravitational torque in the plane of the orbit are investigated. The librational motion of a two-body system on an elliptic orbit is described by the second order system of differential equations with the periodic coefficients. Applying the perturbation techniques the periodic solution of the equations of motion is constructed in the form of power series in a small parameter. Using the proposed approach it is shown that the motion of the two-body system is described by periodic oscillations in the plane of an elliptic orbit. All the relevant symbolic computations are performed with the help of computer algebra systems.

Introduction

We consider the dynamics of a two-body system (satellite and stabilizer) connected by a spherical joint that moves in gravitational field in the plane of an elliptical orbit. The dynamics of various schemes for satellite-stabilizer gravitational orientation systems on a circular orbit was discussed in many papers, some review of them can be found in papers [1, 2, 3].

In the previous works the equilibrium orientations of the system on a circular orbit only in the simplest cases were considered when the spherical joint is located at the intersection of the satellite and stabilizer principal central axis of inertia and in the case where the spherical joint is positioned on the line of intersection between two planes formed by the principal central axes of inertia of the satellite and stabilizer [4, 5, 6].

On a circular orbit, there are spatial oscillations of a system of two connected bodies at the vicinity of equilibria. In paper [7], the eigen oscillations of a system of two bodies were studied and the parameters of the system, optimal in terms of speed, were found for the transition of the system to equilibrium. A detailed study

of the oscillations of a satellite (a rigid body) in the plane of an elliptical orbit and the conditions for their stability were carried out in [8].

In the previous works the planar oscillations of a system of two coupled bodies on an elliptic orbit were carried out only for simple cases, when the centers of mass of the first and second bodies coincide [9], [10]. Here, we study the planar oscillations of a two-body system on an elliptic orbit in case when the spherical joint is located at the intersection of the first and second body principal central axis of inertia. Applying the perturbation techniques and appropriate symbolic computations we construct the periodic solution in the form of a power series in a small parameter.

1. Equations of Motion

We consider the problem of two bodies connected by a spherical joint that move on an elliptic orbit. To write the equations of motion of two-body system, we introduce the following right-handed Cartesian coordinate systems: $OXYZ$ is the orbital coordinate system, the OZ axis is directed along the radius vector connecting the Earth center of mass C and the center of mass O of the two-body system, the OX axis is directed along the linear velocity vector of the center of mass O , and the OY axis coincides with the normal to the orbital plane. The axes of coordinate systems $O_1x_1y_1z_1$ and $O_2x_2y_2z_2$, are directed along the principal central axes of inertia of the first and the second body, respectively. The orientation of the coordinate system $O_ix_iy_iz_i$ with respect to the orbital coordinate system is determined by the aircraft angles α_i (pitch), β_i (yaw), and γ_i (roll) (see [3]).

Suppose that (a_i, b_i, c_i) are the coordinates of the spherical joint P in the body coordinate system $Ox_iy_iz_i$, A_i, B_i, C_i are principal central moments of inertia; $M_1M_2/(M_1 + M_2) = M$; M_i is the mass of the i th body; ω is the angular velocity for the center of mass of the two-body system moving along an elliptic orbit. Then we use the expressions for kinetic energy of the system in the case when $b_1 = b_2 = c_1 = c_2 = 0$ and the coordinates of the spherical joint P in the body coordinate systems are $(a_i, 0, 0)$ and when the motions of the two-body system are located in the plane of the elliptic orbit ($\alpha_1 \neq 0, \alpha_2 \neq 0, \beta_1 = \beta_2 = 0, \gamma_1 = \gamma_2 = 0, \dot{\alpha}_1 = d\alpha_1/dt, \dot{\alpha}_2 = d\alpha_2/dt$, where t is time) in the form [1]

$$\begin{aligned} T &= 1/2(B_1 + Ma_1^2)(\dot{\alpha}_1 + \omega)^2 + 1/2(B_2 + Ma_2^2)(\dot{\alpha}_2 + \omega)^2 \\ &- Ma_1a_2 \cos(\alpha_1 - \alpha_2)(\dot{\alpha}_1 + \omega)(\dot{\alpha}_2 + \omega). \end{aligned} \quad (1)$$

The force function, which determines the effect of the Earth gravitational field on the system of two connected by a joint bodies, is given by [1]

$$\begin{aligned} U &= -3\mu/(2\rho^3)((A_1 - C_1)\sin^2\alpha_1 + (A_2 - C_2)\sin^2\alpha_2) \\ &+ 3/2M\mu/\rho^3((a_1 \sin \alpha_1 - a_2 \sin \alpha_2)^2 + M\mu/\rho^3 a_1 a_2 \cos(\alpha_1 - \alpha_2)). \end{aligned} \quad (2)$$

Here ρ is a radial distance between the center of mass of the Earth C and center of mass of the system O ; $\mu = fM_0$, where f is a gravitational constant, and M_0

is the mass of the Earth; $\omega = \frac{d\vartheta}{dt} = \omega_0(1 + e \cos \vartheta)^2$; $\frac{\mu}{\rho^3} = \omega_0^2(1 + e \cos \vartheta)^3$; ϑ is the true anomaly and e is the orbital eccentricity. On the circular orbit $\omega = \omega_0$, $\frac{\mu}{\rho^3} = \omega_0^2$, $\vartheta = \omega_0 t$.

By using the kinetic energy expression (1) and the expression (2) for the force function, the equations of motion for this system can be written as Lagrange equations of the second kind in the form of a system of second-order ordinary differential equations in variables α_1 and α_2 [1]

$$\begin{aligned}
 & (B_1 + Ma_1^2)(\ddot{\alpha}_1 + \dot{\omega}) - Ma_1a_2(\ddot{\alpha}_2 + \dot{\omega}) \cos(\alpha_1 - \alpha_2) \\
 & - Ma_1a_2((\dot{\alpha}_2 + \omega)^2 - \mu/\rho^3) \sin(\alpha_1 - \alpha_2) \\
 & + 3\mu/\rho^3((A_1 - C_1 - Ma_1^2) \sin \alpha_1 + Ma_1a_2 \sin \alpha_2) \cos \alpha_1 = 0, \quad (3) \\
 & - Ma_1a_2(\ddot{\alpha}_1 + \dot{\omega}) \cos(\alpha_1 - \alpha_2) + (B_1 + Ma_1^2)(\ddot{\alpha}_2 + \dot{\omega}) \\
 & + Ma_1a_2((\dot{\alpha}_1 + \omega)^2 - \mu/\rho^3) \sin(\alpha_1 - \alpha_2) \\
 & + 3\mu/\rho^3((A_2 - C_2 - Ma_2^2) \sin \alpha_2 + Ma_1a_2 \sin \alpha_1) \cos \alpha_2 = 0,
 \end{aligned}$$

which determine the oscillations of the two-body system in the plane of the elliptic orbit in the orbital coordinate system. In (3), the dot denotes differentiation with respect to time t .

One can easily check that the system (3) has the stationary solution

$$\alpha_1 = \alpha_2 = 0. \quad (4)$$

Our goal is to obtain the periodic solution of the equations of motion (3) in the form of a power series in a small parameter e ($e \ll 1$) in the neighborhood of the stationary solution (4).

2. Periodic solutions

To perform the calculations we assume that the oscillations are small and replace the sine and cosine in (4) by their expansions in power series. Doing the substitution $dt = d\vartheta/(\omega_0(1 + e \cos \vartheta)^2)$ in (3) we change the independent variable from t to ϑ and reduce the system to the form

$$\begin{aligned}
 & - (1 + e \cos \vartheta)\alpha_2'' + 2e\alpha_2' \sin \vartheta + (B_1 + Ma_1^2)/(Ma_1a_2)((1 + e \cos \vartheta)\alpha_1'' \\
 & - 2e\alpha_1' \sin \vartheta) - e(1 + e \cos \vartheta)(\alpha_2' + 1)^2 + e(2 \sin \vartheta(1 - (B_1 + Ma_1^2)/Ma_1a_2) \\
 & + (4 + 3((A_1 - C_1) - Ma_1^2)/(Ma_1a_2))) = 0, \quad (5) \\
 & - (1 + e \cos \vartheta)\alpha_1'' + 2e\alpha_1' \sin \vartheta + (B_2 + Ma_2^2)/(Ma_1a_2)((1 + e \cos \vartheta)\alpha_2'' \\
 & - 2e\alpha_2' \sin \vartheta) + e(1 + e \cos \vartheta)(\alpha_1' + 1)^2 + e(2 \sin \vartheta(1 - (B_2 + Ma_2^2)/Ma_1a_2) \\
 & + (2 + 3((A_2 - C_2) - Ma_2^2)/(Ma_1a_2))) = 0.
 \end{aligned}$$

The prime in (5) denotes differentiation with respect to ϑ . It is possible to check that a general solution of nonlinear system (5) cannot be found in analytic form. It is convenient for application of the perturbation techniques [11] and symbolic

algorithms proposed in paper [12, 13]. However, we can seek for an approximate solution in the form of power series in the small parameter e :

$$\alpha_i(\vartheta) = e\alpha_i^{(1)}(\vartheta) + e^2\alpha_i^{(2)}(\vartheta) + \dots, \quad (6)$$

Computation of unknown functions $\alpha_i(\vartheta)$ in (6) is done in accordance with the techniques proposed in [11] and [12, 13] requires quite tedious symbolic computations. In this paper symbolic computations are performed using Wolfram Mathematica [14] functions: TrigExpand, Series, Normal, Replace, DSolve, NDSolve.

Substituting (6) into (5) and collecting coefficients of equal powers of e , we obtain the set of systems of linear differential equations which can be solved in succession. For example, using in (6) only the first linear elements we obtain the corresponding periodic solutions in the form

$$\alpha_1^{(1)}(\vartheta) = \bar{a}_1\sin(\vartheta) + \bar{b}_1\cos(\vartheta), \quad \alpha_2^{(1)}(\vartheta) = \bar{a}_2\sin(\vartheta) + \bar{b}_2\cos(\vartheta), \quad (7)$$

where the coefficients $\bar{a}_1, \bar{b}_1, \bar{a}_2, \bar{b}_2$ can be defined from the linear algebraic system. The amplitudes of the oscillations of the first and the second bodies have the expressions

$$\begin{aligned} R_1^2 &= (\bar{a}_1^2 + \bar{b}_1^2)e^2 = 4\frac{e^2b^2}{d^2}, \\ R_2^2 &= (\bar{a}_2^2 + \bar{b}_2^2)e^2 = 4\frac{e^2\bar{b}^2}{d^2}, \end{aligned} \quad (8)$$

where

$$\begin{aligned} b &= (B_1 + Ma_1(a_1 - a_2))(3(A_2 - C_2) - B_2) - 4Ma_2(a_1B_2 + a_2B_1), \\ \bar{b} &= (B_2 + Ma_2(a_1 - a_2))(3(A_1 - C_1) - B_1) - 4Ma_1(a_1B_2 + a_2B_1), \\ d &= (3(A_1 - C_1) - B_1)(3(A_2 - C_2) - B_2) - 4Ma_1^2(3(A_2 - C_2) - B_2) \\ &\quad - 4Ma_2^2(3(A_1 - C_1) - B_1). \end{aligned} \quad (9)$$

In the present work, we have considered the first approximation of the planar oscillations of a system of two bodies connected by a spherical joint that moves along an elliptic orbit. We have found the expressions of the periodic motion of the system in the linear approximation. All the relevant computations in this work are performed with the computer algebra system Wolfram Mathematica [14]. At the next steps we plan to construct the quadratic and cubic approximation of the periodic solutions which have very cumbersome expressions.

References

- [1] Sarychev, V.A.: Problems of orientation of satellites, Itogi Nauki i Tekhniki. Ser. Space Research, Vol. 11. VINITI, Moscow (1978) (in Russian)
- [2] Rauschenbakh, B.V., Ovchinnikov, M.Yu., McKenna-Lawlor, S.: Essential Spaceflight Dynamics and Magnetospherics. Kluwer Academic Publishers (2003)

- [3] Gutnik, S.A., Sarychev, V.A.: Symbolic computations of the equilibrium orientations of a system of two connected bodies moving on a circular orbit around the Earth. *Math. Comput. Sci.* **15**(2), 407–417 (2021)
- [4] Sarychev, V.A.: Relative equilibrium orientations of two bodies connected by a spherical joint on a circular orbit. *Cosmic Research* **5**, 360–364 (1967)
- [5] Gutnik, S.A., Sarychev, V.A.: Symbolic methods for studying the equilibrium orientations of a system of two connected bodies in a circular orbit. *Programming and Computer Software* **48**(2), 73–79 (2022)
- [6] Gutnik, S.A., Sarychev, V.A.: Computer algebra methods for searching the stationary motions of the connected bodies system moving in gravitational field. *Math. Comput. Sci.* **16**, 1–15 (2022)
- [7] Sarychev, V.A., Mirer, S.A., Sazonov, V.V.: Plane oscillations of a gravitational system satellite-stabilizer with maximal speed of response. *Acta Astronaut.* **3**(9-10), 651–669 (1976)
- [8] Zlatoustov, V.A., Markeev, A.P.: Stability of planar oscillations of a satellite in an elliptic orbit. *Celest. Mech.* **7**(1), 31–45 (1973)
- [9] Penkov, V.I.: Compensation for eccentric oscillations of a satellite with a gravitational stabilization system. *Cosmic Research* **15**(3), 376–383 (1977)
- [10] Clark, J.P.C.: Response of a two-body gravity gradient system in a slightly eccentric orbit. *J. Spacecraft and Rockets.* **7**(3), 294–298 (1970)
- [11] Nayfeh, A.H.: *Introduction to Perturbation Techniques*. John Wiley and Sons, New York (1993)
- [12] Prokopenya, A.N.: Symbolic computation in studying stability of solutions of linear differential equations with periodic coefficients. *Programming and Computer Software* **33**(2), 60–66 (2007)
- [13] Prokopenya, A.N.: Construction of a periodic solution to the equations of motions of generalized Atwood’s machine using computer algebra. *Programming and Computer Software* **46**(2), 120–125 (2020)
- [14] Wolfram, S.: *An elementary introduction to the Wolfram Language*. 2nd ed. Champaign, IL, USA, Wolfram media (2017)

Sergey A. Gutnik
 76, Prospekt Vernadskogo, 119454
 Department of Mathematics, Econometrics and Informatics
 MGIMO University
 Moscow, Russia
 e-mail: s.gutnik@inno.mgimo.ru

Numerical-analytical approach to the study of resonant structures of nearplanetary orbital spaces

Tomilova I.V., Bordovitsyna T.V., Aleksandrova A.G.,
Blinkova E.V. and Popandopulo N.A.

Abstract. A numerical and analytical method for studying the resonant structures of nearplanetary spaces and the results of its application to the construction of such structures for the Earth and the Moon are presented.

Introduction

The idea of joint use of analytical and numerical approaches in the analysis of resonances in dynamic systems was first expressed by B.V. Chirikov [1]. And in problems of celestial mechanics, this idea was first applied in works [2, 3] devoted to the dynamics of objects in GPS systems and the developed GALILEO system.

1. Research methodology

Numerical modeling is used to calculate the orbital evolution of objects over a selected time interval. The software package "Numerical model of the motion of satellite systems" is used. The latest version of software package is described in [4]. The software package is implemented in a parallel computing environment on the supercomputer "SKIF Cyberia" of Tomsk State University.

Numerical modeling allows us to obtain an array of position vectors and osculating orbital elements of all objects under consideration at given moments in time. For the same moments in time, the values of the fast Lyapunov characteristic MEGNO. The components of the frequency basis are determined using numerical and analytical approaches [5].

Formulas for searching for resonance characteristics are found using analytical methods. Formulas for searching for resonance characteristics are found using analytical methods.

Resonance (critical) arguments and resonance relations for orbital (tesseral) resonances are formed using the technique proposed by R. Alan [6, 7], refined by E. D. Kuznetsov [8] for resonance 1:3 and generalized in [9].

To obtain the characteristics of secular and semi-secular resonances, the technique proposed by J. Cook [10] is used. These characteristics are extracted from the argument of the once and twice averaged perturbing function. In our work, we considered the following types of secular (table 1 in [9]) and semi-secular (table 2 in [9]) resonances.

Secular frequencies in satellite motion are calculated both by numerical modeling [11] and by well-known analytical formulas.

2. Results

Using the methodology described above, extensive numerical and analytical experiments were carried out to analyze the resonant structures of near-Earth space (NES) and near-Lunar space (NLS).

The dynamics of NES objects was analyzed in the range of semimajor axes from 8000 to 315000 km with a step of 200 km and inclinations from 0 to 180° with a step of 5°, and an initial eccentricity equal to 0.001.

In this case, disturbances from harmonics of the geopotential up to 10th order and degree were taken into account, as well as disturbances from the Moon and the Sun. Together with the equations of motion, the equations of the parameters of MEGNO, designed to identify chaos in the dynamics of objects, were integrated.

The dynamics of objects in the regions of orbital resonances 1:1 – 1:11 in the direction of decreasing semi-major axis of the satellite’s orbit, as well as 2:1 and 3:1 in the direction of its increase, are examined in detail.

A comparison of the features of the evolution of objects in the non-resonance zone with the evolution of objects moving in the orbital resonance zones showed that the movement in the resonant zones is more chaotic.

If in a non-resonant zone the phenomenon of chaotic movement is rarely observed, then for resonant zones it is a characteristic property. The determining factor in the occurrence of chaos in the movement of objects is the presence in the dynamics of unstable components of the orbital resonance.

The influence of orbital resonance on the occurrence of chaoticity is so great that chaoticity manifests itself even in cases where all components of orbital resonance have circulating resonant arguments, but the resonance ratios repeatedly pass through zero values and all other sources of chaotic occurrence are absent.

The contribution of secular resonances to the emergence of chaos in resonant zones is secondary, but they have an impact on the orbital evolution, which is manifested by an increase in the amplitudes of long-period oscillations of positional variables.

This applies, first of all, to secular resonances of the first order: apsidal geometric resonance of the Lidov–Kozai type $\dot{\underline{\psi}} = \dot{\omega} \approx 0$ and nodal resonance $\dot{\underline{\psi}} = (\dot{\Omega} - \dot{\Omega}'_{S,L}) \approx 0$.

It should be noted that the zone in which the influence of the Lidov–Kozai type resonance is manifested extends along the semi-major axis from 20,000 km to 260,000 km in the region of forward motion and up to 100,000 km in the region of reverse motion. And in terms of inclination, the zone occupies an area from 60 to 120° in the interval of semi-major axes from 20,000 km to 100,000 km; above these values, it is present mainly in the zone of direct movement and is concentrated around an inclination of 90°.

As for the nodal resonance, it appears near inclinations of 0, 90 and 180°, and near inclinations of 0 and 180° – in the range of semi-major axes from 10,000 km to 250,000 km, and in the vicinity of 90° from 10,000 to 110,000 km.

Resonances with the average motion of the third body are present only in low orbits and their influence is insignificant.

It is interesting to note that in the dynamics of objects, the superposition of several stable secular resonances does not lead to the appearance of chaos, and on the contrary, the combined action of stable and unstable secular resonances causes the appearance of chaos in the movement of an object.

To study the dynamic structure of the near-Lunar orbital space using the software "Numerical model of the motion of artificial lunar satellites", the motion of 5180 objects was simulated over a 10-year time interval. The initial position of each satellite was characterized by a circular orbit and its own values of semi-major axis and inclination. The elements a and i were varied in incremental and 5-degree incremental ranges $a \in [1.1R_L; 15R_L]$ with a step of $0.1R_L$ and $i \in [0; 180^\circ]$ with a step of 5°.

The following results were obtained: the short lifetime of objects in low orbits is explained by the direct influence of the complex gravitational field of the Moon; there are no orbital resonances in the motion of the moon's satellites, and semi-secular resonances are still unstable. Thus, the main resonant factor in the motion of the lunar satellites are secular apsidal-nodal resonances, and the Lidov–Kozai type resonance and low-order nodal resonances have the greatest influence.

The Lidov–Kozai type resonance extends in a wide band across the entire considered region of cislunar space in the inclination range from 55 to 110°. Nodal resonance also runs through the entire region and clusters around $i = 90^\circ$.

As was shown in [12] for the 1:1 orbital resonance, the influence of light pressure leads to the appearance of secondary orbital resonances, the areas of action of which above and below along the semimajor axis cover the area of action of the main resonance. Our numerical and analytical modeling allows us to state that all components of all considered orbital resonances have secondary analogues, which leads to a significant expansion of the bands of orbital resonances.

Conclusion

Thus, the numerical-analytical technique makes it possible to obtain a large number of interesting and useful results in the study of resonant structures of near-planetary orbital spaces.

This work was supported by the Russian Science Foundation (Scientific Project No 19-72-10022), <https://rscf.ru/en/project/19-72-10022/>.

The review report was prepared within the state assignment of Ministry of Science and Higher Education of the Russian Federation (theme No. FSWM-2024-0005).

References

- [1] Chirikov B.V., *Nonlinear resonance*. Tutorial. Novosibirsk, NSU, 1977, P. 82.
- [2] Chao, C. and Gick, R., *Long-term evolution of navigation satellite orbits*, Adv. Space Res., 2004, V. 34, pp. 1221–1226.
- [3] Rossi, A., *Resonant dynamics of medium earth orbits: space debris*, Celest. Mech. Dyn. Astron., 2008, V. 100, pp. 267–286.
- [4] Aleksandrova A.G., Avdyushev V.A., Popandopulo N.A., Bordovitsyna T.V., *Numerical Modeling of Motion of Near-Earth Objects in a Parallel Computing Environment*, Russ. Phys. J., V. 64, Iss. 8, p.1566-1575.
- [5] Popandopulo N.A., Aleksandrova A.G., Bordovitsyna T. V., *To the Substantiation of a Numerical-Analytical Method for Revealing Secular Resonances*, Russ. Phys. J., 2022, V. 65, Is. 6, p.959-965
- [6] Allan, R.R., *Resonance effects due to the longitude dependence of the gravitational field of a rotating primary*, Planet. Space Sci., 1967a, vol. 15, pp. 53–76.
- [7] Allan, R.R., *Satellites resonance with the longitude dependent gravity. II. Effects involving the eccentricity*, Planet. Space Sci., 1967b, vol. 15, pp. 1829–1845.
- [8] Kuznetsov E.D., Zakharova P.E., Glamazda D.V., Shagabutdinov A.I., Kudryavtsev S.O., *Light pressure effect on the orbital evolution of objects moving in the neighborhood of low-order resonances*, Sol. Syst. Res., 2012, V. 46, No 6, P. 442–449.
- [9] Tomilova, I.V., Blinkova, E.V., and Bordovitsyna, T.V., *Features of the dynamics of objects moving in the neighborhood of the 1:3 resonance with the Earth's rotation*, Sol. Syst. Res., 2019, V. 53, no. 5, pp. 307-321.
- [10] Cook, G.E., *Luni-solar perturbations of the orbit of an Earth satellite*, Geophys. J., 1962, V. 6, no. 3, pp. 271–291.
- [11] Aleksandrova, A.G., Bordovitsyna, T.V., Popandopulo, N.A., Tomilova, I.V. *A New Approach to Calculation of Secular Frequencies in the Dynamics of Near-Earth Objects in Orbits with Large Eccentricities*, Russ. Phys. J., 2020, V. 63, Is. 1, p.64-70.
- [12] Valk, S., Delsate, N., Lemaitre, A., and Carletti, T., *Global dynamics of high area-to-mass ratios GEO space debris by means of the MEGNO indicator*, Adv. Space Res., 2009, V. 43, no. 7, pp. 1509–1526.

Tomilova I.V.
Scientific Research Institute of Applied Mathematics and Mechanics
National Research Tomsk State University
Tomsk, Russia
e-mail: irisha_tom@mail.ru

Bordovitsyna T.V.
Scientific Research Institute of Applied Mathematics and Mechanics
National Research Tomsk State University
Tomsk, Russia
e-mail: bordovitsyna@mail.ru

Aleksandrova A.G.
Scientific Research Institute of Applied Mathematics and Mechanics
National Research Tomsk State University
Tomsk, Russia
e-mail: aleksandrovaannag@mail.ru

Blinkova E.V.
Scientific Research Institute of Applied Mathematics and Mechanics
National Research Tomsk State University
Tomsk, Russia
e-mail: zbizk322@mail.ru

Popandopulo N.A.
Scientific Research Institute of Applied Mathematics and Mechanics
National Research Tomsk State University
Tomsk, Russia
e-mail: nikas.popandopulos@gmail.com

A non-dissipative tidal evolution of stellar inclination axis in eccentric inclined close binary systems

Pavel Ivanov

Abstract. In this contribution I introduce a new effect of the non-dissipative tidal evolution of stellar rotational axis in inclined eccentric binary systems containing a distributed star and a point-like component. This effect is analogous to the well-known von Zeipel-Kozai-Lidov effect, but, in our case there is no need for a third perturbing body. The effect was discovered in our work together with J. C. B. Papaloizou in 2021 and its theory was later developed in 2023.

Introduction

Tidal interactions play an extremely significant role in the evolution and dynamics of close binary systems and systems containing “Hot” and “Warm Jupiters”. Despite the almost 150-year history of quantitative researches in this area, the complexity of phenomena associated with tides still opens up room for an opportunity to find qualitatively new effects. In particular, in our work [1] we showed that there is a possibility of the evolution of the angle between rotation axis of one of the binary components and the normal to the orbital plane (the inclination angle) due to non-dissipative processes associated with tides. Physically, this possibility arises due to misalignment of the symmetry axis of the tidal bulge and the axis directed to the gravitating center induced by rotation. The corresponding torque leads to the evolution of the inclination angle. This effect operates when the axis of rotation is inclined relative to the orbital plane, and the orbit has a non-zero eccentricity. It turns out that the rate of change of the inclination angle is determined by the rate of precession of the apsidal line. In our subsequent work [2], [3], we examined the evolution of the apsidal line due to all potentially important factors operating in an isolated binary system - tides, the Einstein precession and the effects determined by oblateness of the rotating star. The second component of the system was treated as a point-like source of gravity. It was shown, that in the case when the various terms in the equation describing the evolution of the apsidal line almost cancel

each other (the so-called evolution near a “critical line”), in addition to the effect of non-dissipative tidal evolution of the stellar rotational axis there must be another qualitatively new effect - instead of the usual, uniform evolution of the apsidal line it librates around an equilibrium value. These effects can be observed in three types of astronomical systems, at least, - in close binary systems with an observed anomalous change of the apsidal line, in systems containing neutron stars, where the orbital inclination and eccentricity can be formed during a supernova explosion (e.g. GX-301-2) and the subsequent kick of the compact component, and in systems containing "Warm Jupiters" on inclined eccentric orbits. In the latter case, the effect can be significant when the planet's axis of rotation is inclined, and it can potentially be used to find the angle of inclination and rotational frequency of a planet with suitable orbital parameters. A preliminary analysis of the parameter space of the problem was carried out in order to find a region corresponding to the librational dynamics and it was shown that this region is rather large in the case of a sufficiently large eccentricity of the system (say, the eccentricity e is larger than or of the order of 0.5), and the mass ratio is larger than or of the order of unity. Observational detection of this effect would allow one to exploit new methods of determining of the orbital parameters of the systems, it would also provide some additional information about the internal structure of the distributed stars.

Conclusion

We introduced the new effect of non-dissipative tidal evolution of the inclination angle, which may also lead to librations of the apsidal line. We also pointed out a few of potentially interesting systems, where this effect may take place.

References

- [1] P. B. Ivanov, J. C. B. Papaloizou, *Monthly Notices of the Royal Astronomical Society*, 500, 3335, 2021.
- [2] P. B. Ivanov, J. C. B. Papaloizou, *Monthly Notices of the Royal Astronomical Society*, 526, 3352, 2023.
- [3] P. B. Ivanov, J. C. B. Papaloizou, *Astronomical Reports*, 67, 911, 2023.

Pavel Ivanov
Department of theoretical astrophysics and cosmology
PN Lebedev Physical Institute
Moscow, Russia
e-mail: pavel1000astrophysics@gmail.com

Constructing the Secular System in the Three–Axial Moon’s Rotation Theory in the Trigonometric Form

Tamara Ivanova.

The combined secular system for the evolution parameters of the orbits of the eight major planets and the Moon and the rigid–body rotation of the three–axial Moon is constructed by the method of the General Planetary Theory (GPT) [1] in the trigonometric form without secular and mixed terms. For that the techniques of the GPT and the Poisson Series Processor (PSP) [2] are used. The GPT is based on the ideas of separating the short–period and long–period terms variables and the Birkhoff’ normalizing transformation of the dynamical system. This method allows to reduce the equations of the translatory motion of the major planets and the Moon and the equations of the Earth’s rotation in Euler parameters to the secular system describing the evolution of the planetary and lunar orbits (independent of the Moon’s rotation) and the evolution of the Moon’s rotation (depending on the planetary and lunar evolution) and containing only the long–periodic terms. Therefore, the Moon’s rotation parameters are represented in the form of the GPT coordinates, i.e. in the form of the series in powers of the evolutionary variables with quazi–periodic coefficients with respect to the planetary-lunar mean longitudes.

References

- [1] Brumberg, V.A.: 1995, *Analytical Techniques of Celestial Mechanics*, Springer, Heidelberg
- [2] Ivanova, T.V.: 1995, “PSP: A New Poisson Series Processor”. In: *Dynamics, Ephemerides and Astrometry of the Solar System* (IAU Symposium 172, Paris, 1995, eds. S. Ferraz-Mello, B. Morando and J. -E. Arlot), 283, Kluwer

Tamara Ivanova.
Institute of Applied Astronomy of the Russian Academy of Sciences
Saint-Petersburg, Russian Federation
e-mail: itv@iaaras.ru

Transit trajectories of ballistic capture near libration points for low-energy transfers

Ivanyukhin A.V.

Abstract. One of the approaches to increase the efficiency of interplanetary transfers is the use of low-energy transit orbits, which have a small energy change during transit from one massive body to another. The paper considers an approach to the design of transit trajectories of ballistic capture based on invariant manifolds of libration points L1 and L2. To study transit trajectories and capture duration, an elliptical 3-body problem and an ephemeris 4-body problem are used. The influence of the masses of massive bodies and the eccentricity of the orbit of a smaller body on the ballistic capture and its duration is analyzed. The use of the ΔV impulse to change the velocity of the spacecraft at the libration point to change the plane of the transit trajectory is considered.

Introduction

To improve transfers in a system consisting of several massive bodies, it is necessary to purposefully use the dynamics of three- and four-body problems. This idea led to a new class of spacecraft (SC) flights – low-energy trajectories, in which the change in SC energy during transfer between massive bodies is minimal. One approach to their design is ballistic capture trajectories, which carry out the transit of the SC from one massive body to another. Such trajectories have already been implemented by the Hiten (JAXA), SMART-1 (ESA), Genesis and GRAIL (NASA), Danuri (KARI), etc.

Ballistic capture trajectories in the design of lunar missions began to be studied in the works of V.A. Egorov, V.G. Fesenkov, M.C. Davidson and others. The use of the four-body problem and the WSB (Weak Stability Boundary) trajectory proposed by E.A. Belbruno became important in the design of lunar trajectories.

We call capture the transition of a spacecraft to an orbit with a negative Keplerian energy of a massive body from the outer part of space.

1. The three-body problem

For studying the features of spacecraft motion in a system of two massive bodies, the most useful are the restricted circular and restricted elliptic three-body problems (RC3BP and RE3BP) [1].

The RC3BP analysis shows that transit from one massive body to another with minimal energy change occurs near the L1 and L2 libration points with near-zero velocity [1, 2], which corresponds to the minimal change in the Jacobi constant for the transfer.

Such transit trajectories can be obtained on the basis of stable and unstable invariant manifolds of libration points. Trajectories based on invariant manifolds are in the plane of motion of massive bodies, which determines the planes of satellite orbits that can be obtained from massive bodies without additional maneuvers to change the plane of the orbit. This is a disadvantage for their practical use. The plane (inclination) of the satellite's orbit can be changed by changing the SC's velocity at the libration point.

The capture duration and the suitable orbital parameters are important. The Jacobi integral, Tisserand's parameter and minimum velocity surface are used to study them [1, 3, 4].

In RE3BP, libration points are only a geometric concept and are not a solution in this model. That is, libration points have an instantaneous velocity corresponding to the pulsation of the coordinate system. The region of possible motions (zero velocity curves, Jacobi constant) and transit trajectories depend on the mass parameter of the problem, the eccentricity and the true anomaly of the small massive body [5, 6, 4].

An analysis of the system linearized in the vicinity of the libration point shows that transit at the libration point (with zero velocity in the pulsating coordinate system) is not possible at any moment in time, and depends on the true anomaly of the small body. And for transit, a suitable Jacobi constant is not enough. The correct velocity vector is also necessary [7].

The ranges of true anomaly that allow transit are in the vicinity of 90° and 270° , which correspond to the radial velocity maxima in the orbital coordinate system. In these cases, the transit has a different direction. For example, in the case of the Earth-Moon system for L1 with a true anomaly of $47.64^\circ - 132.90^\circ$, the transit is from the Moon to the Earth, and with $-47.64^\circ - -132.90^\circ$, from the Earth to the Moon [7, 8].

2. The four-body problem

To use these solutions in the perturbed ephemeris model, we will move from a rotating coordinate system associated with the barycenter of the system or the libration point to a stationary coordinate system associated with one of the massive bodies.

It is obvious that in the perturbed four-body model there will be a significant perturbation of the trajectories under consideration. The choice of the date of the libration point flight allows us to determine the transit trajectory formed by invariant manifolds that stays for a sufficiently long time near the small body. For example, for the Earth-Moon system, the duration of stay at the Moon during the flight of the L1 libration point on certain dates is more than 1000 days [7].

Conclusion

A method is proposed for determining the capture orbit near the libration points L1 and L2, based on their invariant manifolds. The analysis of ballistic capture trajectories based on invariant manifolds of libration points is carried out in models of restricted circular, elliptical and perturbed three-body problems. Such transit trajectories were investigated depending on the masses of the bodies and the eccentricity of the orbit in RE3BP. The possibility of determining the trajectories of ballistic capture by selecting the date of the libration point flyby and the velocity vector in the ephemeris model is shown.

Transit trajectories of this type make it possible to obtain ballistic capture orbits suitable for the implementation of low-thrust spacecraft. In particular, such examples in the Earth-Moon system were obtained in [7, 8], and the use of libration points for interplanetary transfers was considered in [9].

The study was supported by the Russian Science Foundation grant No 22-79-10206, <https://rscf.ru/project/22-79-10206/>.

References

- [1] V. Szebehely, *Theory of orbits. The restricted problem of three bodies*, Academic press, New York and London, 1967, p. 679.
- [2] C.C. Conley, *Low energy transit orbits in the restricted three-body problems*, SIAM Journal on Applied Mathematics. 1968. Vol. 16. No. 4. pp. 732-746.
- [3] K.V. Kholshchevnikov, V.B. Titov, *Minimal velocity surface in a restricted circular three-body problem*, Vestnik St. Petersburg University, Mathematics, 2020, Vol. 53, No. 4, pp. 473-479.
- [4] L.G. Luk'yanov, *Energy conservation in the restricted elliptical three-body problem*, Astronomy reports, 2005, Vol. 49, pp. 1018-1027.
- [5] N. Hyeraci, F. Topputo, *The role of true anomaly in ballistic capture*, Celestial Mechanics and Dynamical Astronomy, 2013, Vol. 116, pp. 175-193.
- [6] Z.F. Luo, *The role of the mass ratio in ballistic capture*, Monthly Notices of the Royal Astronomical Society, 2020, Vol. 498, No 1, pp. 1515-1529.
- [7] A.V. Ivanyukhin, V.V. Ivashkin, V.G. Petukhov, S.W. Yoon, *Designing Low-Energy Low-Thrust Flight to the Moon on a Temporary Capture Trajectory*, Cosmic Research, 2023, Vol. 61, No 5, pp. 380-393.

- [8] A.V. Ivanyukhin, V.V. Ivashkin, V.G. Petukhov, S.W. Yoon, *Low-energy lunar transfer design using high- and low-thrust on ballistic capture trajectories*, IAC-23-C1.9.7, Proceedings of the International Astronautical Congress, 74th International Astronautical Congress (IAC), Baku, Azerbaijan, 2023, p. 10.
- [9] S.W. Yoon, V.G. Petukhov, A.V. Ivanyukhin, *An approach for end-to-end optimization of low-thrust interplanetary trajectories using collinear libration points*, Acta Astronautica, 2024, Vol. 221, pp. 12-25.

Ivanyukhin A.V.

Research Institute of Applied Mechanics and Electrodynamics of Moscow Aviation institute

Peoples Friendship University of Russia (RUDN University)

Moscow, Russia

e-mail: ivanyukhin.a@yandex.ru

The case of János Sajnovics as a milestone in history of astronomy, the study of which was inspired by the lectures of Prof. K.V. Kholoshevnikov

Nikolai Kirsanov

Abstract. Prof. **K. V. Kholoshevnikov** presented to us the subject of celestial mechanics in his lectures in a very broad cultural context, which subsequently inspired me to study a number of disciplines related to language - and to think about how one could use the methods of the exact sciences in studying linguistic phenomena (the opposite seems somewhat more difficult, because, paraphrasing Auguste Comte, ok, we now know what the stars are made of, but we will never know what they are really called). Below I will present some considerations and cases from the history of celestial mechanics and linguistics, which it might be interesting to present in courses on the history of the corresponding disciplines.

1. Precession and Assibilation

Precession in astronomy and assibilation in linguistics, though seemingly unrelated, can both serve as valuable "clocks" for pinpointing historical events. Precession, the gradual shift in the orientation of Earth's axis, allows astronomers to date ancient observations by calculating the position of celestial objects at specific times in history. Similarly, assibilation, a phonological change where sounds like "k" or "g" evolve into "ch" or "j" sounds, can help linguists trace the evolution of languages and, by extension, the timelines of linguistic and cultural shifts.

By comparing these two phenomena, one can see how both serve as tools for reconstructing the past. Just as precession helps us understand the chronological context of ancient texts and artifacts by aligning them with specific celestial configurations, assibilation offers insights into the temporal layers of language development, revealing when particular phonetic changes occurred. By using these methods in tandem, we can more accurately place historical events within a broader

temporal framework, deepening our understanding of both human history and the natural world.

2. Lapland Expedition

János Sajnovics, a Hungarian Jesuit priest and scientist, made significant contributions by merging celestial mechanics with historical linguistics during an 18th-century expedition to Lapland. In 1768, Sajnovics joined an astronomical expedition led by Maximilian Hell to observe the transit of Venus. While in Lapland, Sajnovics became interested in the Sámi language, noting its similarities to Hungarian. His interdisciplinary approach led to the publication of "Demonstratio. Idioma Hungarorum et Lapponum idem esse" in 1770, where he provided evidence of the relationship between these languages. Sajnovics' work is notable for being one of the first instances where historical linguistics and celestial mechanics intersected in a single research context, illustrating the potential for interdisciplinary collaboration to enhance scientific understanding. His findings laid the groundwork for future research in Finno-Ugric linguistics and demonstrated the value of cross-disciplinary approaches in advancing scientific knowledge.

3. Intersection

Sajnovics' research during the Lapland expedition was one of the first instances where historical linguistics and celestial mechanics concretely intersected on the same scientific journey. This intersection was influenced by the following factors:

1. The Scientific Interdisciplinarity of the Expedition: Although the main goal of the expedition was astronomical, the scientists involved, like Sajnovics, were also interested in other scientific questions. This allowed for an interdisciplinary approach, where observations from natural sciences and humanistic studies were combined.

2. Cultural Encounter: The journey to Lapland provided Sajnovics with the opportunity to learn about Sámi culture and language. He observed significant similarities between the Sámi and Hungarian languages, particularly in basic vocabulary and grammatical structures. This led him to investigate the common origin of these languages, which is a fundamental question in historical linguistics.

3. Connections Between Disciplines: Sajnovics' work demonstrated that the boundaries between sciences are not absolute and that different fields of study can benefit from each other's methods and findings. His observations on the connections between the Sámi and Hungarian languages were an important step in the study of Finno-Ugric languages and helped to strengthen the theory of their relatedness.

4. Interdisciplinary Approach

János Sajnovics' journey to Lapland exemplifies how interdisciplinary approaches can unlock new methods for dating historical events, much like using precession in astronomy or assibilation in linguistics as a "clock." By observing and documenting the linguistic similarities between Sámi and Hungarian, Sajnovics not only advanced the study of Finno-Ugric languages but also laid the groundwork for using linguistic changes, such as assibilation, as temporal markers. Just as astronomers use precession to date ancient celestial observations, linguists can use phonological shifts to trace the evolution of languages and cultures, thereby refining our understanding of historical timelines.

In my presentation, I will also highlight a few more examples of how methods from celestial mechanics can be applied almost directly in historical linguistics, demonstrating the deep connections between these seemingly distinct fields.

Nikolai Kirsanov

Kantele, Finland

e-mail: nikolai@kirsanov.fi

On the Evolution of Asteroid Orbit in the Restricted Circular Three-Body Problem: External and Internal Cases, New Results

Pavel Krasilnikov and Alexander Dobroslavskiy

Abstract. The spatial circular restricted three-body problem in the nonresonant case is investigated. We apply Gaussian averaging to obtain averaged equations of motion in terms of osculating elements. A Keplerian ellipse with a focus at the main body (the Sun) is taken as an unperturbed orbit. We derive a twice-averaged disturbing function in the form of an explicit analytical series with coefficients that are expressed in terms of Gauss and Clausen hypergeometric functions. For a reduced system, phase portraits of oscillations in the plane of are shown in the fourth approximation. The radius of convergence of the power series for fixed values of Lidov-Kozai integral was investigated. It is shown that the power series is asymptotic in the sense of Poincaré in the regions of divergence. The asymptotic nature of the series allows the use of perturbation theory methods in regions of divergence, excluding uniformly close orbits. An estimate of the number of retained members of the series is obtained, which guarantees the reliability of constructing phase portraits.

Introduction

We investigate the classical problem of the Keplerian orbit evolution for a massless body in the gravitational field of two primaries (the Sun and Jupiter). This problem was first considered by Gauss in 1809. Zeipel [1] continued these studies by investigating Lindstedt series of solutions to the problem. A detailed study of Hill's case is contained in the articles [2, 3]. The main goal of the report is to obtain new results using modern information technologies.

1. Statement of the problem

We consider the circular spatial restricted three-body problem. Assume that a massless body (asteroid, or satellite) P is in the gravitational field of two primaries

moving in a circular orbit of radius r_J . The central body S (Sun) of mass m_S affects the asteroid with the force F_J , and the second body J (Jupiter) of mass m_J has a disturbing effect with the force F_J . Assume that the unperturbed trajectory of the satellite is a Keplerian ellipse with a focus at S , and its plane Π makes an angle of i with the plane Π_0 of motion of the attracting bodies (Fig. 1).

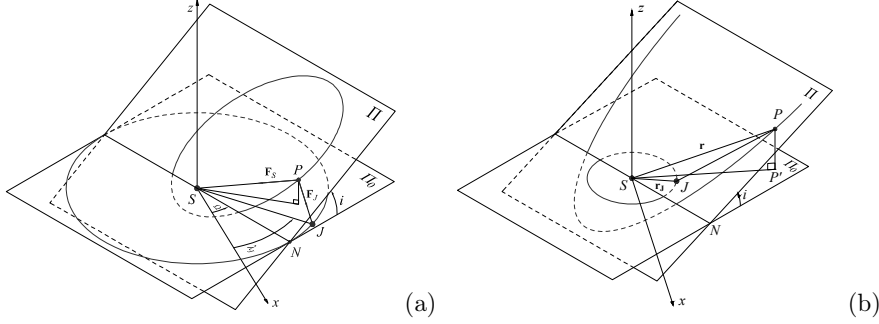


FIGURE 1. Internal (a) and external (b) cases

2. Averaged perturbation function

The perturbation functions of the problem and their twice averaging are the following:

| Internal case | External case |
|---|---|
| $R = \frac{fm_J}{r_J} \sum_{n=2}^{\infty} \left(\frac{r}{r_J}\right)^n P_n(\cos \gamma),$ | $R = \frac{fm_J}{r} \left(1 + \frac{r_J^3 - r^3}{r_J^2 r} + \sum_{n=2}^{\infty} \left(\frac{r_J}{r}\right)^n P_n(\cos \gamma)\right),$ |
| $R^{**} = \frac{fm_J}{r_J \sqrt{1-e^2}} \sum_{n=1}^{\infty} D_n \left(\frac{a}{r_J}\right)^{2n},$ | $R^{**} = \frac{fm_J}{a} \left(1 + \frac{1}{\sqrt{1-e^2}} \sum_{n=1}^{\infty} D_n \left(\frac{r_J}{a}\right)^{2n}\right),$ |
| $D_n = (1+e)^{2n+2} P_{2n}(0) \times$ $\left(F_{2,1} \left(\frac{1}{2}, 2n+2; 1; \frac{2e}{e-1} \right) \times$ $P_{2n}(0) P_{2n}(\cos i) +$ $2 \sum_{k=1}^n (-1)^k A_{2k}^{(2n)}(e, i) \cos 2k\omega \right).$ | $D_n = (1+e)^{1-2n} P_{2n}(0) \times$ $\left(F_{2,1} \left(\frac{1}{2}, 1-2n, 1; \frac{2e}{e-1} \right) \times$ $P_{2n}(0) P_{2n}(\cos i) +$ $2 \sum_{k=1}^n A_{2k}^{(2n)}(e, i) (-1)^k \cos 2k\omega \right).$ |

Here $r = \frac{a(1-e^2)}{1+e \cos \nu}$, γ is the angle between r_J and r , $P_n(\cos \gamma)$ is the Legendre polynomial, $F_{2,1}$ and $F_{3,2}^{reg}$ is the Gaussian and Clausen functions.

3. Phase portraits of oscillations in a reduced system

We have three first integrals of the evolution equations:

$$a = c_0, \quad (1 - e^2) \cos^2 i = c_1, \quad R^{**} = h$$

The reduced equations have the following

$$\frac{de}{dt} = -\frac{\sqrt{1-e^2}}{na^2e} \frac{\partial \hat{R}}{\partial \omega}, \quad \frac{d\omega}{dt} = \frac{\sqrt{1-e^2}}{na^2e} \frac{\partial \hat{R}}{\partial e}, \quad \hat{R} = R^{**}|_{(1-e^2) \cos^2 i = c_1}$$

Phase portraits of oscillations in the fourth approximation ($n = 4$) are shown in Fig.2

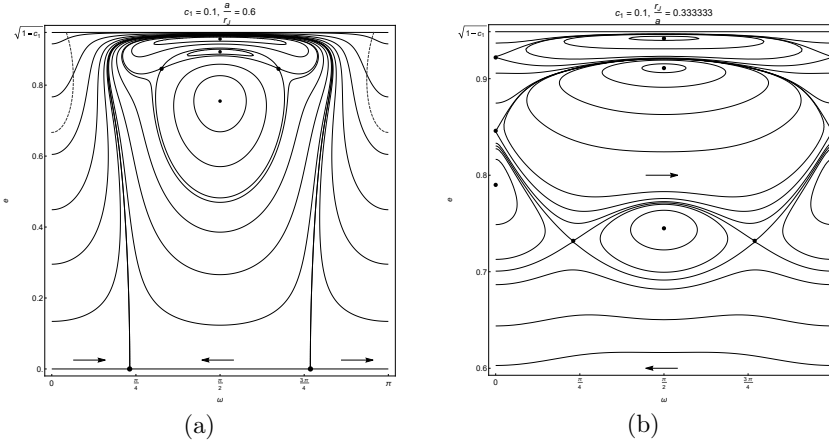


FIGURE 2. Phase portraits (a) internal case $c_1 = 0.1$, $a/r_J = 0.6$,
(b) external case $c_1 = 0.1$, $a/r_J = 0.333$

4. Convergence and divergence regions of power series of averaged perturbation function

The convergence radius of function $\hat{R}(a, e, \omega, c_1)$ is calculated using the Cauchy-Hadamard formula:

$$\rho(e, \omega, c_1) = \left(\overline{\lim}_{n \rightarrow \infty} \sqrt[n]{|D_n|} \right)^{-1}$$

The curves isolines $\rho(e, \omega, c_1) = const$ in plane (e, ω) for $c_1 = 0.1$ and $n = 100$ are shown in the following figures [4]. The power series of $\hat{R}(a, e, \omega, c_1)$ diverges above the curve $\rho(e, \omega, c_1) = \mu$ when μ is the parameter of expansion. Below this curve, the series converges.

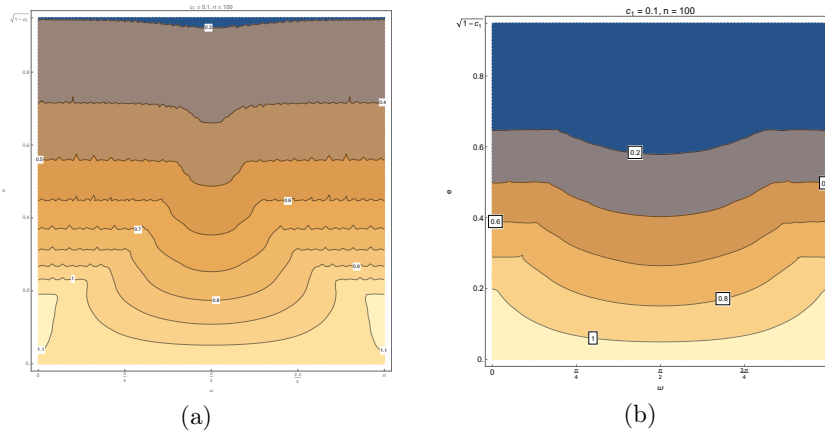


FIGURE 3. Convergence radius (a) internal case, (b) external case

5. On Poincaré asymptoticity of a power series

We investigated [4] the behavior of a power series in regions of divergence. It is shown numerically that this series is asymptotic in the sense of Poincaré, i.e.

$$\left\| \hat{R} - \hat{R}_k \right\| \sim O(\varepsilon^{k+1})$$

over a finite period of time where \hat{R}_k is partial sum of a series. Here k is the number of retained members of the series. It follows from the calculations that the partial sum of seventy terms approximates the function with high accuracy. The asymptotic nature of the series allows, using traditional methods of perturbation theory, to study the evolution of Keplerian orbital elements for all values of μ from the interval $[0, 1)$, excluding the case $\mu \approx 1$.

References

- [1] von Zeipel H. *Sur l'application des séries de M. Lindstedt a l'etude du mouvement des cometes periodiques*. Astronomische Nachrichten. 1910. V. 183. pp. 345–418. Available at <https://doi.org/10.1002/asna.19091832202>
- [2] Lidov M. L. *Evolution of the orbits of artificial satellites of planets as affected by gravitational perturbation from external bodies*. Artificial Earth Satellite. 1961. V. 8. pp. 5–45.
- [3] Kozai Y. *Secular perturbations of asteroids with high inclination and eccentricity*. Astronomical Journal. 1962. V. 67. No. 9. pp. 591–598.
- [4] Krasilnikov P. S. and Dobroslavskiy A. V. *On the Asymptotic Behavior of the Secular Perturbation Function in the Circular Restricted Three-Body Problem* Cosmic Research. 2024. V. 62. No. 3. pp. 266–275.

Pavel Krasilnikov
Department of Theoretical Mechanics and Mechatronics,
Moscow Aviation Institute (National Research University),
Moscow, Russia
e-mail: krasil06@rambler.ru

Alexander Dobroslavskiy
Department of Theoretical Mechanics and Mechatronics,
Moscow Aviation Institute (National Research University),
Moscow, Russia
e-mail: a.dobroslavskiy@gmail.com

On the paper of K.V. Kholshchevnikov about the exactness of epicyclic theory

H.A. Krayani and N.Y. Sotnikova

Abstract. This work briefly describes the paper of K.V. Kholshchevnikov devoted to Ptolemy's geocentric model. The author defends the originality and authenticity of Ptolemy's work and argues his point of view. He then lists the advantages of this model and establishes a theoretical limit of the accuracy of the ancient model in R^3 space. He shows how high they are and that the potential accuracy of Ptolemy's model is tens of times higher than the accuracy of real models up to Tycho Brahe.

References

- [1] K. V. Kholshchevnikov , *The exactness of epicyclic theory*. Studies in the History of Astronomy **24** ,181-191 (1994). (In Russian)

H.A. Krayani
Department of Astrophysics
St.Petersburg University
Higher School of International Educational Programs
Peter the Great St.Petersburg Polytechnic University
St.Petersburg, Russia
e-mail: huseinkrayani@hotmail.com

N.Y. Sotnikova
Department of Celestial Mechanics
St.Petersburg University
St.Petersburg, Russia
e-mail: nsot-astro@mail.ru

Semi-analytical theories of motion for the study of the dynamical evolution of planetary systems

Eduard Kuznetsov and Alexander Perminov

Abstract. We present the results of construction and use of semi-analytical theories of planetary motion initiated by Professor Konstantin Kholshevnikov. Theories of motion for two- and four-planet systems, as well as their applications to the study of long-period evolution, stability, and occurrences of chaos in the Solar System and extrasolar planetary systems are discussed. We announce the development of an eight-planet theory of motion and a version of the theory to account for mean-motion resonances.

Introduction

From the 18th century until the mid-20th century, all the theories of planetary motion needed for practice were constructed analytically by the small parameter method. In the early 20th century, Lyapunov and Poincaré established the convergence of the corresponding series for a sufficiently small time interval. Subsequently, K. Kholshevnikov estimated this interval to be on the order of several tens of thousands of years, which is in agreement with numerical experiments. The first works describing analytically (in the first approximation) the evolution on cosmogonic time scales appeared in the first half of the 19th century (Laplace, Lagrange, Gauss, Poisson). The averaging method was developed in the early 20th century based on these works. In the first half of the 20th century, the averaging method introduced by Gauss as an approximate one became an exact one, at least formally (the series were handled as polynomials), through the works by H. Zeipel, N.M. Krylov, and N.N. Bogolyubov. In the 1960s, G. Hori and, independently, A. Deprit suggested a method of Lie transforms. Detailed reviews of the works on the orbital evolution of Solar System major planets see in [6].

Powerful analytical and numerical methods have made significant progress in describing the orbital evolution of planetary systems. In this work we present the results of construction and use of semi-analytical theories of planetary motion initiated by Professor Konstantin Kholshevnikov. Theories of motion for two-

and four-planet systems, as well as their applications to the study of long-period evolution, stability, and occurrences of chaos in the Solar System and extrasolar planetary systems are discussed. We are also announcing the development of an eight-planet theory of motion and a version of the theory to account for mean-motion resonances.

1. Semi-analytical theory of motion of a two-planet system

The construction of the theory of planetary motion was carried out with the aim to study the evolution of solar-type planetary systems. We used the Jacobi coordinate system as the most suitable coordinate system for studying the evolution of planetary orbits [15]. The form of the Poisson expansion of the Hamiltonian in all elements was given in [4]. In [5], the expansion coefficients for the Hamiltonian of the two-planet Sun–Jupiter–Saturn problem were obtained using a simple algorithm reduced to the calculation of multiple integrals of elementary functions, the convergence domain was found, and the summation limits and the number of coefficients of the desired expansion were estimated. In [10], the expansions of the Hamiltonian of the two-planet problem into the Poisson series in all elements were constructed with the help of the PSP Poisson Series Processor [2].

We used the Hori–Deprit method to construct the averaged Hamiltonian of the two-planetary problem and the right-hand sides of the equations in average elements accurate to the third order of a small parameter, the generating function of the transform and the change of variables expressions to the second order of a small parameter [12]. Analytical transformations were performed with the help of the rational version of the echeloned Poisson series processor EPSP [3]. The evolution of the two-planet Sun–Jupiter–Saturn system was studied by numerically over 10 Gyr [11, 12].

The constructed theory was used to study the stability of planetary systems with respect to masses [7]. The study of Lagrange stability with respect to masses allows us to obtain upper limits for masses of extrasolar planets. In the Solar System, when the masses of Jupiter and Saturn increase by 20 times, these planets can have close approaches on a time scale of 1 Myr. Close approaches appear when analyzing osculating elements; they are absent in the mean elements. A similar situation takes place in the case of studied exoplanetary systems.

Our results established the bounds of applicability of the theorem that the area integral is conserved during averaging transformations: taking into account a finite number of terms in the series representing the averaged Hamiltonian, only one of the three components of the area vector is conserved, namely, the one corresponding to the longitudes measuring plane. We concluded that the non-conservation of the components σ_x and σ_y of the area integral is due to a failure to include small terms that are neglected when representing the averaged Hamiltonian in the form of a Poisson series.

We proposed the method for describing the resonance properties of planetary systems [8]. Our estimates of the resonance values of the semi-major axes and widths of resonance zones in relative units for characteristic values of the small parameter of the problem make it easy to classify and describe the resonance properties of planetary systems.

2. Enhancement of the semi-analytic theory of motion of the N -planet system

The development of the constructed semi-analytic theory became the theory of motion of four-planet systems [14]. The Hamiltonian expansion of the four-planetary problem into the Poisson series in elements of Poincaré second system is constructed up to third degree in the small parameter. The averaged Hamiltonian and the equations of motion in averaged Poincaré elements are constructed by the Hori–Deprit method up to third degree of the small parameter. The functions for the change of variables are obtained in second approximation and used for the transformation between osculating and averaged orbital elements. The transformations were performed analytically using the Piranha computer algebra system [1]. The constructed analytical equations of motion are applied to the study of the orbital evolution of the Solar System’s giant planets on long time scales. The amplitudes and periods of the planetary motion are in good agreement with numerical theories. The investigation of the dynamical evolution of the chosen extrasolar planetary systems was performed in the framework of the theory of motion of the second order in planetary masses [13].

The next stage in the development of the semi-analytic theory of planetary motion is the construction of the eight-planet theory of motion and a version of the theory to account for mean-motion resonances.

Conclusion

Productive ideas on the development of the semi-analytical theory of the N -planet problem laid down by Professor Konstantin Kholshchevnikov continue to be realised in new versions of the theory, bringing new scientific results.

The study was supported by the Russian Ministry of Science and Higher Education via the State Assignment Project FEUZ-2020-0038.

References

- [1] F. Biscani, *The Piranha computer algebra system*, 2019, <https://github.com/bluescarni/piranha>
- [2] T.V. Ivanova, *Poisson Series Processor (PSP)*, Preprint of Institute of Theoretical Astronomy, Russian Academy of Sciences, St. Petersburg, 1997, No. 64.

- [3] T. Ivanova, *A New Echeloned Poisson Series (EPSP)*, *Celest. Mech. Dyn. Astron.*, 2001, Vol. 80, pp. 167–176.
- [4] K.V. Kholoshevnikov, A.V. Greb, and E.D. Kuznetsov, *The Expansion of the Hamiltonian of the Planetary Problem into the Poisson Series in All Keplerian Elements (Theory)*, *Sol. Syst. Res.*, 2001, Vol. 35, pp. 243–248.
- [5] K.V. Kholoshevnikov, A.V. Greb, and E.D. Kuznetsov, *The Expansion of the Hamiltonian of the Two-Planetary Problem into a Poisson Series in All Elements: Estimation and Direct Calculation of Coefficients*, *Sol. Syst. Res.*, 2002, Vol. 36, pp. 68–79.
- [6] K.V. Kholoshevnikov and E.D. Kuznetsov, *Review of the Works on the Orbital Evolution of Solar System Major Planets*, *Sol. Syst. Res.*, 2007, Vol. 41, pp. 265–300.
- [7] K.V. Kholoshevnikov and E.D. Kuznetsov, *Stability of planetary systems with respect to masses*, *Celest. Mech. Dyn. Astron.*, 2011, Vol. 109, pp. 201–210.
- [8] E.D. Kuznetsov, *Resonance Properties of Extra-Solar Two-Planet Systems*, *Astron. Rep.*, 2010, Vol. 54, pp. 550–561.
- [9] E.D. Kuznetsov, *The Conservation of Area Integrals in Averaging Transformations*, *Astron. Rep.*, 2010, Vol. 54, pp. 562–569.
- [10] E.D. Kuznetsov and K.V. Kholoshevnikov, *Expansion of the Hamiltonian of the Two-Planetary Problem into the Poisson Series in All Elements: Application of the Poisson Series Processor*, *Sol. Syst. Res.*, 2004, Vol. 38, pp. 147–154.
- [11] E.D. Kuznetsov and K.V. Kholoshevnikov, *Dynamical Evolution of Weakly Disturbed Two-Planetary System on Cosmogonic Time Scales: the Sun–Jupiter–Saturn System*, *Sol. Syst. Res.*, 2006, Vol. 40, pp. 239–250.
- [12] E.D. Kuznetsov and K.V. Kholoshevnikov, *Orbital evolution of two-planetary system the Sun–Jupiter–Saturn*, *Vestnik St. Petersburg University, Ser. 1*, 2009, Iss. 1, pp. 139–149.
- [13] A.S. Perminov and E.D. Kuznetsov *Orbital evolution of the extrasolar planetary systems HD 39194, HD 141399, and HD 160691*, *Astron. Rep.*, 2019, Vol. 63, pp. 795–813.
- [14] A. Perminov and E. Kuznetsov *The orbital evolution of the Sun–Jupiter–Saturn–Uranus–Neptune system on long time scales*, *Astrophysics and Space Science*, 2020, V. 365, Id. 144, 21 p.
- [15] M.F. Subbotin, *Vvedenie v teoreticheskuyu astronomiyu (An Introduction into Theoretical Astronomy)*, Moscow: Nauka, 1968.

Eduard Kuznetsov
 Dept. of Astronomy, Geodesy, Ecology and Environmental Monitoring
 Ural Federal University
 Yekaterinburg, Russia
 e-mail: eduard.kuznetsov@urfu.ru

Alexander Perminov
 Dept. of Astronomy, Geodesy, Ecology and Environmental Monitoring
 Ural Federal University
 Yekaterinburg, Russia
 e-mail: alexander.perminov@urfu.ru

On the algebraic properties of difference approximations of Hamiltonian systems

Mikhail Malykh, Lubov' Lapshenkova and Marina Konyaeva

Abstract. We consider difference approximations of dynamic systems with a polynomial Hamiltonian that define birational correspondences between the initial and final positions of the system.

1. Introduction

One of mathematical models most widespread in celestial mechanics is a dynamic system described by a Hamiltonian system of ordinary differential equations. In applications, the Hamiltonian is often a polynomial or an algebraic function of coordinates q_1, \dots, q_n and momenta p_1, \dots, p_n . As a rule, from physical reasons a few integrals of motion are known, but they are not sufficient to reduce the system of differential equations to Abel quadratures.

Unable to reduce the system to quadratures, we are forced to solve it numerically. Having solved the many-body problem using the explicit Runge-Kutta method, we can only sadly watch as the mechanical energy of the system changes, and closed trajectories turn out to be open.

In the 1990s, the concept of geometric integrators emerged, i.e. numerical methods that in some sense inherit the analytical properties of the original Hamiltonian system. Historically, the first approach to designing difference schemes was proposed, in which the transition from one time layer to another is carried out using a canonical transformation. Such difference schemes were called symplectic. The simplest example of a symplectic scheme is the midpoint scheme.

This scheme perfectly imitates a Hamiltonian system with a quadratic Hamiltonian, for example, a harmonic oscillator with Hamiltonian $H = p^2 + q^2$. According to Cooper's theorem, the energy integral is preserved exactly in the scheme, and the approximate solution itself is a sequence of points $\mathfrak{x}_n = (p_n, q_n)$ of the circle

$p^2 + q^2 = C$. Each step of the approximate solution is a rotation by an angle

$$\Delta u = \int_{r_n}^{r_{n+1}} \frac{dq}{\sqrt{C - q^2}},$$

which does not depend on n [1]. Thus, even in calculations with a very coarse time step, energy is conserved exactly, and the motion occurs along closed trajectories.

However, in the nonlinear case, the conservation of symplecticity does not entail the inheritance of other properties of the original Hamiltonian system. What principles should be used as the basis for the design of difference schemes that imitate Hamiltonian systems with a polynomial Hamiltonian?

2. Conservative schemes

The obvious approach is to abandon symplecticity in favor of the exact preservation of all algebraic integrals.

In [2] we introduced additional variables for the many-body problem, namely distances and reciprocal distances between bodies, and wrote down a system of differential equations with respect to the coordinates, velocities, and the additional variables. In this case, the system lost its Hamiltonian form, but all the classical integrals of motion of the many-body problem under consideration, as well as new integrals describing the relationship between the coordinates of the bodies and the additional variables are described by linear or quadratic polynomials in these new variables. Therefore, any symplectic Runge–Kutta scheme preserves these integrals exactly.

Ten classical integrals are sufficient to reduce the two-body problem to quadratures. However, as our computer experiments have shown, preserving them in the difference scheme is not sufficient for the points of the approximate solution to lie on an ellipse (or at least on a closed curve). Thus, preserving the integrals of motion also does not entail inheriting other properties of the original Hamiltonian system.

3. Kahan's Method and the Cubic Hamiltonian

From general considerations, it follows that any mechanical system should define a one-to-one correspondence between the initial and final positions of the system. In order to construct a difference scheme that imitates this property, we can try to approximate the original Hamiltonian system by equations that define a birational correspondence between the points \mathbf{r} and $\hat{\mathbf{r}}$.

It is easy to see that this can always be done for systems with a cubic Hamiltonian, using a method that arose in the field of solitons [3]; some authors associate it with the name of W. Kahan, others with the names of Hirota and Kimura

[4, 5]. We came to it when searching for a discrete analogue of the Painlevé theory [6, n. 3.2].

A Hamiltonian system with a cubic Hamiltonian is reduced to a quadrature

$$\int \frac{dq}{H_p} = t,$$

and the differential dq/H_p is an integral of the first kind on the elliptic curve $H(p, q) = C$, which is inverted in elliptic functions. After the Kahan discretization, the energy integral is inherited [4] and therefore the points of the approximate solution also lie on some elliptic curve, and the scheme itself can be written as a quadrature

$$\Delta u = \int_{\mathfrak{r}_n}^{\mathfrak{r}_{n+1}} v dq,$$

where $v dq$ is again an elliptic integral of the first kind [7]. Thus, the Kahan difference scheme inherits both the form of the trajectory (a closed elliptic curve), and the quadrature, and even the possibility of representing the solution as a meromorphic function of time [7]. The symplectic structure is not preserved exactly, but is inherited [4]. Thus, Kahan's method allows imitating an elliptic oscillator to the same extent as the midpoint scheme allows imitating a linear oscillator.

The subtlety is that when designing the difference scheme we have included a property that is not present in the original Hamiltonian system, but which should be present in any mechanical system from general considerations. The point is that in the nonlinear case the general solution of the elliptic oscillator defines a birational transformation on the integral curve $H(p, q) = C$, which does not extend to a birational transformation of the entire phase space pq . Using Kahan's method we approximate this solution by a birational transformation of the entire space, for which we correct the integral curve, preserving its genus. Thus, Kahan's scheme imitates the elliptic oscillator, but does not reproduce its properties exactly. This makes it extremely difficult to find such schemes.

4. Appelroth Method and polynomial Hamiltonian

Transferring the developed technique to the case of equations with a polynomial right-hand side does not cause significant difficulties, since back at the beginning of the 20th century G.G. Appelroth [8] proposed a method that allows, by increasing the number of unknowns, to reduce a system with a polynomial right-hand side to a system with a quadratic right-hand side. This procedure was later called quadratization [9].

Computer experiments have shown that the relationships between new and old variables, which are valid for the exact solution, are no longer valid for the approximate solution, which is especially noticeable near moving singular points of the solution.

5. Discussion

Designing schemes that imitate systems with polynomial Hamiltonians raises a question that lies at the interface between algebra and physics: should the correspondence between the initial and final positions of the system be a one-to-one correspondence? Since Jacobi, we have known that the quadrature

$$\int \frac{dq}{H_p} = t$$

does not allow q to be represented as a single-valued analytic function of t if the genus of the curve $H(p, q) = C$ exceeds 1. However, we can approximate the solution of such a system using Cremona transformations by combining the methods of Appelroth and Kahan. Thus, the analytic properties of the difference approximation are simpler than those of the original Hamiltonian model. Does this mean that such models are better than continuous ones?

References

- [1] Gerdt V. P. et al. *On the properties of numerical solutions of dynamical systems obtained using the midpoint method*, Discrete and Continuous Models and Applied Computational Science. 2019. Vol. 27, no. 3. P. 242–262.
- [2] Yu Ying et al. *On the Quadraticization of the Integrals for the Many-Body Problem*, Mathematics. 2021. Vol. 9, no. 24: 3208.
- [3] Kahan W., Ren-Chang Li. *Unconventional Schemes for a Class of Ordinary Differential Equations – With Applications to the Korteweg–de Vries Equation*, Journal of Computational Physics. 1997. Vol. 134. P. 316–331.
- [4] Celledoni, E. et al. *Geometric properties of Kahan’s method*, J. Phys. A: Math. Theor. 2013. Vol. 46. P. 025201.
- [5] Petrera M. et al. *Geometry of the Kahan discretizations of planar quadratic Hamiltonian systems*, Proc. R. Soc. A. 2019. Vol. 475. P. 20180761.
- [6] Ayryan E. A. et al. *Finite Differences Method and Integration of the Differential Equations in Finite Terms*. Dubna, 2018. Preprint no. P11-2018-17.
- [7] Malykh M. D. et al. *Finite Difference Models of Dynamical Systems with Quadratic Right-Hand Side*, Mathematics 2024, 12, 167.
- [8] Appelroth, G. G. *Die Normalform eines Systems von algebraischen Differentialgleichungen*, Mat. Sb. 1902, 23, pp. 12–23.
- [9] Bychkov A. Pogudin G. *Quadraticization for ODE Systems*, In Combinatorial Algorithms, Springer: Cham, 2021, pp. 122–136.

Mikhail Malykh
 Department of Applied Probability and Informatics
 Peoples' Friendship University of Russia,
 Moscow, Russia

e-mail: malykh_md@pfur.ru

Lubov' Lapshenkova
Department of Applied Probability and Informatics
Peoples' Friendship University of Russia,
Moscow, Russia

e-mail: lapshenkova-lo@pfur.ru

Marina Konyaeva
Department of Applied Probability and Informatics
Peoples' Friendship University of Russia,
Moscow, Russia

e-mail: 1032217044@pfur.ru

Dynamics of self-gravitating ellipsoids

Ivan Mamaev and Ivan Bizyaev

Abstract. We investigate the figures of equilibrium of a self-gravitating ideal fluid with a stratified density and a steady-state velocity field. As in the classical formulation of the problem, it is assumed that the figures, or their layers, uniformly rotate about an axis fixed in space.

Introduction

This paper is concerned with exact solutions to the problem of (axisymmetric) figures of equilibrium of a self-gravitating ideal fluid with density *stratification*. First of all, we briefly recall the well-known results:

For *homogeneous* fluid, the following ellipsoidal equilibrium figures for which the entire mass *uniformly rotates as a rigid body* about a fixed axis are well known: the Maclaurin spheroid (1742), the Jacobi ellipsoid (1834). In addition, in the case of a homogeneous fluid there also exist *figures of equilibrium with internal flows*: the Dedekind ellipsoid (1861), the Riemann ellipsoids (1861).

On the other hand, Hamy [3], Volterra [4] and Pizzetti [5] showed that for a stratified fluid mass rotating as a rigid body there exist no figures of equilibrium in the class of ellipsoids.

Hamy proved this theorem for the case of a finite number of ellipsoidal layers with constant density, Volterra generalized this result to the case of continuous density distribution for a homothetic stratification of ellipsoids, and Pizzetti gave the simplest and most rigorous proof in the general case for both continuous and piecewise constant density distribution.

Inhomogeneous figures with isodensity distribution of the angular velocity of layers

If one admits the possibility that the angular velocity of fluid particles is not constant for the entire fluid mass, then equilibrium figures for an arbitrary axisymmetric form of the surface and density stratification are possible. For example,

Chaplygin [2] explicitly showed a spheroidal equilibrium figure with a nonuniform distribution of angular velocities for the case of homothetic density stratification. It turns out that the surfaces with equal density $\rho(\vec{r}) = \text{const.}$ do not coincide with the surfaces of equal angular velocity $\omega(\vec{r}) = \text{const.}$ S. A. Chaplygin tried to use the resulting solution to explain the dependence of the angular velocity of rotation of the outer layers of the Sun on the latitude.

In [6] an explicit solution of another kind was found for which the equilibrium figure is a spheroid consisting of two fluid masses of different density $\rho_1 \neq \rho_2$ separated by the spheroidal boundary confocal to the outer surface, with each layer rotating at constant angular velocity such that $\omega_1 \neq \omega_2$. A generalization of this solution to the case of an arbitrary finite number of ‘‘confocal layers’’ was obtained by Esteban [1].

In this paper we obtain a generalization of this solution to the case of an arbitrary confocal (both continuous and piecewise constant) density stratification. For comparison, we also present Chaplygin’s solution for the homothetic stratification.

For an arbitrary confocal stratification the angular velocity on the outer surface of the inhomogeneous spheroid is the same as the angular velocity ω_0 of the Maclaurin spheroid with density $\langle \rho \rangle$:

$$\frac{\omega_0^2}{2\pi G \langle \rho \rangle} = \mu_0((1 + 3\mu_0^2)\text{arctg}(\mu_0) - 3\mu_0), \quad \mu_0 = \frac{b}{\sqrt{a^2 - b^2}} \quad (1)$$

where $\langle \rho \rangle$ is the average density of the spheroid.

To keep track of the dependence of the angular velocity of the layers on the change in density, we consider an inhomogeneous spheroid with different functions of density distribution of the following form:

$$\rho(\mu) = \rho_n^{(0)}(1 - \alpha_n \mu^n), \quad n = 2, 4, 6, \quad (2)$$

where $\rho_n^{(0)}$ and α_n are some constants ($\rho_n^{(0)}$ has the meaning of density at the center of the spheroid). We will determine their values from the given average density of the body $\langle \rho \rangle = \frac{\int \rho dV}{\int dV}$ and the given ratio between the density on the surface and the average density of the body $\varepsilon = \frac{\langle \rho \rangle}{\rho(\mu_0)}$,

$$\alpha = \frac{(1+n)(3+n)(1+\mu_0^2)(1-\varepsilon)\mu_0^{-n}}{(3+n)(1-\varepsilon(1+n)(1+\mu_0^2)) + 3(1+n)\mu_0^2}$$

$$\rho_0 = \langle \rho \rangle \frac{(3+n)(\varepsilon(1+n)(1+\mu_0^2) - 1) - 3(1+n)\mu_0^2}{n\varepsilon((1+n)\mu_0^2 + 3+n)}.$$

As an example, assume that the eccentricity e_0 and the quantity ε , which are the same as the data of the Earth:

$$e_0 = 0.08181, \quad \varepsilon = 2.5.$$

Figure 1 shows the dependences of $\frac{\rho}{\langle \rho \rangle}$ on the coordinate of the layer μ for (2). As we can see, the density increases most sharply at the center of the spheroid for $n = 2$ and then, as n increases, the density decreases.

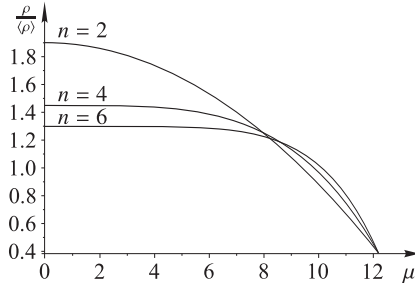


FIGURE 1. A graph showing the dependence of the relation $\frac{\rho}{(\rho)}$ on the layer μ

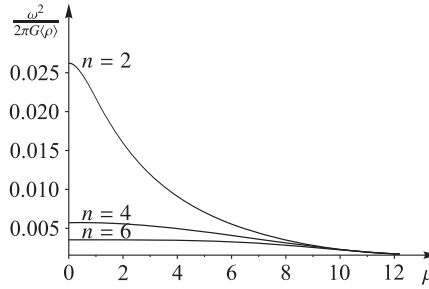


FIGURE 2. A graph showing the dependence of the angular velocity on the layer μ

To find the angular velocity, we substitute the density distributions and obtain the dependence of the angular velocity on the layer. A graph of this dependence is shown in Fig. 2. Since the explicit formulae for $\omega(\mu)$ are unwieldy, we do not present them here.

For the angular velocity with density distribution (2) one may draw the following conclusion from Fig. 2: *the closer the center of the spheroid, the larger the angular velocity; specifically, the larger the value of density at the center of the spheroid (with $n = 2$), the larger the increase in the angular velocity.*

References

- [1] Esteban, E.P., Vasquez, S. *Rotating Stratified Heterogeneous Oblate Spheroid in Newtonian Physics*, 2001, Celestial Mech. Dynam. Astronom, vol. 81, no. 4, pp. 299–312.
- [2] Chaplygin, S. A. *Steady-State Rotation of a Liquid homogeneous spheroid* In Collected works: Vol. 2. Hydrodynamics. Aerodynamics. Gostekhizdat, Moscow 1948.
- [3] Hamy M. *Étude sur la Figure des Corps Célestes*, Ann. de l’Observatoire de Paris, 1889, vol. 19, pp. 1–54.
- [4] Volterra V. *Sur la Stratification d’une Masse Fluide en Equilibre*. Acta Math, 1903, vol. 27, no. 1, pp. 105–124.
- [5] Pizzetti P. *Principii della Teorïa Meccanica della Figura dei Pianeti*. Enrico Spoerri, Libraio-Editore, Pisa 1913.
- [6] Montalvo D., Martínez F. J., Cisneros J. *On Equilibrium Figures of Ideal Fluids in the Form of Confocal Spheroids Rotating with Common and Different Angular Velocities*, 1983, vol. 5, no. 4, pp. 293–300.

Ivan Mamaev
Ural Mathematical Center
Udmurt State University
Universitetskaya 1, Izhevsk 426034, Russia
e-mail: mamaev@rcd.ru

Ivan Bizyaev
Ural Mathematical Center
Udmurt State University
Universitetskaya 1, Izhevsk 426034, Russia
e-mail: bizyaevtheory@gmail.com

On estimating the magnitude of perturbations in the rotational dynamics of asteroids approaching the Earth

Alexander Melnikov and Kristina Lobanova

Abstract. In numerical experiments, the rotational dynamics of asteroids as they approach the Earth is considered. It is shown that close encounters can lead to noticeable perturbations in the asteroid's rotational speed and the orientation of the rotational axis. The influence of uncertainty in knowing the figure of an asteroid on the assessment of the magnitude of perturbations in its rotation has been studied. Estimates of perturbations in the rotational dynamics of the asteroid (99942) Apophis during its approach to the Earth in 2029 were obtained.

Introduction

In terms of asteroid-comet hazard, it is of great importance to study different aspects of near-Earth asteroids (NEAs) dynamics. Investigation of the dynamics of small (diameter 10–100 m) NEAs is of special interest since they engage frequently in close encounters with our planet at a distance of about 10 Earth radii (R_E). The rotational and orbital dynamics of an asteroid are closely interrelated and influence one another [1, 2]. In particular, perturbations in the rotation of an asteroid affect its orbital motion due to the changes in the value of the Yarkovsky effect [3, 4]. We have designed [4] numerical methods for modeling the rotational motion of an asteroid during its approach to the planet and investigated the dynamics of a number of small asteroids during their close encounters with the Earth. We present the main results of our numerical experiments with the following example of asteroid (99942) Apophis whose rotational dynamics during 2029 approach to the Earth was studied. By means of numerical experiments, the estimates of the change in the rotational period $\Delta P = P_{\text{final}} - P_0$ and the angle between the rotational axis and the normal to the orbital plane $\Delta\gamma = \gamma_{\text{final}} - \gamma_0$ were acquired, where P_0 and γ_0 are the values before the approach.

1. Influence of the orbit

An important issue is defining the size of an area of the space around the planet where disturbances in the rotational dynamics of an asteroid are significant. Figure 1 shows dependences of the magnitudes of perturbations in the rotation of Apophis on the parameters of its geocentric orbit (d , e), where $d = a(e - 1)$ is the pericentric distance, a the semimajor axis and e the eccentricity. It can be seen that significant perturbations occur within $d \leq 10R_E$, where R_E is the Earth radius. We made a similar conclusion from the analysis of the dynamics of other small NEAs ((367943) Duende, 2012 TC4, 2023 BU).

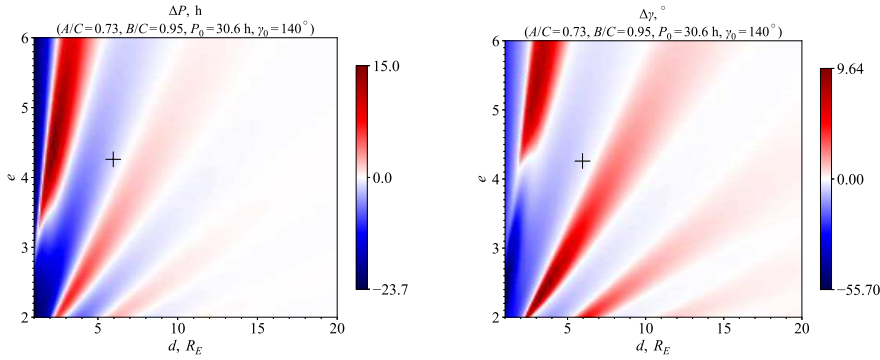


FIGURE 1. Dependences of ΔP and $\Delta \gamma$ for Apophis due to its approach to the Earth in 2029 on the orbital parameters $d = a(e - 1)$ (within Earth's radii) and e . The cross indicates current position of Apophis [5]

2. Influence of the initial rotational state

The estimates of perturbations in the rotational dynamics of asteroids during approaches to the Earth have shown that for the asteroids with relatively slow rotation ($P > 5$ h) perturbations may be large. Figure 2 demonstrates the perturbations in the rotation of Apophis during its approach to the Earth in 2029. It can be seen that the rotational period may change by tens of hours, and variations in the orientation of the rotational axis may reach ten degrees. In case of the asteroids with extremely fast rotation ($P < 1$ h), which includes, for example, asteroids 2012 TC4 and 2023 BU, the perturbations in the rotational motion during approach to the Earth are negligibly small.

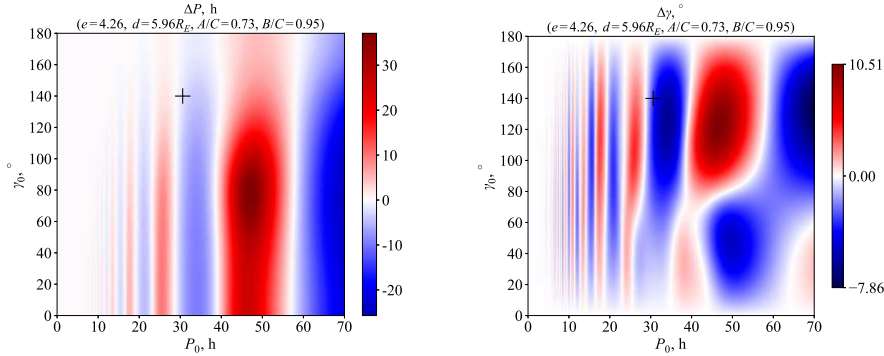


FIGURE 2. Dependences of ΔP and $\Delta\gamma$ for Apophis due to its approach to the Earth in 2029 on the possible initial (before the moment of approach) values of P_0 and γ_0 . The cross indicates current position of Apophis [5]

3. Influence of the figure

The shape of small asteroids is usually unknown or poorly defined. We studied the influence of the asteroid's shape (which may be described through its moments of inertia $A < B < C$) on ΔP and $\Delta\gamma$. It follows from the example shown on Figure 3 that, in case of Apophis, the errors in determining the asteroid figure (which is approximated by a triaxial ellipsoid with the semi-axes $a > b > c$) may lead to significant underestimates of the values of perturbations. Similar results were obtained for other asteroids with slow rotation. In the case of asteroid with fast rotation, its shape has little influence on the estimates of the perturbation values.

Conclusion

Our numerical modeling of small asteroids approaching the Earth has shown that significant perturbations in the rotational dynamics of an asteroid take place only when it approaches the planet at a distance of less than 10 Earth radii. In case of asteroids with the rotational period $P > 5$ h encounters with the Earth may lead to noticeable changes in the rotational speed and the orientation of the rotational axis. In addition, precise knowledge of the asteroid figure is needed for the accurate estimation of the perturbation value. On the contrary, for the asteroids with fast rotation ($P < 1$ h) perturbations in the rotational motion are negligible, and the shape of an asteroid has little influence on their value.

The study was funded by a grant Russian Science Foundation № 23-22-00306, <https://rscf.ru/project/23-22-00306/>.

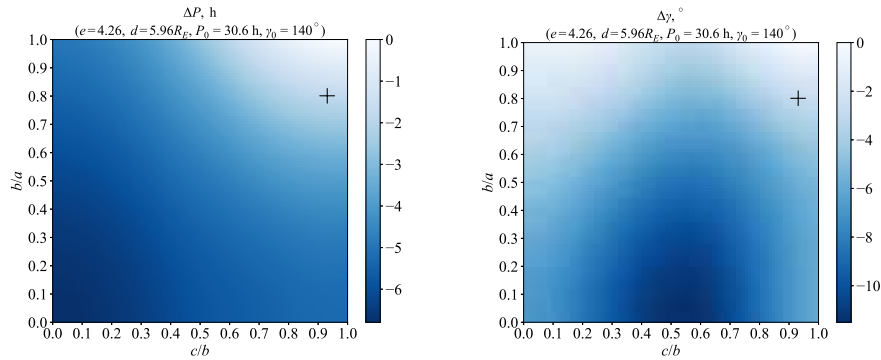


FIGURE 3. Dependences of ΔP and $\Delta \gamma$ for Apophis due to its approach to the Earth in 2029 on the parameters c/b and b/a , characterizing the figure of the asteroid. The cross indicates current position of Apophis [5]

References

- [1] L.A.G. Boldrin, R.A.N. Araujo and O.C. Winter, *On the rotational motion of NEAs during close encounters with the Earth*, European Physical Journal Special Topics, v. 229, Issue 8, pp. 1391–1403, 2020.
- [2] A.V. Melnikov, *Rotational dynamics of asteroids approaching planets*, Solar System Research, v. 56, Issue 4, pp. 241–251, 2022.
- [3] A.A. Martyusheva and A.V. Melnikov, *Influence of planetary encounters on the magnitude of the Yarkovsky effect in asteroid dynamics*, Solar System Research, v. 57, Issue 5, pp. 486–494, 2023.
- [4] K.S. Lobanova and A.V. Melnikov, *Disturbances in the rotational dynamics of asteroid (99942) Apophis at its approach to the Earth in 2029*, Solar System Research, v. 58, Issue 2, pp. 208–219, 2024.
- [5] P. Pravec, P. Scheirich, J. Ďurech et al., *The tumbling spin state of (99942) Apophis*, Icarus, v. 233, pp. 48–60, 2014.

Alexander Melnikov
 Pulkovo Observatory
 Saint-Petersburg, Russia
 e-mail: melnikov@gaoran.ru

Kristina Lobanova
 Pulkovo Observatory
 Saint Petersburg State University
 Saint-Petersburg, Russia
 e-mail: st068189@student.spbu.ru

The effect of encounters with interstellar objects of planetary and substellar masses on the Solar system dynamics

D.V. Mikryukov and I.I. Shevchenko

Abstract. We consider the effect of close encounters of interstellar objects of planetary and substellar masses on the dynamics of the Solar System. By means of massive numerical experiments and analytical considerations, the both immediate and long-term consequences of such events for the Solar system dynamics are identified and explained.

Introduction

A free-floating planet (FFP) is understood as a planet that is not gravitationally bound to any star. The upper mass limit for a planet is about $13M_J$ (Jupiter masses); within a larger mass object, deuterium is ignited in the core and the object thus represents a brown dwarf (BD). The upper mass limit for BD is about $75M_J$.

Currently, ordinary planetary systems (including circumbinary ones) are considered to be the main source of origin of FFPs. An opportunity of the FFP formation in interstellar space via gravitational collapse of interstellar gas blobs is also not excluded. Various formation mechanisms may provide, in sum, the FFP presence in the Galactic thin disc in the range from 0.24 to 200 pc^{-3} [1].

Studies of interactions of planetary systems with massive interstellar objects (MISOs), such as FFPs or BDs, is of great interest, since such interactions directly concern the problem of stability and long-term dynamics of planetary systems.

Model set-up

There can be many scenarios for interaction of the Solar system with a MISO, since the choice is broad not only for the MISO mass but also for its orbit's

initial conditions. Here, we limit ourselves to studying two nominal approach trajectories of MISOs. We consider the hyperbolic orbits of real interstellar objects 1I/'Oumuamua and 2I/Borisov, which visited the Solar system in 2017 and 2019. These both orbits passed through the inner Solar system.

For each approach orbit, the initial state of the system (positions and velocities) is set to be the same in all our numerical experiments, only the MISO masses is varied. The number of experiments is rather large (about 2000 per orbit), because the MISO mass is varied in small steps over a wide range, see table 1.

| MISO type | Mass range, M_J | Step in mass, M_J | ρ , au | τ , yr |
|-----------|-------------------|---------------------|-------------------|-----------------|
| FFP | 0–13 | 0.01 | 1.2×10^4 | 5×10^6 |
| BD | 13–45 | 0.05 | 6×10^4 | 2×10^6 |

TABLE 1. MISO mass range and quantities ρ and τ denoting, respectively, the maximum interaction distance and the integration time interval.

The gravitational interaction of the Sun, MISO and eight major planets (from Mercury to Neptune) is considered. At the initial epoch T_0 , the MISO is at a distance ρ from the Sun and is approaching the Solar system. After passing the perihelion, the MISO moves further on, and, on reaching the same distance ρ from the Sun, is excluded from the integration. The integration of the perturbed planetary configuration is however continued and is eventually stopped when the time elapsed since the epoch T_0 becomes equal to τ . If, during this time interval, any planet is ejected, the integration is as well stopped. The adopted quantities ρ and τ are given in table 1.

In each numerical experiment, we calculate the maximum values of the planetary eccentricities and inclinations

$$e_{\max}^j = \max e_j, \quad i_{\max}^j = \max i_j, \quad 1 \leq j \leq 8, \quad (1)$$

as well as quantities

$$\begin{aligned} d_{\min}^1 &= \min(a_3(1 - e_3) - a_1(1 + e_1)), \\ d_{\min}^j &= \min(a_j(1 - e_j) - a_{j-1}(1 + e_{j-1})), \quad 2 \leq j \leq 8, \end{aligned} \quad (2)$$

which provide estimates of the distance between two elliptical orbits, see e.g. [2]. To calculate all 24 quantities $e_{\max}^j, i_{\max}^j, d_{\min}^j$, $1 \leq j \leq 8$, a time step of 5 yr is used, and the maxima and minima on the RHS of (1) and (2) are taken over the total integration time interval (starting from T_0). At the time moment of the MISO exclusion from the system, the values of the osculating semimajor axes, eccentricities and inclinations

$$a_{\text{imm}}^j, \quad e_{\text{imm}}^j, \quad i_{\text{imm}}^j, \quad 1 \leq j \leq 8,$$

are recorded. The accuracy of calculations in each experiment was controlled by checking the conservation of the energy integral.

All calculations were performed by the IAS15 high-precision non-symplectic integrator implemented in the REBOUND package [3]. The computing resources of the Joint Supercomputer Center of the Russian Academy of Sciences were used. Each MPI (Message Passing Interface) process ran one instance of REBOUND with a given orbit and a given value of the MISO mass.

Results and conclusions

In the case of substellar-mass (> 13 Jovian masses) interlopers, i.e. free-floating BDs, the general conclusions about the influence of the flyby on the subsequent evolution of the planetary system are as follows.

(1) The immediate (on the timescale of $\sim 10 - 100$ yr) consequence of the passage is a significant increase in orbital inclinations and eccentricities of the outermost planets Uranus and Neptune.

(2) On the intermediate timescale ($\sim 10^3 - 10^5$ yr), Neptune or Uranus (more likely) can be ejected from the system due to close encounters with Saturn, as well as with each other.

(3) On the secular timescale ($\sim 10^6 - 10^7$ yr), the major perturbation wave caused by the secular interactions of the planets reaches the inner part of the Solar system.

Regarding immediate and long-term outcomes with planetary mass intruders, it is found that a FFP flyby is able to cause an immediate entering of a pair of planets into a chaotic mean motion resonance; this, in turn, may cause disruption of the Solar system on a secular timescale.

Any MISO flyby typically sets the planetary system into a more chaotic state; however, a stronger chaos, implying a smaller Lyapunov time, does not necessarily cause a more rapid disintegration, because the Lyapunov timescales and chaotic diffusion timescales can be interrelated in various fashions [4, 5]; and the system, in fact, can be left in a state of “stable chaos,” with no disruption following. Besides, the distributions of disruption times of gravitational systems of the considered type are heavy-tailed [6, 7]; therefore, the disruptive effect of an encounter can occasionally be quite prolonged, with respect to values typically observed in simulations.

Concluding, the long-term stability of the Solar System can be disrupted even if the interstellar object is not very massive (a Jovian mass is enough) and does not experience close encounters with the planets. The disintegration of the planetary system does not necessarily appear immediately, but may take place in several million years.

From the data obtained, it also follows that it is unlikely that the Solar system, which has an age of more than 4 Gyr, in its past was subject to numerous encounters with objects of giant-planet and substellar masses, because such encounters induce large planetary eccentricities and inclinations and may even lead to ejections of outermost planets.

A more detailed discussion of the results obtained, as well as consideration of their differences due to changes in the encounter orbit and the MISO's mass can be found in [8].

References

- [1] N. Goulinski, and E.N. Ribak, *Capture of free-floating planets by planetary systems*, Monthly Notices of the Royal Astronomical Society (2018), v. 473, pp. 1589–1595.
- [2] D.V. Mikryukov, and R.V. Baluev, *A lower bound of the distance between two elliptic orbits*, Celestial Mechanics and Dynamical Astronomy (2019), v. 131, id. 28.
- [3] H. Rein, and D.S. Spiegel, *IAS15: a fast, adaptive, high-order integrator for gravitational dynamics, accurate to machine precision over a billion orbits*, Monthly Notices of the Royal Astronomical Society (2015), v. 446, pp. 1424–1437.
- [4] I.I. Shevchenko, *Dynamical Chaos in Planetary Systems*. Springer Nature Switzerland AG, Cham, 2020.
- [5] P.M. Cincotta, C.M. Giordano, and I.I. Shevchenko, *Revisiting the relation between the Lyapunov time and the instability time*, Physica D (2022), v. 430, id. 133101.
- [6] V.V. Orlov, A.V. Rubinov, and I.I. Shevchenko, *The disruption of three-body gravitational systems: lifetime statistics*, Monthly Notices of the Royal Astronomical Society (2010), v. 408, pp. 1623–1627.
- [7] I.I. Shevchenko, *Hamiltonian intermittency and Lévy flights in the three-body problem*, Physical Review E (2010), v. 81, id. 066216.
- [8] D.V. Mikryukov, and I.I. Shevchenko, *Rendez-vous with massive interstellar objects, as triggers of destabilization*, Monthly Notices of the Royal Astronomical Society (2024), v. 528, pp. 6411–6424.

D.V. Mikryukov
Department of Celestial Mechanics
Saint Petersburg State University
Saint Petersburg, Russia
e-mail: d.mikryukov@spbu.ru

I.I. Shevchenko
Department of Celestial Mechanics
Saint Petersburg State University
Saint Petersburg, Russia
Institute of Applied Astronomy
Saint Petersburg, Russia
e-mail: i.shevchenko@spbu.ru

4D Modeling of the Kinematics of a Selected Subsystem of the Milky Way

Igor' I. Nikiforov

Abstract. When solving inverse problems of kinematic modeling of the Milky Way, even for a homogeneous subsystem of objects, the traditional difficulty is to take into account all the variances of the problem: the natural (dynamic) dispersion of the subsystem (ellipsoid of velocities), as well as the measurement uncertainties of the velocity components and heliocentric distances. The standard approach is 3D modeling, in which only velocity measurement errors are taken into account, often without assuming natural dispersion, and the solution is within the framework of the least squares method. However, ignoring the uncertainty of distances, as well as natural dispersion, can lead to significant systematic errors. This problem became especially relevant after the appearance of mass joint determinations of proper motions and trigonometric parallaxes (Galactic masers, Gaia catalog), since objects with large linear and relative errors in distances are inevitably present in such catalogs. The correct solution of the problem with the determination of all spatial-kinematic characteristics, as well as the velocity ellipsoid, taking into account variances of all types, is possible only within the framework of the maximum likelihood method. The corresponding algorithm—4D modeling—is developed and implemented in this paper. It involves minimizing the squares of relative deviations of the model from the observed radial velocity, proper motions, and distant characteristics with natural dispersions as unknown parameters. A distant characteristic is understood as a trigonometric parallax (in the case of absolute distances) or a distance modulus (in the case of relative, i.e. photometric, distances). The constructed iterative algorithm includes optimization of the smoothness of the rotation law and a flexible procedure for eliminating outliers in the data, generalized to a four-dimensional field of residuals. The new method allows us to obtain individual corrections for distances to sample objects. The method was tested on Galactic masers of the HMSFR type. It is shown that the inclusion of distance uncertainties in the probabilistic model greatly reduces estimates of natural velocity dispersions, and also significantly reduces the value of the distance from the Sun to the center of the Galaxy, R_0 , obtained from masers. New estimate is $R_0 = 7.88 \pm 0.12$ kpc. Estimates of a number of other fundamental Galactic characteristics have been obtained.

Igor' I. Nikiforov
Department of Celestial Mechanics, Faculty of Mathematics and Mechanics
Saint Petersburg State University
Saint Petersburg, Russia
e-mail: i.nikiforov@spbu.ru

Finite-point approximations of fields of attraction and their verification

Nikonov Vasily and Burov Alexander

Abstract. Approaches to constructing finite-point approximations of the gravitational fields of celestial bodies with complex shapes that are far from spherical are discussed. The study shows good agreement between the parameters of body mass distribution models obtained using both the K -means method and a system of balls with centers on a straight line.

Introduction

In modern celestial mechanics, a lot of attention is paid to the study of motion in the vicinity of small celestial bodies, in particular, asteroids and comets. The actuality of the related issues is provided by the intensification of research in connection with the problem of asteroid danger, as well as with the design and implementation of missions to work both in the vicinity of such celestial bodies and on their surface.

As is known (see, e.g., [1, 2, 3, 4, 5, 6]), celestial mechanics relies on the development of the potential energy of Newton's gravitational attraction into a series. Such a development is based on a natural small parameter, expressing the ratio of the characteristic sizes of the attracting bodies to the distance between them. The second-order truncation is usually sufficient to accurately describe and predict the dominant dynamic effects of mutual attraction. However, numerous small celestial bodies are of a complex shape. At the same time, many small celestial bodies have a rather complex shape. The correct description of the fields of attraction generated by them requires the use of higher approximations. Currently, the so-called Werner-Scheeres approach is of the most widely used. Its main provisions of which are set out in publications [7, 8]. The Werner-Scheeres approach is effective for numerical calculations in the case when a celestial body is assumed to be homogeneous or, more generally, such a body can be represented as a set of homogeneous disjoint components. Assuming that the surface of a small celestial body is defined by a triangulation grid, the Werner-Scheeres method allows us

to represent its potential of attraction as the sum of the potentials of individual tetrahedra, with a common vertex and bases in the triangulation cells. This sum consists of a large number of terms. In an order this number is comparable to the number of elements of the graph defining the triangulation grid. It is clear that such an approximation is essentially unsuitable for a preliminary analytical study of motion in the vicinity of a small celestial body. In this regard, the problem of constructing a system of equigravitating bodies seems being very important. For such a system, the components of the Euler-Poinsot tensor, otherwise known as inertia integrals, must coincide with the corresponding components of such a tensor for the initial body for the highest possible order.

The problem of the approximation of the field of attraction of a celestial body by the field of attraction of a set of “elementary” bodies is the subject of this study. The goal is to find such approximate configurations for which the components of the Euler-Poinsot tensor will coincide with the corresponding components for the initial body not only for the second, but also for a higher order. The results obtained are compared with the results obtained earlier using the K -means method, applied in conditions where the assumptions of the Werner — Scheeres theorem on the approximation of the potential of a body are valid. As examples, models of a number of small celestial bodies are considered.

1. On K-means method

H. Steinhaus [9] proposed a novel approach to dividing sets of points into non-overlapping groups, which is widely used in the field of pattern recognition. Let A be a set of a finite number of points located in three-dimensional Euclidean space in some way. Let A_1, \dots, A_k be disjoint subsets of A such that their union is exactly equal to A :

$$A = A_1 \cup \dots \cup A_k, \quad A_i \cap A_j = \emptyset, \quad i \neq j. \quad (1)$$

Let S_1, \dots, S_k be the centroids of these subsets and $\rho_{ij} = |S_i S_j|$ be the pairwise distance between them. Let us denote $\rho = \min_{i \neq j} \rho_{ij}$ as the minimum distance between centroids.

According to Steinhaus [9], we are looking for a partition of the set A that satisfies the requirements (1) such that the minimum distance between the centroids of the subsets is maximised: $\rho_* = \max_A \rho$. If such a partition exists, it is said that the subsets in the partition are “as far apart as possible”. Since the iteration is finite, there is at least one partition of A into disjoint subsets that achieves the maximum ρ_* , and this partition is not necessarily unique.

Lloyd [10] proposed an iterative algorithm that approximates ρ_* . The algorithm never repeats splitting, and it is guaranteed to converge, see, e.g., [10, 11].

Suppose that the surface of a body can be represented as a polyhedron, which consists of a given set of vertices and a set of triangular faces that are consistently oriented. The application of the Steinhaus approach and Lloyd’s algorithm to

the centroids of these tetrahedra equipped with corresponding oriented volumes ([12]) made it possible to construct two-, three- and four-point approximations for asteroids (2063) Bacchus, (216) Kleopatra, (433) Eros, (1620) Geographos and comet (67P) Churyumov-Gerasimenko [13, 14, 15]

2. Comparison with finite-point approximations obtained otherwise

According to [14], the K -means method defines a triple of points P'_1 , P'_2 and P'_3 with masses $m'_1 = 2.001 \cdot 10^{15}$, $m'_2 = 2.608 \cdot 10^{15}$ and $m'_3 = 2.057 \cdot 10^{15}$ kg, respectively. At the same time $|P'_1P'_3| = 17.983$, $|P'_2P'_3| = 9.897$, $|P'_1P'_2| = 8.783$. The triangle $\Delta P'_1P'_2P'_3$ is obtuse, with an obtuse angle $\angle P'_1P'_2P'_3 = 2.592524415$ rad, close to the straight one.

On the other hand, the Grebenikov-Demin-Aksenov method (see, e.g., [16]) gives a triple of collinear points P_1 , P_2 and P_3 with masses $m_1 = 1.656 \cdot 10^{15}$ kg, $m_2 = 2.696 \cdot 10^{15}$ kg and $m_3 = 2.313 \cdot 10^{15}$ kg. At the same time $|P_1P_3| = 19.896$ km, $|P_2P_3| = 10.312$ km, $|P'_1P'_2| = 9.584$ km.

Mass discrepancies amounting to

$$\frac{|m_1 - m'_1|}{\min(m_1, m'_1)} \approx 0.2083, \quad \frac{|m_2 - m'_2|}{\min(m_2, m'_2)} \approx 0.0337, \quad \frac{|m_3 - m'_3|}{\min(m_3, m'_3)} \approx 0.1245,$$

does not exceed 21 percent.

Similarly calculated differences in distances amounting to

$$\delta_{12} \approx 0.106, \quad \delta_{23} \approx 0.042, \quad \delta_{13} \approx 0.091, \quad \delta_{ij} = \frac{||P'_iP'_j| - |P_iP_j||}{\min(|P'_iP'_j|, |P_iP_j|)},$$

does not exceed 11 percent.

It remains to be noted that Steinhaus' approach is purely geometric. Its use does not imply at least some knowledge about the gravitational potential of the studied celestial body.

The study shows a good agreement between the parameters of body mass distribution models obtained using both the K -means method and a system of balls placed along a straight line.

References

- [1] Sretensky L. N. *Newtonian Potential Theory*. M.-L.: Gostekhizdat. 1946. (in Russian)
- [2] Duboshin G. N. *Theory of attraction*. M.: GIFML. 1961. (in Russian)
- [3] Brouwer D., Clemence G. *Methods of Celestial Mechanics*. New-York, London: Academic Press. 1961.
- [4] Antonov V. A., Kholshevnikov K. V. *On the Possibility of Using a Laplace Series for the Gravitational Potential at the Surface of a Planet - Part One*. Soviet Astronomy. 1980. V. 24, no 6. P. 761-765.

- [5] Antonov V. A., Kholoshevnikov K. V. *On the Possibility of Using a Laplace Series for the Gravitational Potential at the Surface of a Planet - Part Two*. Soviet Astronomy. 1982. V. 26, no. 4. P. 464-467
- [6] Antonov V. A., Timoshkova E. I., Kholoshevnikov K. V. *Introduction to the Theory of Newtonian Potential*. M.: Nauka. 1988. (in Russian)
- [7] Werner R. A. *The gravitational potential of a homogeneous polyhedron or don't cut corners*. Cel. Mech. & Dyn. Astr. 1994. V. 59, no. 3. P. 253-278.
- [8] Werner R. A., Scheeres D. J. *Exterior gravitation of a polyhedron derived and compared with harmonic and mascon gravitation representations of asteroid 4769 Castalia*. Cel. Mech. & Dyn. Astr. 1996. V. 65, no. 3. P. 313-344.
- [9] Steinhaus H. *Sur la division des corp matériels en parties*. Bull. Acad. Polon. Sci. Cl.III. 1956. V. 4. P. 801 - 804
- [10] Lloyd S. P. *Least squares quantization in pcm*. IEEE Transactions on Information Theory. 1982. V. 28, no. 2. P. 129 - 136.
- [11] Arthur D., Vassilvitskii S. *On the Worst Case Complexity of the k-means Method*. Technical Report. Stanford, Stanford University. 2005. 17 P.
- [12] Chanut T.G.G., Aljbaae S., Carruba V. *Mascon gravitation model using a shaped polyhedral source*. Monthly Notices of Roy. Astr. Soc. 2015. V. 450. P. 3742 - 3749
- [13] Burov A. A., Guerman A. D., Raspopova E. A., Nikonov V. I. *On the use of the K-means algorithm for determination of mass distributions in dumbbell-like celestial bodies*. Rus. J. Nonlin. Dyn. 2018. V. 14, no. 1. P. 45-52.
- [14] Burov A. A., Guerman A. D., Nikonov V. I. *Using the K-means method for aggregating the masses of elongated celestial bodies*. Cosmic Res. 2019. V. 57, no. 4. P. 266-271.
- [15] Burov A. A., Guerman A. D., Nikonova E. A., Nikonov V. I. *Approximation for attraction field of irregular celestial bodies using four massive points*. Acta Astronautica. 2019. V. 157. P. 225-232.
- [16] Beletsky V. V. *Essays on the motion of celestial bodies*. Basel; Boston; Berlin: Birkhäuser. 2001.

Nikonov Vasily

Department of Mechanics № 24

Federal Research Center "Computer Science and Control" of the Russian Academy of Sciences

Moscow, Russian Federation

e-mail: nikon_v@list.ru

Burov Alexander

Department of Mechanics №24

Federal Research Center "Computer Science and Control" of the Russian Academy of Sciences

Moscow, Russian Federation

e-mail: jtm@yandex.ru

APPROXIMATE THEORY OF A GYROSCOPE AND ITS APPLICATIONS TO THE MOTION OF SPACE OBJECTS

Petrov A.G.

Abstract. The motion of an axisymmetric rigid body with a fixed point under the action of a periodic torque is considered. Two small parameters are introduced: the first characterizes the smallness of the amplitude of the torque, and the second characterizes the smallness of the component of the kinetic moment perpendicular to the axis of symmetry. The smallness of the second small parameter is usually the basis for using the approximate theory of the gyroscope. Using this approximation, one can quite simply find the precession velocity of the top under the action of a small periodic torque. It is shown that the relative accuracy of the velocity calculated in this way is practically independent of the second small parameter, which does not exceed a value of the order of unity. In this way, a simple formula is found for the precession of the Earth's satellite under the action of the Earth's gravitational field. The resulting simple formula for the velocity of the Lunar-Solar precession of the Earth agrees well with astronomical observations.

Introduction

The motion of an axisymmetric rigid body is described by an equation for a unit vector \mathbf{e} lying on the axis of symmetry [1]. The exact equation includes the second derivatives of the vector \mathbf{e} with respect to time. In the case of rapid rotation, the approximate theory of a gyroscope proposes to ignore them. Then there remains a first-order equation with respect to the vector \mathbf{e} , which is called the equation of the precession theory of a gyroscope. From this equation, the precession velocity under the action of a periodic torque is easily found by the averaging method [2]. It is shown that the relative accuracy of the precession velocity is proportional to the amplitude of the torque and does not significantly depend on the component of the kinetic moment perpendicular to the axis of the top.

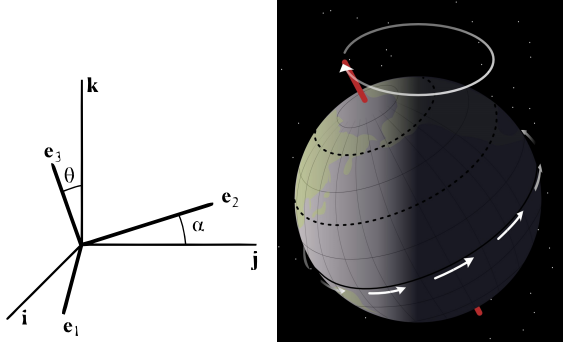


FIGURE 1. Angles of precession and nutation. Lunisolar precession.

1. Exact equations

The motion of an axisymmetric body with a fixed point lying on the axis of symmetry is conveniently described using a unit vector $\mathbf{e} = \mathbf{e}_3$ lying on the axis of symmetry. In this case, information about the rotation of the body about the axis of symmetry will not interest us. The equation for the vector can be obtained from the law of change of the kinetic moment [1]

$$\begin{aligned} \frac{d\mathbf{K}}{dt} &= \mathbf{Mom}, \quad \mathbf{K} = A\mathbf{e} \times \frac{d\mathbf{e}}{dt} + C\mathbf{r}\mathbf{e} \\ \frac{d\mathbf{K}}{dt} &= A\mathbf{e} \times \frac{d^2\mathbf{e}}{dt^2} + Cr\frac{d\mathbf{e}}{dt} + C\mathbf{e}\frac{dr}{dt} = \mathbf{Mom} \end{aligned} \quad (1)$$

where \mathbf{K} is the kinetic moment, \mathbf{Mom} is the moment of force applied to a point on the axis of symmetry, \mathbf{e} is a unit vector directed along the axis of symmetry, A , C are the moments of inertia of a rigid body, r is the projection of the angular velocity onto the axis of symmetry. It is assumed that the vector \mathbf{Mom} is a periodic function of the argument $\tau = \omega t$, ω is the frequency.

Let us introduce two dimensionless parameters $\varepsilon = \frac{\max|\mathbf{Mom}|}{Cr\omega}$, $\varepsilon_1 = \frac{A\omega}{Cr}$ and assume that the projection of the moment of forces \mathbf{Mom} on the axis $\mathbf{e} = 0$.

Then the system will be reduced to the following dimensionless form for angles of precession α and nutation θ (fig.1)

$$\begin{aligned} -\varepsilon_1 \left(\ddot{\alpha} \sin \theta + 2\dot{\theta}\dot{\alpha} \cos \theta \right) + \dot{\theta} &= \varepsilon M_1(\theta, \alpha, \tau), \\ \varepsilon_1 \left(\ddot{\theta} - \dot{\alpha}^2 \sin \theta \cos \theta \right) + \dot{\alpha} \sin \theta &= \varepsilon M_2(\theta, \alpha, \tau), \quad \tau = \omega t \end{aligned} \quad (2)$$

Here the dots denote the derivatives with respect to τ . The parameter ε_1 determines the ratio of the first terms on the left-hand side of the equations to the second. For $\varepsilon_1 \ll 1$, the approximate theory of the gyroscope is usually used, in

which the first terms are discarded [1]

$$\frac{d\theta}{d\tau} = \varepsilon M_1(\theta, \alpha, \tau), \quad \frac{d\alpha}{d\tau} \sin \theta = \varepsilon M_2(\theta, \alpha, \tau) \quad (3)$$

For the components of the moment with a small parameter ε , the (3) system can be easily studied by the averaging method.

It seems obvious that the relative error of the approximate theory of the gyroscope (3) is proportional to the parameter ε_1 . However, this is not so. It is shown that the relative error of the nutation and precession angles determined by the approximate theory of the gyroscope (3) is proportional to the parameter ε for almost all values of the parameter ε_1 limited by a number of the order of unity. The importance of this statement follows from the fact that there are many problems in mechanics in which the parameter ε_1 significantly exceeds the parameter ε in magnitude.

2. Formulation of the theorem and examples of its application

Theorem For the complete system of equations (2) with 2π periodic in τ components of the moment of force M_i with small parameters ε and ε_1 , the precession angle is determined from the system of equations (3) with a relative error of the order of ε and for almost any small values of ε_1 is approximated by the averaged system (3).

Example 1. Precession of a body in the two-body problem. Consider the circular two-body problem, in which the first body is a rigid body of mass m , and the second has mass M . The bodies are attracted by the law $\mathbf{F} = -\gamma Mm \frac{\mathbf{r}}{|\mathbf{r}|^3}$.

A body of mass m moves under the action of force \mathbf{F} along a circle of radius R_1 , the center of which is located at the center of mass of the bodies. Due to the inhomogeneity of the field, a moment of force acts on a solid body of mass relative to its center of mass

$$\mathbf{Mom}(\omega t) = \frac{3\gamma Mm}{R^3} (A - C) \tilde{\mathbf{M}}, \quad \tilde{\mathbf{M}} = ((\mathbf{r}_0/R) \cdot \mathbf{e}) ((\mathbf{r}_0/R) \times \mathbf{e}) \quad (4)$$

where \mathbf{r}_0 is the radius vector from the center of the body of mass m to the center of the body M , A and B are the moments of inertia of the body relative to the axis of symmetry and the axis perpendicular to it $R = |\mathbf{r}_0|$.

The bodies move in circular orbits relative to the center of mass and the distance between the bodies remains constant. The circular orbit is in the plane of vectors \mathbf{i}, \mathbf{j} .

According to the theorem, it is sufficient to solve the simplified system of equations

$$\begin{aligned} \frac{d\theta}{d\tau} &= \varepsilon M_1(\theta, \alpha, \tau), & Cr \frac{d\alpha}{d\tau} \sin \theta &= \varepsilon M_2(\theta, \alpha, \tau), & \frac{dr}{d\tau} &= 0 \\ M_1 &= \sin \theta \cos(\tau - \alpha) \sin(\tau - \alpha), & M_2 &= -\sin \theta \cos \theta \cos^2(\tau - \alpha). \end{aligned}$$

By averaging the right-hand sides, we obtain

$$\dot{\alpha} = -\frac{1}{2}\varepsilon \cos \theta, \quad \dot{\theta} = 0, \quad \varepsilon = \frac{3\gamma M}{R^3 r \omega} \delta = 3\frac{\omega}{r} \left(1 + \frac{m}{M}\right)^{-1}$$

From here we obtain the formula for the angular velocity of precession

$$\frac{d\alpha}{dt} = -\frac{3}{2} \left(\frac{\omega}{r}\right)^2 \delta \cos \theta \left(1 + \frac{m}{M}\right)^{-1}$$

Example 2. Lunisolar precession (fig 1). It consists of the angular velocities of the solar and lunar precessions

$$\frac{d\alpha_1}{dt} = \frac{3}{2} \frac{\omega_1^2}{r} \delta \cos \theta_1, \quad \frac{d\alpha_2}{dt} = \frac{3}{2} \frac{\omega_2^2}{r} \delta \cos \theta_2 (1 + m/M)^{-1}$$

The angle of inclination of the plane of the Earth's equator to the plane of the Earth's rotation around the Sun varies periodically between the values $22.5^\circ < \theta < 24.5^\circ$ [4, 5]. The angle of inclination of the plane of the Moon's rotation around the Earth to the plane of the Earth's rotation around the Sun varies within the range of $5^\circ < \phi < 5.28^\circ$.

Following Beletsky, we accept the following average values

$$\theta_1 = \theta_2 = 23.5^\circ, \quad \phi = 0^\circ, \quad \omega_1 = (360/N_1) \circ / \text{day}, \quad \omega_2 = (360/N_2) \circ / \text{day}, \\ r = 360^\circ / \text{day}, \quad N_1 = 365 \text{day}, \quad N_2 = 28 \text{day}, \quad \delta = 0.0033$$

The ratio of the masses of the Earth and the Moon is $m/M = 81$, and the ratio of the masses of the Earth and the Sun is neglected. Substituting these data for the velocity and period of precession, we get

$$\frac{d\alpha}{dt} = \frac{3}{2} \delta \cos \theta \left(\frac{\omega_1^2}{r} + \frac{\omega_2^2}{r} (1 + m/M)^{-1} \right) \frac{\circ}{\text{day}}, \quad P = \frac{360}{N_1 d\alpha/dt} = 26171 \text{year}$$

Modern observations give a close value of $P = 25772 \text{year}$.

Remark. After averaging the force function over the precession angle, and then over the true anomaly for the precession period, Beletski obtained a formula for the precession period that was similar in structure ([3] p. 209), but it was apparently given with typos.

The work was carried out on the topic of state assignment No. 124012500443-0.

References

- [1] Zhuravlev V.F. Fundamentals of theoretical mechanics. M.: Nauka, 1997. 320 c. (in Russian)
- [2] Zhuravlev V.F., Klimov D.M. Applied methods in the theory of vibrations. Moscow: Nauka, 1988. 326 p. (in Russian)
- [3] Beletski V.V. Motion of a satellite relative to the center of mass in a gravitational field. Moscow: Moscow State University Press, 1975. 308 p. (in Russian)
- [4] Kulikovski P.G. Handbook of amateur astronomy. Editorial URSS. 2002, 688 p. (in Russian)

- [5] Reference manual on celestial mechanics and astrodynamics. Moscow: Nauka, 1976, 864 p. (in Russian)

Petrov A.G.
Ishlinsky Institute for Problems in Mechanics RAS, Moscow, Russia
e-mail: petrovipmech@gmail.com

Dangerous asteroids and the study of their orbits

Petrov N.A.

Abstract. As a result of a numerical experiment using a new method, asteroids have been found, during the movement of which possible close approaches and collisions with the Earth occur, Jupiter, Mars, other planets of the Solar system, with the Moon. The paper describes the method and gives only a part of the structured results obtained, including the cumulative probabilities of collisions of some asteroids with planets The solar system and the Moon, as well as the probability of a possible collision with the Earth and the Moon, depending on the number of virtual asteroids. It is important that asteroids that do not yet belong to the number of "near-Earth asteroids", whose perihelion distance is greater than 1.3 au, can also pose a danger to the Earth. The definition of such objects has become possible with the use of modern computing tools.

Introduction

The Department of Celestial Mechanics of St. Petersburg State University for searching for possible collisions and approaches of asteroids with planets. The first method has been developed since about 2009. It assumes a search of the data on a one-dimensional manifold, minimization of the planetocentric distribution of the asteroid and a number of other techniques (as, for example, in [1, 2]). With this method, many previously unknown impacts of dangerous asteroids have been found, including for Apophis. The use of the Monte Carlo method is difficult in this method due to the high computational complexity. In this regard, a new method was proposed in 2021 [3], which made it possible to identify a large number of asteroids, to identify dangerous ones according to for which close approaches and collisions with the Earth, Moon and other planets are possible. Estimates of the probabilities of these events using the Monte Carlo method are also obtained. Asteroids that are usually dangerous to the Earth are searched for among those q less than 1.3 AU (near-Earth asteroids, NEA). However, the orbits of asteroids evolve, especially strongly in close encounters with planets. As a result, it is possible to switch to the ASP class of the object that was in As is known, the approach

to Jupiter can significantly change the orbit of the asteroid, the approach to Mars is significantly less. In order to distinguish the NEA class from a large number of asteroids, a numerical study of the possible movements of a large number of known asteroids was carried out. Asteroids have been found with perihelion distances exceeding 1.3 au. Next, we examined these 24 asteroids in detail using the first method. They have close approaches and even collisions with the Earth, Moon and other planets in the time interval of 2020-2200 years.

1. Description of the numerical experiment

Let's describe a numerical experiment developed at the Department of Celestial Mechanics St. Petersburg State University in 2021-2023, using a software package [3]. Asteroids with a perihelion distance q greater than 1.8 au and at the same time having an aphelion distance (data were taken on 03/06/2021 from the above-mentioned NASA database [4, 5]). Small asteroids with an absolute value of $H > 26$ are also excluded. Of all the known asteroids (about a million are known), thousands of objects. Here are the stages of a numerical experiment to find dangerous asteroids. The technique of the experiment is that at each stage we exclude asteroids that do not approach planets less than a given distance. For each real asteroid under study, N is the number of virtual asteroids. The motion of virtual asteroids is being studied in the time interval 2132 years. The first stage. For each real asteroid out of the remaining (127 thousand objects), at $N=2000$ virtual asteroids, possible approaches are searched for - standing less than 1000 radii of one of the planets or the Moon. If there are no it is excluded. There are 11 thousand asteroids left, which are taken to the next second stage. For each of the remaining objects, at $N=20$ thousand virtual asteroids, possible approaches to a distance of less than 100 radii of one of the planets or the Moon are searched. If there are none, the asteroid is excluded over 3,000 asteroids left, which are being taken to the next stage. The third stage. Each remaining asteroid is modeled by $N = 200,000$ separate virtual instances. Possible approaches of 100, 10 and 1 radius are being searched for each of the planets and the moon.

2. Some results of the numerical experiment

The results of the numerical experiment are presented on the website [6]. In particular asteroids with a perihelion distance of more than 1.3 au have been found, having possible approaches to the Earth at a distance of less than 100 o . For almost all of these asteroids, approaches and possible collisions with Jupiter have been recorded, and there are many approaches to Mars. A other planets have also been found. Let's take asteroid 2011 XD3 as an example. Here data: the perihelion distance is 1.53 AU, the accuracy is 0.0008 au (1 sigma). The maximum distance is 5.16 AU, the accuracy is 0.07 AU (1 sigma). As a result of the experiment, we obtain two approaches to the Earth by less than 100 of its radii, 6 approaches to

Mars by less than 100 of its radii, 3751 approaches to Jupiter by less than 100 of its radii, 512 approaches to Jupiter by less than 10 of its radii, 103 possible collisions with Jupiter. Asteroids with perihelion distance 1.3 and more.e. and convergent with the Earth at a distance of less than 100 and its radius to 2132 year: 2020 KH, 2011 XD3, 2006 CQ, 2020 RJ8, 2019 YH3, 2010 UC8, 2019 WY6, 2019 UQ10, 2009 LB. Note that for the asteroid 2006 CQ, we found a possible collision with the Earth in 2169. The cumulative probabilities of collisions of various asteroids with planets and the Moon are multiplied by 200,000 for ease of recording and comparison. Then we will write down the cumulative collision probabilities obtained in the form of a list below: — Earth: 2000 SG344 — 709, 2008 HJ — 53, — Moon: 2015 AZ43 — 12, 2008 JL3 — 9, — Mercury: 2009 UM1 — 5, 2018 VB1 — 2, — Venus: 2009 CE — 144, 2020 MA1 — 132, — Mars: 2007 WD5 — 34, 2006 BX39 — 9, — Jupiter: 2018 BJ11 — 463, 2019 JD14 — 303. Let's explain the meaning of these numbers using the example of asteroid 2000 SG344. At the third stage of the experiment, 200,000 virtual asteroids were started. For the asteroid under consideration, 709 possible impacts with the Earth were obtained in the time interval 2020 — 2132 years. This means that the probability of impact is $709/200000=3.5e-3$. On the NASA website, in the dangerous asteroids section, the probability for this asteroid is $2.7e-3$ in the time interval 2069-2122 years. This is logical for other asteroids. The change in probabilities depending on the number of virtual asteroids was also considered. For asteroid 2021 the probabilities P (multiplied by 10^5) of an impact with the Earth and the Moon are in Table 1.

| N | Earth ($P * 10^5$) | Moon ($P * 10^5$) |
|--------|----------------------|---------------------|
| 10^4 | 10.0 | 10.0 |
| 10^5 | 13.0 | 6.0 |
| 10^6 | 16.0 | 5.3 |
| 10^7 | 15.0 | 4.5 |

TABLE 1. The probability of impact (multiplied by 10^5) with the Earth and the Moon asteroid 2021 QM1, depending on the number of virtual asteroids

Conclusion

As a result of a numerical experiment using a new method, asteroids have been found, the movement of which possible close approaches and collisions with the Earth occur, Jupiter, Mars, other planets of the Solar system, with the Moon. The paper describes the method and gives only a part of the structured results obtained, including the cumulative probabilities of collisions of some asteroids with planets The solar system and the Moon, as well as the probability of a possible collision wi and the Moon, depending on the number of virtual asteroids. It is important that

asteroids that do not yet belong to the number of "near-Earth asteroids", whose perihelion distance is greater than 1.3 au, can also pose a danger to the Earth. The definition of modern computing tools.

References

- [1] Petrov N, Sokolov L., Polyakhova E., Oskina K. Predictions of asteroid hazard to Earth for the 21st century // AIP Conference Proceedings 1959, 040012 (2018); doi: 10.1063/1.5034615
- [2] Petrov N.A., Vasiliev A.A., Kuteeva G.A., Sokolov L.L. On the trajectories of asteroids 2015 RN35 and Apophis colliding with the Earth // Astronomical Bulletin Exploration of the Solar system. 2018. Vol. 52. No. 4. C. 330-342.
- [3] Balyaev I. A. Acceleration of numerical integration of the equations of motion of asteroids, Sol. Syst. Res. 54, 557–566 (2020). [https://doi.org/ 10.1134/S0038094620330011](https://doi.org/10.1134/S0038094620330011)
- [4] Jet Propulsion Laboratory. California Institute of Technology. Small-Body Database Lookup. Electronic resource: [https : //ssd.jpl.nasa.gov /](https://ssd.jpl.nasa.gov/) (accessed March 30 , 2024)
- [5] Jet Propulsion Laboratory. California Institute of Technology. Electronic resource [https : //sneos.jpl.nasa.gov /](https://sneos.jpl.nasa.gov/) (accessed March 30, 2024)
- [6] Astronomy at St. Petersburg University. Electronic resource: [http : //www.astro.spbu.ru/sites/default/files/stats 2 00000.xls](http://www.astro.spbu.ru/sites/default/files/stats_2_00000.xls) (accessed March 30 , 2024)

Petrov N.A.
Mathematical and mechanical faculty
Saint-Petersburg State University
Saint-Petersburg, Russian Federation
e-mail: n.petrov@spbu.ru

A new example of stable chaotic orbit in asteroid belt: 2022 QB59 and 2022 RM50

Rosaev Alexey

Abstract. We report about a new example of stable chaotic motion. Two asteroids (2022 QB59 and 2022 RM50) are moving in an almost identical orbit, close to a 3:11 resonance with Earth. The orbits are very stable, despite the chaotic fluctuations of the semi-major axis.

Introduction

(5026) Martes and 2005 WW113 are listed in the paper by Vokrouhlicky and Nesvorny between pairs with a low relative velocity [1]. Later, Pravec, Vokrouhlicky [2] noted that the pair is perturbed by irregular jumps over a weak mean motion resonance. Briefly, identification with 3:11 E resonance was mentioned in paper by Rosaev, Plavalova [3].

Recently, three asteroids close to this pair have been discovered: 2011 RF40, 2022 QB59 and 2022 RM50 (Vokrouhlicky, et al, (2024)). Consequently, the group associated with 5026 Martes becomes a very young family. The discovery is very important for understanding the origin of this cluster because the direct separation of 2005 WW113 from 5026 Martes requires notably large relative velocity or unrealistic values of the Yarkovsky effect.

1. Result of the new members of Martes family orbits integrations

Here we study these new members with an emphasis on their resonant perturbations. First, we integrate the orbits of the new members with the perturbations of the large planets only. Note that the three of new members (2011 RF40, 2022 QB59 and 2022 RM50) orbited closer to the 3:11E resonance as well as 5026 Martes. Therefore their separation is easier than 2005 WW113. Two new members (2022 QB59 and 2022 RM50) are moving in an almost identical orbit. The result is shown in fig 1. The minimum distance between 2022 QB59 and 2022 RM50 is

about 4500 km in the epoch 17.003 thousand years ago. Despite the intersection of the resonance about 3, 6, 16, 21 thousand years ago, the distance between them does not exceed 0.28 AU during the entire considered interval (Fig.2). This means that 2011 RF40, 2022 QB59 and 2022 RM50 orbited in a very stable region of phase space which is interesting in itself. However, the closest encounter with 5026 Martes occurred an about 17.45 kyr ago.

This conclusion is confirmed by our integration with Ceres and Vesta effect. The orbits of 2022 QB59 and 2022 RM50 remain unchanged, while the orbits of 2011 RF40 and 5026 Martes slightly change the mean semimajor axis.

Moreover, the orbit of 2011 RF40 in the time interval between 31 and 24 thousand years ago becomes the same as the orbits of 2022 QB59 and 2022 RM50. The minimum distance between 2022 QB59 and 2022 RM50 is about 1720 km at 17.075 kyr. However, the closest encounter with Martes takes place an about 15.45 kyr ago for this case.

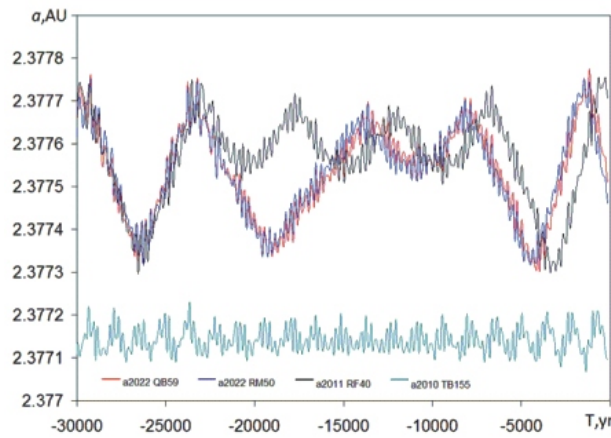


FIGURE 1. The semimajor axis evolution of 2011 RF40, 2022 QB59 and 2022 RM50

Conclusion

In the paper we report about a new example of stable chaotic motion. Two asteroids (2022 QB59 and 2022 RM50) are moving in an almost identical orbit, close to a 3:11 resonance with Earth. The orbits are very stable, despite the chaotic fluctuations of the semi-major axis.

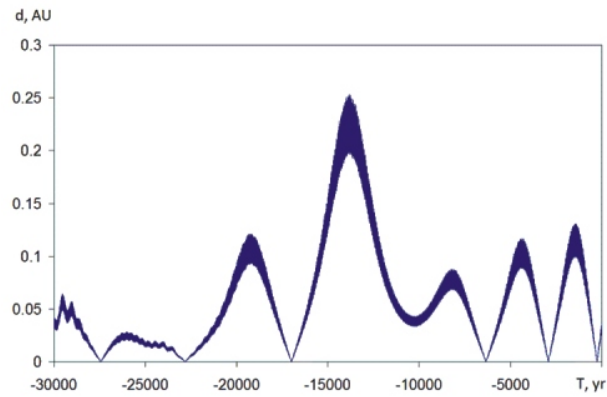


FIGURE 2. Distance between 2022 QB59 and 2022 RM50 evolution

References

- [1] D. Vokrouhlicky, D. Nesvorny, *Pairs of asteroids probably of a common origin.* , The Astronomical Journal, 136, 280-290, 2008.
- [2] P.Pravec, D. Vokrouhlicky, *Significance analysis of asteroid pairs.*, Icarus 204, 580-588, 2009
- [3] A.E.Rosaev, E. Plavalova, *Some of the most interesting cases of close asteroid pairs perturbed by resonance*, Proceedings of the International Astronomical Union, Volume 364, 226-231 (2022).
- [4] D. Vokrouhlicky, et al., *Debiased population of very young asteroid families.* , A&A, 681, A23 (2024)

Rosaev Alexey
 Research and Educational Center "Nonlinear Dynamics"
 Yaroslavl State University
 Yaroslavl, Russia
 e-mail: hegem@mail.ru

Localized trajectories of cosmic particles near libration points

Tatiana Salnikova and Eugene Kugushev

Abstract. We discuss a new behavior of a dynamic system near an unstable equilibrium position. We call corresponding trajectories located in the selected neighborhood of unstable equilibrium as localized trajectories.

The use of topological methods for proving the existence of localized trajectories makes possible to abandon the condition of analyticity of the first integrals and the condition of non-resonance of purely imaginary roots of the characteristic equation for the systems of Lyapunov.

As an important application, we consider perturbed motion in libration points vicinity of the restricted circular three-body problem. Numerical simulations for the parameters of the Earth-Moon system convincingly illustrate our theoretical study.

Introduction

Let us consider a dynamical system whose equilibrium position is non-degenerate and unstable in Lyapunov sense, and its degree of instability is greater than zero and less than the number of degrees of freedom. When considering the behavior of a mechanical system near an equilibrium position or near a steady state of motion, when higher-order terms in the expansions of kinetic and potential energies are also taken into account, one has a system of differential equations with additional non-linear terms. A.M. Lyapunov showed that, under very general assumptions, such a system admits periodic solutions of a certain type and indicated an effective way to calculate these solutions.

Our work deals with a situation where a mechanical system with $n > 1$ degrees of freedom has a non-degenerate Lyapunov unstable equilibrium position, the degree of instability of which ν lies within $1 \leq \nu \leq n - 1$. The energy at the equilibrium position is assumed to be zero. It is shown that for any sufficiently small positive value of the total energy of the system, there is a motion of the system with a given energy value that begins at the boundary of the region where

motion is possible and does not leave a small neighborhood of the equilibrium position. We call such motions as localized motions.

An essential condition for the presence of such movements is the limitation of system movements in “unstable directions.” For natural systems with gyroscopic and dissipative forces, this is ensured by the conservation or non-increase of the total mechanical energy. The use of topological Ważewski method applying the Borsuk concept of retract [1, 2] in the analysis of such motions makes possible to abandon the condition of analyticity of the first integrals and the condition of non-resonance of purely imaginary roots of the characteristic equation. The presence of time-dependent gyroscopic and dissipative forces, as well as forces with incomplete dissipation, does not interfere with the proof of the existence localized solutions [3].

As an example, we consider the planar restricted circular three-body problem. Two triangular libration points have an even degree of instability. For certain mass ratios of the two main bodies they are gyroscopically stable, and we don't consider them in our application.

Three collinear libration points have degree of instability equal to unity, therefore, according to the Kelvin-Chetaev theorem, they cannot be stabilized by adding dissipative and gyroscopic forces. Nevertheless, in accordance with our research, localized trajectories should exist near these unstable collinear libration points. Numerical simulations for the parameters of the Earth-Moon system convincingly illustrate our theoretical study.

1. Perturbed linear system of the second order.

We consider the following system:

$$\ddot{x} = A(t)x + B(t)\dot{x} + \mu g(x, \dot{x}, t), \quad x \in W \subseteq R^n, \quad t \geq 0; \quad (1)$$

where $\mu \geq 0$ — parameter, W — an open domain containing point $x = 0$.

It is assumed that in the domain W for $t \geq 0$ the matrices $A(t)$, $B(t)$ and the function $g(x, t)$ are continuous in (x, t) and norm-bounded:

$$\|A(t)\| \leq a, \quad \|B(t)\| \leq b, \quad \|g(x, t)\| \leq d, \quad x \in W, \quad t \geq 0, \quad (2)$$

for some constants a, b, d .

Definition For $\varepsilon > 0$ we introduce an open neighborhood $U_\varepsilon = \{x : \|x\| < \varepsilon, x \in R^n\}$. A solution $x(t)$ of system (1) will be called localized in a neighborhood of U_ε , if it begins at $t = 0$ in this neighborhood, exists for $t \geq 0$, and does not leave U_ε for $t \geq 0$.

Theorem.

Let the matrix A be symmetric for $t \geq 0$, its characteristic numbers are positive, bounded, and separated from zero uniformly in t , i.e.

$$c\|x\|^2 \leq (A(t)x, x) \leq a\|x\|^2, \quad \text{for } t \geq 0, \quad \forall x \in R^n \quad (3)$$

where $c > 0$ — some constant, and

$$c - b\sqrt{a} > 0.$$

Let also the matrix \dot{A} be non-negative definite, and the matrix $B(t)$ be non-positive definite, and the perturbation $g(x, \dot{x}, t)$ is dissipative, for all $x \in U_\varepsilon$, $t \geq 0$:

$$(\dot{A}(t)\dot{x}, \dot{x}) \geq 0, \quad (B(t)\dot{x}, \dot{x}) \leq 0, \quad (g(x, \dot{x}, t), \dot{x}) \leq 0, \quad \forall \dot{x} \in R^n. \quad (4)$$

And let for $t \geq 0$ the function $g(x, t)$ satisfy the Lipschitz condition uniformly in t , i.e. there is $L > 0$ such that

$$\|g(x_1, t) - g(x_2, t)\| \leq L\|x_1 - x_2\|, \quad \text{for } t \geq 0. \quad (5)$$

Let us choose an arbitrary $\varepsilon > 0$ such that $U_\varepsilon \subseteq W$. Then there is $\mu^0 > 0$ that for all values of the parameter μ such that $0 \leq \mu < \mu^0$, there exists a solution of system (1), localized in a neighborhood of U_ε .

2. Collinear libration points

Lagrange equations of perturbed planar restricted three-body problem read:

$$\begin{aligned} \ddot{x}_1 &= -\omega^2 x_1 + c\dot{x}_2 + f_1(\mathbf{x}, \dot{\mathbf{x}}) \\ \ddot{x}_2 &= \alpha^2 x_2 - c\dot{x}_1 + f_2(\mathbf{x}, \dot{\mathbf{x}}), \end{aligned} \quad f_i = O(\mathbf{x}^2 + \dot{\mathbf{x}}^2), \quad i = 1, 2, \quad (6)$$

where c — some constant (possibly, $c(t)$), intensity of gyroscopic forces.

We fix $h > 0$. Area of possible of motion of unperturbed problem is the following: $\omega^2 x_1^2 - \alpha^2 x_2^2 \leq 2h$. Let us define a closed subdomain W in it: $\alpha^2 x_2^2 \leq 4h$. Figure 1 shows the trajectories starting with zero-velocity (acceleration is greater than zero) from the left part of the boundary of W . Libration point $L1$ is in the center of W — point $(0, 0)$. The upper part of the trajectories leave the vicinity of the libration point through the upper part of the boundary, the lower part of the trajectories leave through the lower part of the border. It means, that for each energy level at least one trajectory starting on the left side of the boundary will remain in the vicinity of the libration point, which is proven in Theorem.

Conclusion

For natural systems with two degrees of freedom, localized motions are periodic, similar to the result of the corresponding theorem for Lyapunov systems. In the general case, our proof does not require the conditions of non-resonance of purely imaginary roots of the characteristic equation and the presence of an analytical first integral of the dynamical system. With addition of gyroscopic forces and of dissipative forces (with or without complete dissipation), and possibly time-dependent ones, the existence of localized motions is also proven.

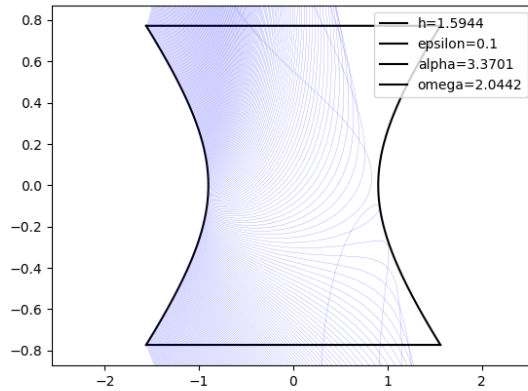


FIGURE 1. L1 vicinity

References

- [1] K.Borsuk, *Theory of retracts*, Polish Scientific Publishers, 1967.
- [2] D.Reissig, G.Sansone, and R.Conti, *Qualitative theorie nichtlinearer differentialgleichungen*, Roma: Edizioni Cremonese, 1963.
- [3] E.I.Kugushev, T.V.Salnikova *Existence of localized motions in the vicinity of an unstable equilibrium position*, Proceedings of the Steklov Mathematical Institute. 2024, V. 4.

Tatiana Salnikova
 Dept. of Mechanics and Mathematics
 Lomonosov Moscow State University
 Moscow, Russia
 e-mail: tatiana.salnikova@gmail.com

Eugene Kugushev
 Dept. of Mechanics and Mathematics
 Lomonosov Moscow State University
 Moscow, Russia
 e-mail: kugushevei@yandex.ru

Norm of orbit displacement in a problem with perturbing acceleration varying inversely with the square of the heliocentric distance

T. N. Sannikova

Abstract. Let a point of zero mass move under the influence of attraction to the Sun and a small perturbing acceleration $\mathbf{P}' = \mathbf{P}/r^2$, where r is the heliocentric distance. The components of the vector \mathbf{P} are assumed to be constant in one of the two reference frames: \mathcal{O}_1 , associated with the radius vector, and \mathcal{O}_2 , associated with the velocity vector. Here are the expressions for the Euclidean (root-mean-square over the mean anomaly) norm of displacement $\varrho^2 = \|d\mathbf{r}\|^2$ in two reference frames for this problem, where $d\mathbf{r}$ represents the difference between the position vectors in the osculating and mean orbit. Using these expressions, the ϱ displacement of model asteroids with different orbital eccentricities due to the Yarkovsky effect is estimated.

Introduction

We considered the motion of the asteroid \mathcal{A} under the influence of attraction to the Sun \mathcal{S} and additional perturbing acceleration \mathbf{P}' . Let the acceleration \mathbf{P}' vary inversely with the square of the r distance from \mathcal{S} , that is, $\mathbf{P}' = \mathbf{P}/r^2$. We introduced two orbital reference frames \mathcal{O}_1 and \mathcal{O}_2 with a origin \mathcal{S} . The axes for the \mathcal{O}_1 frame are directed along the radius vector, the transversal (perpendicular to the radius vector in the osculating plane in the direction of motion), and the binormal (directed along the angular momentum vector). The axes for the \mathcal{O}_2 frame are directed along the velocity vector, the main normal to the osculating orbit and the binormal.

Let the acceleration \mathbf{P}' be small in comparison with the main acceleration κ^2/r^2 :

$$\max \frac{|\mathbf{P}'|}{\kappa^2 r^{-2}} = \max \frac{|\mathbf{P}|}{\kappa^2} = \mu \ll 1,$$

where $\mathbf{r} = \mathcal{S}\mathcal{A}$, $r = |\mathbf{r}|$, κ^2 is the product of the gravitation constant by the mass \mathcal{S} . The vector \mathbf{P} has components S, T, W in the system \mathcal{O}_1 and components $\mathfrak{T}, \mathfrak{N}, W$ in the system \mathcal{O}_2 . We assume that they are constant and small on the order of μ .

Sannikova and Kholshchevnikov [1] applied an averaging procedure to the Euler-type equations of motion and obtained mean-elements motion equations and formulas for the transition from osculating elements to the mean ones in the first order of smallness for this problem (we neglected the second order quantities). For this problem in the \mathcal{O}_1 system, the paper [2] obtained the Euclidean (root mean square over the mean anomaly) displacement norm $\rho^2 = \|d\mathbf{r}\|^2$, where $d\mathbf{r}$ represents the difference between the position vectors on the osculating and mean orbit. The expression for the Euclidean norm in the \mathcal{O}_2 reference frame is also presented below. Using these expressions, it is possible to estimate the magnitude ρ of short-period orbital disturbances arising due to the presence of a small perturbing acceleration \mathbf{P}' varying inversely with the square of the heliocentric distance, e.g. due to the Yarkovsky effect.

1. Equations

The Euclidean norm of the difference between osculating and mean elements in the \mathcal{O}_1 is

$$\varrho_1^2 = \|d\mathbf{r}\|^2 = \frac{a^2}{\kappa^4}(A_1S^2 + A_2T^2 + A_3W^2), \quad (1)$$

where

$$\begin{aligned} A_1 &= \frac{1}{2}(2 + 3e^2), \\ A_2 &= \frac{1}{(1 - e^2)^2} \left(16 + \frac{3365e^2}{32} - \frac{12601e^4}{1152} - \frac{13327e^6}{2048} - \frac{226339e^8}{163840} - \mathcal{O}(e^{10}) \right), \\ A_3 &= 1 - \frac{39e^2}{32} + \frac{101e^4}{576} + \frac{599e^6}{6144} + \frac{19889e^8}{307200} + \mathcal{O}(e^{10}), \end{aligned} \quad (2)$$

a is the semi-major axis and e is the eccentricity. The expressions (2) give acceptable accuracy for $e < 0.6$. More accurate expressions of the A_n functions in the form of series in powers of e and in powers of $\beta = e/(1 + \sqrt{1 - e^2})$ were obtained in [2].

The Euclidean norm of the difference between osculating and mean elements in the \mathcal{O}_2 is

$$\varrho_2^2 = \|d\mathbf{r}\|^2 = \frac{a^2}{\kappa^4}(B_1\mathfrak{T}^2 + B_2\mathfrak{N}^2 + B_3W^2). \quad (3)$$

where

$$\begin{aligned} B_1 &= \frac{1}{(1 - e^2)^2} \left(16 + \frac{1121e^2}{8} + \frac{10793e^4}{512} - \frac{239033e^6}{18432} - \frac{17713751e^8}{18874368} - \mathcal{O}(e^{10}) \right), \\ B_2 &= \frac{1}{(1 - e^2)^2} \left(1 + \frac{29e^2}{8} - \frac{2221e^4}{288} + \frac{1907e^6}{512} - \frac{265501e^8}{491520} - \mathcal{O}(e^{10}) \right), \end{aligned}$$

$$B_3 = 1 - \frac{39e^2}{32} + \frac{101e^4}{576} + \frac{599e^6}{6144} + \frac{19889e^8}{307200} + \mathcal{O}(e^{10}). \quad (4)$$

The expressions (4) give acceptable accuracy for $e < 0.6$. The derivation of the displacement norm in the \mathcal{O}_2 is being prepared for publication; more precise expressions for the B_n functions will also be given there.

Let's compare the ρ_1^2 and ρ_2^2 norms. The formulas for the main results (1) and (3) are identical up to the replacement of the components of the perturbing acceleration. In both cases, the $\|d\mathbf{r}\|^2$ norm depends only on the components of the \mathbf{P} vector (positive definite quadratic form), the semimajor axis (proportional to the second power) and the eccentricity of the osculating ellipse. The $A_n(e)$ and $B_n(e)$ functions are series in even degrees of eccentricity. The $A_3(e)$ and $B_3(e)$ functions coincide, since the W component is the same for both reference systems. In the \mathcal{O}_1 frame the $A_1(e)$ function is a polynomial of the second degree, while in the \mathcal{O}_2 system $B_1(e)$ is an infinite series, $A_2(e)$ and $B_2(e)$ are series in both systems. Since at zero eccentricity the $(-\mathfrak{N}, \mathfrak{T}, W)$ trihedron is identical to the (S, T, W) trihedron, then $A_1(0) = B_2(0)$, $A_2(0) = B_1(0)$ and $A_3(0) = B_3(0)$, that is, the free terms of (2) and (4) coincide, as it should be.

2. Application

| e | $\mathfrak{T}, 10^{-14}$ AU ³ /day ² | $\mathfrak{N}, 10^{-14}$ AU ³ /day ² | $\varrho_2,$ m | $\varrho_1,$ m |
|-------|---|---|-------------------|-------------------|
| 0.001 | -5.10168 | -9.91079 | 129.185 | 129.185 |
| 0.01 | -5.10155 | -9.91054 | 129.245 | 129.231 |
| 0.10 | -5.08887 | -9.88585 | 135.127 | 133.848 |
| 0.20 | -5.04976 | -9.80969 | 152.479 | 147.865 |
| 0.30 | -4.98212 | -9.67805 | 180.585 | 171.674 |
| 0.40 | -4.88179 | -9.48280 | 219.968 | 206.987 |
| 0.50 | -4.74156 | -9.20998 | 273.527 | 258.152 |
| 0.60 | -4.54897 | -8.83547 | 348.406 | 335.067 |
| 0.70 | -4.28099 | -8.31451 | 461.304 | 461.827 |
| 0.80 | -3.88832 | -7.55138 | 658.382 | 711.424 |
| 0.90 | -3.22864 | -6.26976 | 1136.522 | 1448.588 |
| 0.99 | -1.53792 | -2.98595 | 5562.831 | 14545.945 |

TABLE 1. Tangential \mathfrak{T} and normal \mathfrak{N} components, the ϱ_1 and ϱ_2 displacements, calculated at different eccentricities e

The article [3] considers model objects with different orbital eccentricities from 0 to 0.99, and other orbital and thermophysical characteristics, like asteroid Bennu, and finds the mean-orbital values of the \mathbf{P} vector components in the \mathcal{O}_1 and \mathcal{O}_2 systems. Turning to the results [3], let us calculate the ϱ_1 and ϱ_2

orbit displacements for these model objects. The following constants were used in the calculations: $1 \text{ AU} = 1.495978707 \times 10^{11} \text{ m}$, $\kappa^2 = 1.32712440041279419 \times 10^{20} \text{ m}^3 \text{ s}^{-2}$, $1 \text{ day} = 86400 \text{ s}$. For all cases $a = 1.126391025894812 \text{ AU}$, $S = 9.91079 \times 10^{-14} \text{ AU}^3/\text{day}^2$, $T = -5.10168 \times 10^{-14} \text{ AU}^3/\text{day}^2$, $W = 0$. The table 1 contains the other initial data and calculation results.

From the table 1 it is clear that as e increases, the magnitude of periodic disturbances caused by the Yarkovsky effect increases, although the modulo values of the \mathfrak{T} and \mathfrak{N} components decrease. In the \mathcal{O}_1 system, the S and T components do not depend on e , but the increase in ϱ_1 at high e is more pronounced than in the \mathcal{O}_2 system. This may indicate an overestimation of the short-period orbital disturbances for objects in highly elliptical orbits when it is calculated in the \mathcal{O}_1 system.

In general, at low perturbing acceleration characteristic of the Yarkovsky effect, the displacement of the osculating orbit relative to the mean one is small and can be neglected, taking into account only the secular drifts of the orbital elements, as was shown in [2].

Conclusion

Expressions for the Euclidean (root mean square over the mean anomaly) norm of the difference between osculating and mean elements are represent in two orbital frames of reference: \mathcal{O}_1 , associated with the radius vector, and \mathcal{O}_2 , associated with the velocity vector. The short-period orbit disturbances of model asteroids with different orbital eccentricities due to the Yarkovsky effect is estimated.

This work was supported by ongoing institutional funding as part of the state assignment (topic No. 22022400207-0).

References

- [1] T. N. Sannikova & K. V. Kholoshevnikov, *The Averaged Equations of Motion in the Presence of an Inverse-Square Perturbing Acceleration*, *Astron. Rep.*, v. 63, p. 420, 2019.
- [2] T. N. Sannikova, *Displacement Norm in the Presence of an Inverse-Square Perturbing Acceleration in the Reference Frame Associated with the Radius Vector*, *Astron. Rep.*, v. 68, p. 331, 2024.
- [3] T. N. Sannikova, *Accounting for the Yarkovsky Effect in Reference Frames Associated with the Radius Vector and Velocity Vector*, *Astronomy Reports*, v. 66, p. 500, 2022.

T. N. Sannikova

Laboratory of small solar system bodies of the Solar Physics and Solar System Department

Crimean Astrophysical Observatory of the Russian Academy of Sciences

Nauchny, Crimea, Russia

e-mail: tnsannikova@craocrimea.ru

Collocation integrator based on Legendre polynomials

V.Sh. Shaidulin

Abstract. This work presents an algorithmic implementation of a collocation integrator based on Legendre polynomials. Issues about effective implementation, application conditions, and numerical stability are considered. The presented integrator already has a software implementation.

Introduction

Collocation integration methods are a different interpretation of the class of Runge–Kutta methods first noted by Hammer and Hollingsworth [1, 2]. The essence of this interpretation is to present the solution in a polynomial form. It is interesting to note that, unlike other integration methods, we obtain a continuous solution at each step. This work presents an algorithmic implementation of a collocation integrator based on Legendre polynomials.

1. Collocation polynomial

Suppose we have a system of ordinary differential equations, represented in the form

$$\dot{\mathbf{y}} = \mathbf{f}(t, \mathbf{y}), \quad \mathbf{y} \in \mathbb{O} \subseteq \mathbb{R}^n, \quad \mathbf{f} : \mathbb{R} \times \mathbb{O} \rightarrow \mathbb{R}^n. \quad (1)$$

Collocation integration methods propose to approximately represent the solution of a system at a step of size h with a beginning at t_0 in the form of a collocation polynomial \mathbf{u} of a given degree s :

$$\mathbf{y}(t_0 + h\tau) \approx \mathbf{u}(\tau),$$

where τ is dimensionless time varying on the interval $[0, 1]$. We can define the polynomial $\mathbf{u}(\tau)$ as a linear combination over some basis $P_k(\tau)$:

$$\mathbf{u}(\tau) = \sum_{k=0}^s \boldsymbol{\alpha}_k P_k(\tau), \quad \boldsymbol{\alpha}_k \in \mathbb{R}^n.$$

The coefficients α_k are implicitly determined by a system of nonlinear equations obtained from (1) for some set of nodes c_j of size s :

$$\begin{aligned} \sum_{k=1}^s \alpha_k P'_k(c_j) &= \mathbf{f}(t_0 + hc_j, \mathbf{y}_j)h, & \mathbf{y}_j &= \sum_{k=0}^s \alpha_k P_k(c_j), \\ \alpha_0 + \sum_{k=1}^s \alpha_k P_k(0) &= \mathbf{y}(t_0). \end{aligned} \quad (2)$$

2. Calculation of coefficients α_k

For efficient calculations, we rewrite system (2) in the form:

$$\sum_{k=1}^s \alpha_k P'_k(c_j) = \mathbf{f}(t_0 + hc_j, \mathbf{y}_j)h, \quad \mathbf{y}_j = \mathbf{y}(t_0) + \sum_{k=1}^s \alpha_k (P_k(c_j) - P_k(0)).$$

This allows us to move on to the matrix notation of this system of equations:

$$\mathcal{A}\mathcal{C}^T = \mathcal{F}.$$

Here α_k for $k = 1, \dots, s$ are collected into a matrix \mathcal{A} of size $n \times s$, $\mathbf{f}(t_0 + hc_j, \mathbf{y}_j)h$ into a matrix \mathcal{F} of size $n \times s$ and $P'_k(c_j)$ into a matrix \mathcal{C} of size $s \times s$. In the matrices \mathcal{A} and \mathcal{F} , the columns are the corresponding vectors in ascending order of the indices k and j . In the matrix \mathcal{C} , index k lists the columns and j lists the rows.

The calculation of matrix \mathcal{A} is done iteratively and is efficient when using modern linear algebra libraries.

3. Application conditions

Let's write it like this:

$$\mathcal{A} = \mathcal{F}\mathcal{C}^{-T}, \quad (3)$$

The iterative process of calculating the matrix \mathcal{A} , given by the equation (3), will converge if the norm of the Jacobian matrix of the right side of the equation (3) is strictly less than one:

$$\left\| \frac{\partial(\mathcal{F}\mathcal{C}^{-T})}{\partial\mathcal{A}} \right\| < 1.$$

We use the definitions given earlier and obtain a restriction for the right-hand side function \mathbf{f} :

$$\max_p \sum_{q=1}^n \sum_{i=1}^s \left| \left(\frac{\partial f_p}{\partial y^{(q)}} \right)_{\mathbf{y}=\mathbf{y}_i} \right| < \frac{1}{hsbz}. \quad (4)$$

Here:

$$b = \max_{j,k} |P_k(c_j) - P_k(0)|, \quad z = \max_{j,k} |(\mathcal{C}^{-T})_{j,k}|.$$

4. Numerical stability

Along with the convergence of the iterative process of calculating the matrix \mathcal{A} , it is important to ensure that there is numerical stability so that rounding errors don't significantly affect the result. As can be seen from equation (3), the numerical stability will be determined by the value of z introduced earlier. The smaller it is, the better.

Conclusion

The presented algorithm for the collocation integrator already has a software implementation (<https://github.com/shvak/collo>). It proved the efficiency of calculating matrix \mathcal{A} using equation (3). This work tries to determine how successful the choice of Legendre polynomials is as a basis for different quadrature grids.

References

- [1] Hammer P. C., Hollingsworth J. W., *Trapezoidal methods of approximating solutions of differential equations* // Math. Tables Aids Comput. — 1955. — Vol. 9. — P. 92–96.
- [2] Hairer E., Wanner G., Lubich C., *Geometric Numerical Integration: Structure-Preserving Algorithms for Ordinary Differential Equations. Second Edition*. Springer, 2006. — P. 644.

V.Sh. Shaidulin

The Department of Celestial Mechanics

Saint Petersburg State University

Saint Petersburg, Russia

e-mail: v.shaidulin@spbu.ru

Adiabatic approximation in dynamical studies of exoplanetary systems in mean-motion resonance

Vladislav Sidorenko

Abstract. If in a planetary system the ratio of the time periods of revolution of two planets around the host star is approximately equal to the ratio of two small integers, then such a situation is characterized as mean motion resonance (MMR). Available observational information indicates that MMR are quite common in exoplanetary systems. Analytical studies of MMR are carried out mainly within the framework of restricted or general three-body problem. In 1985, J. Wisdom proposed an approach that makes it possible to study the properties of the resonant motions of celestial bodies without any restrictions on the eccentricities and inclinations of their orbits. Since the application of this approach is associated with the construction of a special approximate integral of the problem (adiabatic invariant), it is often called the adiabatic approximation. We give a brief description of J. Wisdom's approach to the analysis of MMR and its subsequent development, illustrated by the results of the systematic use of this approach in our studies.

Introduction

Investigations of resonant motions in satellite and planetary systems are an important element in the study of their dynamical “skeleton”, the properties of which determine the properties of many other physical processes in these systems. Classical approaches are focused primarily on the construction and study of periodic solutions of equations of motion (see, for example, [1]). In 1985, J. Wisdom, relying on the theory of adiabatic invariants (AI), showed how regions with chaotic dynamics are formed in the phase space of the three-body problem in the vicinity of resonant solutions [2]. A strict justification of Wisdom's constructions and estimates of the diffusion rate of AI at MMR 3:1 were given by A.I. Neistadt [3].

Adiabatic approximation in the study of resonances

The description of MMR in Wisdom's approach is completely equivalent to the picture of resonance effects given in textbooks on the modern theory of Hamiltonian systems (for example, [4]). The behavior of the system at MMR is characterized by the presence of dynamical processes with three time scales: "fast", "semi-fast" and "slow". A "fast" dynamical process is the orbital motion of resonant bodies. The "semi-fast" process is a variation of the resonant phase (a combination of mean longitudes, longitudes of periastrons and longitudes of the ascending nodes). The "slow" dynamical process consists of the secular evolution of the shape and orientation of the orbits of celestial bodies.

For a qualitative analysis of secular effects within the Wisdom's approach, double averaging of the equations of motion is applied. Averaging is carried out in two stages. The first stage consists of averaging over "fast" processes. After a series of transformations in the averaged equations, one can write down a subsystem that describes a "semi-fast" process, and a subsystem that describes "slow" processes. If we fix the values of the "slow" variables, the "semi-fast" system turns into an integrable Hamiltonian system with one degree of freedom (allowing a transition to "action-angle" variables). Averaging along its solutions of the right-hand sides of the equations of the "slow" subsystem completes the construction of evolutionary equations used to study secular effects.

In the general case, a "semi-fast" subsystem can be considered as a Hamiltonian system with slowly varying parameters, the role of which is played by slow variables. From this interpretation it follows that the "action" variable corresponding to this subsystem will be an approximate integral of the problem - an adiabatic invariant. Taking into account the existence of this AI, Wisdom characterized his approach as an adiabatic approximation.

An important difference between the adiabatic approximation and other approaches to MMR analysis is that it allows the consideration of possible transitions between resonant modes of motion (in which the resonant phase oscillates) and non-resonant modes (the resonant phase rotates). Each such transition is accompanied by a small quasi-random change in AI and a deviation of the true motion from what is predicted by the averaged equations. Repeated changes in the mode of motion lead to the diffusion of AI (in particular, we will see as the phase trajectory of the original system eventually fills a certain region in the phase space, called the region of adiabatic chaos).

Examples of the application of the adiabatic approximation in studies of MMR

J. Wisdom proposed his approach while studying MMR 3:1 in planar restricted three-body problem. The use of this approach to study other resonances required the introduction of various modifications taking into account their specifics.

To analyze MMR in exoplanetary systems, Wisdom's approach was adapted to the general three-body problem (more precisely, to the planetary variant of this problem when two low-mass bodies are moving in slightly perturbed Keplerian orbits around a significantly more massive body).

In our talk we present some properties of MMR 1:1 and 3:1 in the planar planetary problem, established using the Wisdom's approach [5]. Different scenarios of secular evolution were found and possible manifestations of chaotic dynamics were identified.

References

- [1] A.D. Bruno, *Resricted three-body problem*. Nauka, 1990 (in Russian).
- [2] J. Wisdom, *A perturbative treatment of motion near the 3/1 commesurability*. *Icarus*. 1985. V. 63. P. 272–286.
- [3] A.I. Neishtadt, *Jumps of the adiabatic invariant on crossing the separatrix and the origin of the 3:1 Kirkwood gap*. *Sov. Phys. Dokl.* 1987. V. 32. P. 571–573.
- [4] V.I. Arnold, V.V. Kozlov, A.I. Neishtadt, *Mathematical aspects of classical and celestial mechanics*. 3rd edition. Springer New York, 2006.
- [5] V.V.Sidorenko, *Secular evolution of co-orbital motion of two exoplanets. Semi-analytical investigation*. *Celestial Mechanics and Dynamical Astronomy*. 2024. V. 136. 25 P.

Vladislav Sidorenko
Keldysh Institute of Applied Mathematics RAS
Moscow, Russia
e-mail: sidorenk@keldysh.ru

Lerman separatrix map for the problem of satellite attitude motion

Vladislav Sidorenko

Abstract. The attitude motion of an axisymmetric satellite under the influence of a gravitational torque is studied. The satellite's center of mass moves in a circular orbit in a central gravitational field. If the projection of the satellite's angular momentum vector onto its axis of symmetry is zero, then so-called "planar" motions are possible. In planar motions the axis of symmetry moves in the orbital plane and, therefore, the angular velocity vector of the satellite is perpendicular to this plane. To analyze the properties of the motions of the satellite, which are close to planar ones, perturbation theory is applied. A map is constructed that approximates the map generated by the phase flow of the system. Using this map, we were able to establish some previously unknown properties of the satellite's attitude motion in a gravitational field.

1. Problem formulation

The investigations of the attitude motion of natural and artificial celestial bodies is an important area of space flight mechanics and celestial mechanics [1].

The aim of our study is to analyze the properties of the motion of an axisymmetric satellite relative to its center of mass under the influence of a gravitational torque. It is assumed that the satellite's center of mass moves in a circular orbit in a central gravitational field.

Let \mathbf{L} be the vector of the angular momentum of the satellite relative to its center of mass O . If the projection of \mathbf{L} onto the symmetry axis of the satellite is zero, then so-called "planar" motions are possible - motions in which the symmetry axis is always in the orbital plane, and the angular velocity vector is perpendicular to this plane. In the phase space of a Hamiltonian system with two degrees of freedom, which describes the motion of an axisymmetric satellite relative to the center of mass, planar motions are associated with phase trajectories lying on a two-dimensional invariant manifold. The behavior of phase trajectories on

this manifold is similar to the behavior of trajectories on the phase portrait of a mathematical pendulum - separatrices separate trajectories corresponding to the rotations and oscillations of the satellite relative to the local vertical.

In [2, 3], the stability of planar motions of an axisymmetric satellite was studied. We tried to describe in as much detail as possible the dynamics of the system in the case when the phase trajectories are located in the vicinity of the separatrix contour.

2. Methods

L.M. Lerman developed a general approach to study Hamiltonian systems with two degrees of freedom, in the phase space of which there is an invariant manifold with separatrix loop [4]. The main idea of this approach is to construct, using perturbation theory methods, a map that approximates the map generated by the phase flow of the system.

The approximating map is obtained as a composition of a rotation operator that describes the behavior of the phase flow in the vicinity of an unstable equilibrium (which is part of the separatrix loop), and a linear map that describes the behavior of the phase flow in the vicinity of the separatrices. The map depends on parameters, finding the values of which is a separate task.

Lerman's approach was used in [5] to analyze the dynamics of a specific mechanical system - certain version of a double pendulum. Planar oscillations of an axisymmetric satellite near the local vertical differ from oscillations of a pendulum by the physical nonequivalence of situations corresponding to different directions of relative angular velocity. Therefore, we needed to introduce a number of modifications to the construction of the separatrix mapping used in [4, 5].

Another approach to constructing a map that approximates the phase flow for the similar problem can be found in [6, 7]. It should be noted that in [6, 7] the center of mass of the satellite moves in an elliptical orbit, and the consideration is limited to planar motions only.

3. Results of investigations

A map was constructed that approximates the phase flow in the problem of attitude motion of axisymmetric satellite. Its correctness was checked by comparison with the numerically constructed Poincaré sections of the phase flow.

Using this map, we were able to describe a series of bifurcations, as a result of which families of spatial periodic motions of the satellite are born from planar motions. The stability of the found families of periodic motions is studied for different values of the ratio of the longitudinal and transverse moments of inertia of the satellite.

The stability of the separatrix loop separating the planar rotational and oscillatory motions of the satellite has been studied. The critical value of the ratio

of the moments of inertia of the satellite is found, at which the loss of stability of this separatrix loop occurs.

Also the fractal nature of the dynamical structure of the phase space of the problem was revealed (by dynamical structure we mean, in particular, stationary and periodic solutions, stable and unstable invariant manifolds adjacent to these solutions).

All this allows us to conclude that the constructed map makes it possible to carry out a detailed study of the dynamics of an axisymmetric satellite in a significantly more efficient manner in comparison with previously used approaches.

References

- [1] V.V. Beletsky, *Motion of an artificial satellites around its center of mass*. NASA, 1966.
- [2] A.P. Markeev, *Stability of planar oscillations and rotations of the satellite in circular orbit*. Cosmic Research. 1975. V. 13. P. 322–336.
- [3] A.P. Markeev, B.S. Bardin, *On the stability of planar oscillations and rotations of a satellite in a circular orbit*. Celestial Mechanics and Dynamical Astronomy. 2003. V. 85. P. 51–66.
- [4] L.M. Lerman, *Hamiltonian systems with loops of a separatrix of a saddle-center*. Sel. Math. Sov. 1991. V. 10. P. 297–306.
- [5] C. Grotta Ragazzo, *On the stability of double homoclinic loops*. Commun. Math. Phys. 1997. V. 184. P. 251–272.
- [6] A.A. Burov, *On the oscillations of a satellite in an elliptical orbit*. Cosmic Research. 1984. V. 22. P. 133–134.
- [7] I.I. Shevchenko, *The separatrix algorithmic map: application to the spin-orbit motion*. Celestial Mechanics and Dynamical Astronomy. 1999. V. 73. P. 259–268.

Vladislav Sidorenko
Keldysh Institute of Applied Mathematics RAS
Moscow, Russia
e-mail: sidorenk@keldysh.ru

Identifying mean-motion and secular resonances with large language models and classical machine learning

Evgeny Smirnov

Abstract. The usage of the machine learning techniques in astronomy is experiencing significant growth, including various challenges such as predicting orbital stability, classifying celestial objects, and analyzing images. A new approach in this field is the use of large language models (LLMs), which rely on natural language processing and explicit task definitions instead of traditional statistical algorithms or probabilistic models. This talk will demonstrate the capabilities of LLMs, particularly GPT-4o and other proprietary and open-source alternatives, in analyzing visual patterns and accurately classifying asteroids. Remarkably, this is achieved without any training, fine-tuning, or coding beyond writing an appropriate natural language prompt. The overall accuracy can reach even 100 per cent. This new approach signifies a new paradigm in astronomical data analysis. The implications extend beyond the tasks discussed, as the methodology can be applied to various astronomical problems.

Evgeny Smirnov
Belgrade Astronomical Observatory
Volgina 7, Belgrade, Serbia
e-mail: smirik@gmail.com

General three body problem in the shape space

Vladimir Titov

Abstract. The general three-body problem is considered in the shape space, the space reduced by translation and rotation. In this space the symmetric periodic orbits are studied, as well as the degenerate (collinear and isosceles) orbits. The Lemaitre regularization are used to regularize the collisions for degenerate orbits. The regions of possible motion for different values of angular momentum are constructed in the shape space.

1. Introduction

The shape space is the quotient of \mathbb{R}^n by translations, rotations and scaling. For N -body problem we have several ways to reduce configuration space by translations. We can use, for example, barycentric coordinates. The more convenient way is to use Jacobi coordinates:

$$\begin{aligned}\mathbf{Q}_1 &= \mathbf{r}_2 - \mathbf{r}_1, \\ \mathbf{Q}_2 &= \mathbf{r}_3 - \frac{m_1\mathbf{r}_1 + m_2\mathbf{r}_2}{m_1 + m_2},\end{aligned}$$

So, for planar problem we have 4-dimensional configuration space.

The sphere in the space of Jacobi coordinates $(\mathbf{Q}_1, \mathbf{Q}_2)$ is \mathbb{S}^3 , and, by eliminating rotations, we obtain \mathbb{S}^2 . Thus, we naturally arrive at the classical Hopf transformation ($\mathcal{S}^1 \hookrightarrow \mathcal{S}^3 \rightarrow \mathcal{S}^2$):

$$\begin{aligned}\xi_1 &= \frac{1}{2}\mu_1|\mathbf{Q}_1|^2 - \frac{1}{2}\mu_2|\mathbf{Q}_2|^2, \\ \xi_2 + i\xi_3 &= \sqrt{\mu_1\mu_2}\mathbf{Q}_1\bar{\mathbf{Q}}_2.\end{aligned}\tag{1}$$

2. Periodic Orbits

In [1] it is shown that the symmetry groups of the general planar three-body problem are exhausted by 10 groups. Three of these groups served as the basis for the search for symmetric periodic solutions [2]. The found trajectories can

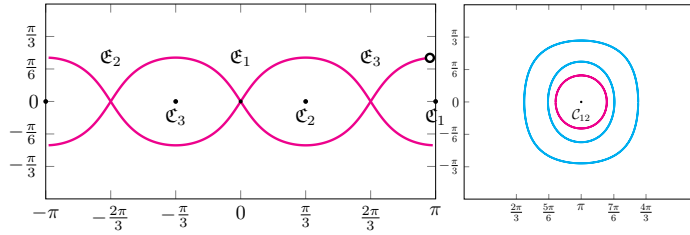


FIGURE 1. Figure-eight (left) and 2–1-symmetry orbits (right) on shape sphere

be mapped into the shape space, such a transformation is unambiguous up to the rotation of the original barycentric system. Since the distance from the origin varies little in the shape space for these trajectories (within $\pm 10\%$), then for qualitative analysis we can limit ourselves to their projection onto the sphere of shapes.

Three symmetries from the list of planar three-body problem symmetries are studied: simple choreography (only one orbit – the figure-eight), 2-1 choreographies (where two masses must be equal), and linear symmetry (where all masses differ from each other). The obtained solutions are analyzed.

Some of symmetrical orbits are shown on fig. 1.

3. The Regions of Possible Motion

If the energy constant is negative (for example, $h = -1/2$), there are five topologically distinct regions of possible motion, depending on the value of the angular momentum constant J . The type of region changes when J reaches values corresponding to the Lagrange points $L_{4,5}$, L_3 , L_2 , and L_1 . The situation is analogous to well-known surfaces of zero-velocity or Hill's surfaces in Restricted Three-Body Problem. Indeed, in the case for general three-body problem we have five topological type of surfaces depending on the value of angular momentum. It should be noted that the zero velocity surfaces in the circular restricted three-body problem are constructed in a rotating coordinate system, while in our case, they are in the shape space[3].

4. Regularization and Degenerate Orbits

For degenerate cases (collinear and isosceles trajectories) one need eliminate the singularity. For shape space the Lemaitre regularization is convinient enough. For the orbits under consideration a parameterization is constructed that allows the equations of motion for these degenerate cases, free from singularities. A lot of such orbits have been obtained numerically.

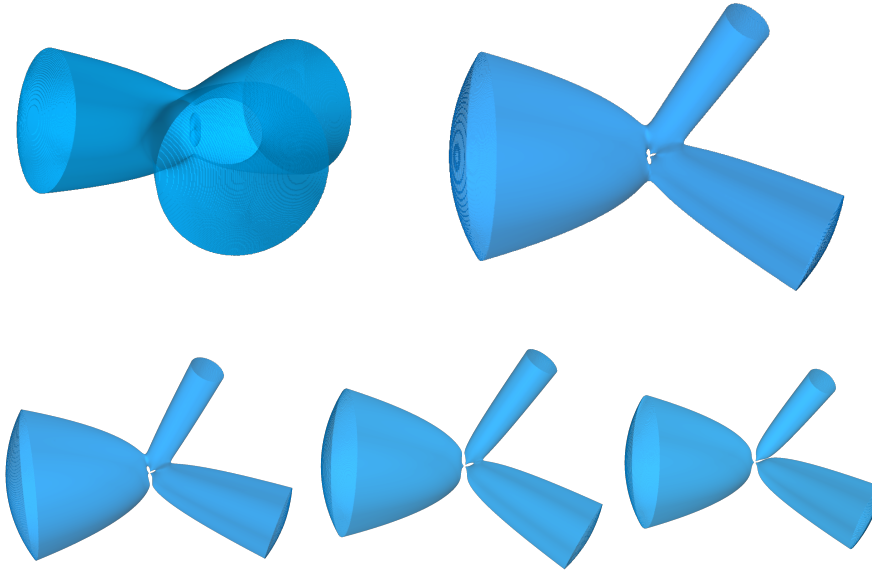


FIGURE 2. Regions of possible motion

The preimages of figure-eight orbit in configuration space regularized by Lemaitre space are very closed to circles.

5. Conclusion

The three-dimensionality of this space makes it possible to simplify the analysis of solutions, and at least simply visualize the space of solutions.

The study of periodic orbits in the shape space allows us to conclude that at least some of them have a simple form on the shape sphere: the trajectories (topologically) are a circle in the center of which lies either a singular point \mathcal{C}_i , or an Eulerian point \mathcal{E}_i .

The shape space makes it possible to construct easily the zero-velocity surfaces, and, therefore, areas of possible motion.

The Lemaitre transform allows you to simply regularize degenerate orbits. Using the given parameterizations, we regularize the Hamiltonian, and solve the equations of motion, which have no singularities, numerically. At the same time, the properties of the solutions allow us to conclude that the motion is chaotic. The corresponding orbits are given for collinear and isosceles configurations.

References

- [1] Barutello, V., Ferrario D., and Terracini S., *Symmetry groups of the planar 3-body problem and action-minimizing trajectories*. ArRMA: **190**, 2. 2008.
- [2] Titov V., *Symmetrical periodic orbits in the three body problem - the variational approach*. Annales Universitatis Turkuensis, Series 1A. Astronomica–Chemica–Physica–Mathematica: **358**, 9–15. 2006.
- [3] Titov V., *The regions of possible motion of the general planar three-body problem (in russian)*. Zap. nauchn. sem. POMI: **517**, 225–249. 2022.

Vladimir Titov
Math-mech. department
Saint-Petersburg State University
Saint-Petersburg, Russia
e-mail: tit@astro.spbu.ru

Neural network simulating the Schuster periodogram

Vladislav V. Topinskiy and Roman V. Baluev

Abstract. The search for periodic components in a time series is an important aspect of data analysis. In most cases, Schuster's periodograms or Lomb-Scargle periodograms are used depending on the homogeneity of the distribution of the original data over time. Calculating spectra is not a computationally intensive task; however, difficulties arise when processing large quantities of time series data and assessing the existence of periodic components within them. For preliminary analysis of large data sets, a convolutional neural network simulating the operation of Schuster's periodogram is suitable.

Introduction

This work represents our initial step towards accelerating the primary processing of signals in the task of exoplanet detection. Initially, a two-layer perceptron was designed to determine the existence of a sinusoidal component in a signal consisting of 128 samples by means of its Fourier transform. Each layer is defined by the following formula:

$$x_k^{i+1} = f \left(\left(\sum_{j=1}^n w_j^i x_j^i \right) + b_k^i \right), \quad (1)$$

where f – layer's activation function (sigmoid were used), w_j^i – weight, b_k^i – bias. Training time series were generated for network training and subsequent testing. Bayes factor, as described in the paper [1], was used to assess prediction accuracy.

The first attempt was not very successful: the accuracy reached only 90% for series with high amplitudes. Increasing accuracy required increasing the number of neurons, which in turn resulted in numerous "extra" connections in the network that needed to be optimized through training, consequently increasing the amount of required data. Therefore, it was decided to restructure the network to reduce

the number of neural connections while improving accuracy. In this case, the best alternative was to introduce convolutional layers into the structure.

Model description

Replacing regular layers with convolutional layers reduces the number of trainable connections and allows for an increase in the number of neurons in each layer. To

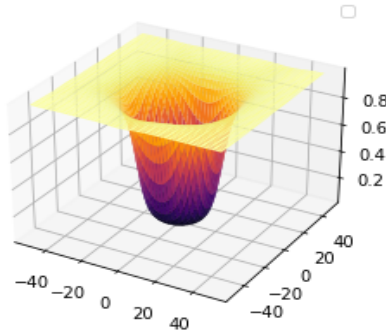


FIGURE 1. Network structure, first layer. Response graph of a 16-neuron block to a pair of real and imaginary parts of a signal sample

optimize training, weights from pre-trained models' layers were used. The network structure now consists of 2 convolutional layers processing a pair of Fourier components (Figure 1.), a technical flattening layer, and 2 regular layers responsible for finding the maximum and outputting the result as the probability of a sinusoidal component in the signal. The neural network was implemented using Python 3.8, and the network structures were taken from the module keras. Training took place over 300 epochs, with the adadelta optimizer, accuracy metric, and binary cross-entropy loss function. The choice of optimizer was based on its precise and rapid weight minimization, as determined through empirical testing.

Tests

Tests were conducted on synthesized datasets with approximately $N \sim 10^6 - 10^7$. The amount of data containing a sinusoidal component and data consisting solely of noise was equal. This volume allowed achieving a signal detection accuracy of 99% of the theoretical maximum with a small number of trainable network neurons (Figure 2.). Additionally, no overfitting issue affecting the network's response was observed.

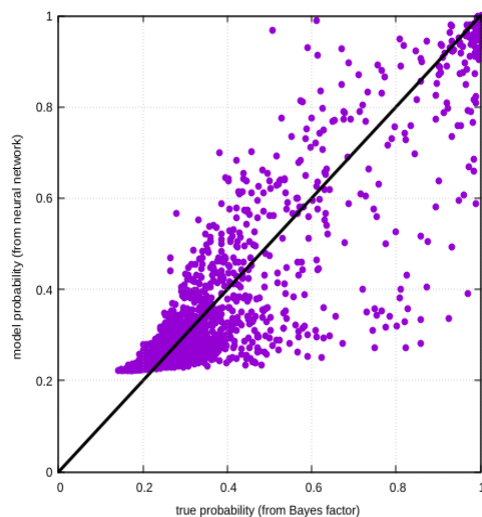


FIGURE 2. The ratio of the model probability of the existence of a signal with the theoretically possible

Conclusion

This work presented a brief description of a convolutional neural network model solving the signal detection problem. The described structure is currently not well-suited for real data; hence work is underway to expand its functionality, specifically introducing weights to time series and processing non-uniform series (simulating the operation of Lomb-Scargle periodograms). The synthesis of training datasets will also be revised for more efficient training. These steps will enable obtaining results from real data.

References

- [1] Roman V. Baluev, *Comparing the frequentist and Bayesian periodic signal detection: rates of statistical mistakes and sensitivity to priors*. preprint (2022), available at <https://arxiv.org/abs/2203.08476>.

Vladislav V. Topinskiy
Saint Petersburg State University
Saint Petersburg, Russia
e-mail: st076660@student.ru

Roman V. Baluev

Saint Petersburg State University, 7–9 Universitetskaya Emb., St Petersburg 199034,
Russia

Special Astrophysical Observatory, Russian Academy of Sciences, Nizhnii Arkhyz, 369167,
Russia

e-mail: r.baluev@spbu.ru

Towards understanding the astronomical orientation of the Old Kingdom pyramids

Irina Tupikova

Key words and phrases. Pyramids, Old Kingdom, astronomical orientation, precession.

The remarkable northern orientation of some of the Old Kingdom pyramids—Snofru’s Meidum, Bent und Red pyramids, Khufu’s, Khafre’s, Menkaure’s (4th Dynasty), and Neferirkare’s (5th Dynasty) pyramids—was formerly presumed to be a consequence of the constructions having been aligned to the position of the North Celestial Pole (NCP). However, in the range of the widely agreed upon Egyptian chronologies,¹ the maximal azimuthal deviation of the star closest to the NCP (Thuban) from true north varied between $\pm 1^\circ$ and $\pm 1^\circ 40'$; and thus couldn’t support the measured precision of the orientation of the pyramids in the range from $-35.4'$ to $30'$ (with the precision of the orientation of Khafre’s pyramid better as $-3.7'$). In 1984 an important observation was published by S. Haack [5] that the orientation of the pyramids of the Fourth Dynasty follows a special pattern of digression from true north and this progressive deviation in orientation was understood to be a consequence of the pyramids having been aligned to a star whose celestial position changed due to the effect of the general precession of the rotational axis of the Earth. S. Haack proposed that the primary alignment direction was true east, which was determined by observation of β *Scorpii* as first visible at its rising; however one couldn’t explain why the orientation of the pyramids was based upon adjustment to a relatively faint star in the east. Instead of a single star, later publications considered a possible usage of some notable stellar configurations exhibiting an azimuthal trend similar to the trend in the orientation of pyramids. All these publications considered the astronomical data to be known with great precision and treated the conventional Egyptian chronologies of this period as only relative. Accordingly, the discrepancies between the azimuths of the sides of the pyramids and the azimuths of the proposed stellar alignments

¹Several chronologies of the period are available; the three most agreed-upon chronologies are von Beckerath’s [1], Malek’s [2], and Hornung et al. [3], all modified according to Stadelmann’s [4] proposal by having 48-years for the duration of Snofru’s reign.

were interpreted purely as a consequence of erroneous historical dating and the astronomical data were used to anchor the archeological data in time. Such attempts at explanation forced researches to shift the existing Old Kingdom chronologies by some significant (and different) number of years. We have evaluated the aforementioned proposals² with the help of the actual long-term precession theory [10] and analyzed for each variant the corresponding errors of the alignments of the pyramids to the selected stellar configurations against the conventional or proposed chronologies of the Old Kingdom; it was shown that practically all the methods reveal a secular trend in the alignments and do not match the trend properly.

We assume that some other ideas played a role in the orientation of pyramids—e.g. a vertical alignment of stars might have been considered as a sort of a stellar elevator to the celestial realm, the king's final destination as stated in the *Pyramid Texts*:³ "A stairway to the sky is set for you among the Imperishable Stars [Circumpolar stars]." A remarkable geometrical configuration of stars is known for us as the constellation Little Dipper where two sides of the Dipper can each be observed as a vertical configurations at low altitude. We propose and discuss a new solution based upon the vertical alignment of Kochab and ζ UMi which shows an impressive degree of agreement with the trend in the orientation of the pyramids for von Beckerath's classical chronology and thus do not demand any temporal shift in dating of the pyramids. The special pattern of digression in the orientation of the pyramids from true north is displayed in Figure 1 where the y-axis gives the azimuths of the east sides of the pyramids,⁴ the trendline 'c' is running as a guide to the eye through these azimuths,⁵ and the time-axis follows von Beckerath's chronology. The dashed line 'a' is a trendline through the points corresponding to the azimuth of the vertical alignment of Kochab and ζ UMi at the lower position. The precision of the orientation towards this stellar alignment calculated for every pyramid along trendline 'c' separately is at a surprisingly high level: the mean deviation of the orientation of the pyramids towards the stellar vertical is ca. $-4'$ with a standard deviation of $2'$ (Tupikova [16], Fig. 30). Such a small deviation is, in fact, close to the limit of naked-eye observations.

Even better match can be obtained for the west sides of the pyramids where only scarce measurements are available. As shown in Figure 2, the precision of this orientation is very impressive and cannot be questioned for the Meidum, Bent and Khufu's pyramids. The only visible deviation from the trendline 'a' is for Menkaure's pyramid. One should take into account, however, that because the

²Spence [6]; Rawlins and Pickering [12]; Belmonte [8]; Puchkov [9].

³Faulkner [11], 156, Nt. 773–74.

⁴The azimuths to the west from true north are given as negative and to the east as positive numbers. With this counting, azimuth becomes equivalent to the deviation of a direction from true north.

⁵The known problem of the orientation of Khafre's pyramid, however, is that it is identical with that of Khufu's pyramid in spite of more than 30 years between the accession dates of the two kings. The proposed hypotheses to explain this were copying of alignment [12] or that two pyramids were laid down simultaneously ("Khufu's double project", see [13], [14] and [15]).

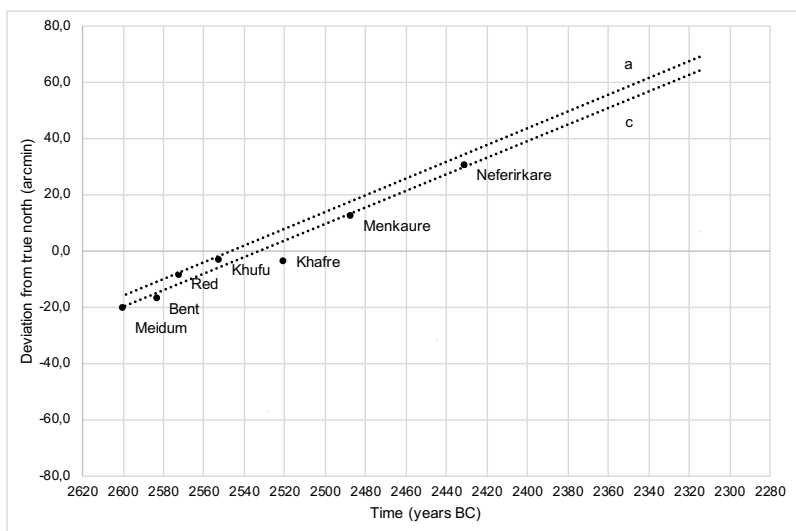


FIGURE 1. Deviation of pyramid orientations (east sides) from true north over time vs. azimuth of the lower vertical alignment of Kochab and ζ UMi (von Beckerath's chronology).

foundation of the pyramid was covered with rubble, Nell and Ruggles [17] were only able to survey the alignment of courses of stones on the pyramid itself. The results for two block courses (9th and 11th) were given with orientations of $29.5'$ and $19.7'$, correspondingly; for the latter figure, the azimuth of the west side of Menkaure's pyramid would lie exactly on the line 'a' (this position is marked at Fig. 2 with a cross).

Another remarkable stellar alignment could have been used as a crossover check for the orientation of pyramids. As we have shown, in the time of the Old Kingdom two other prominent bright stars aligned horizontally—Alioth and Mizar in the constellation Big Dipper—support von Beckerath's chronology with Mizar being a target of observations at the moment of such alignment (Tupikova [16], Figs. 19–21). It was shown that the azimuths of these two different stellar alignments would match the trend in the orientation of the pyramids with similar precision. That these alignments occurred at the time of the construction of the Old Kingdom pyramids close to true north is, in our opinion, a fortuitous event which is mainly responsible for the remarkable northern orientation of these pyramids.

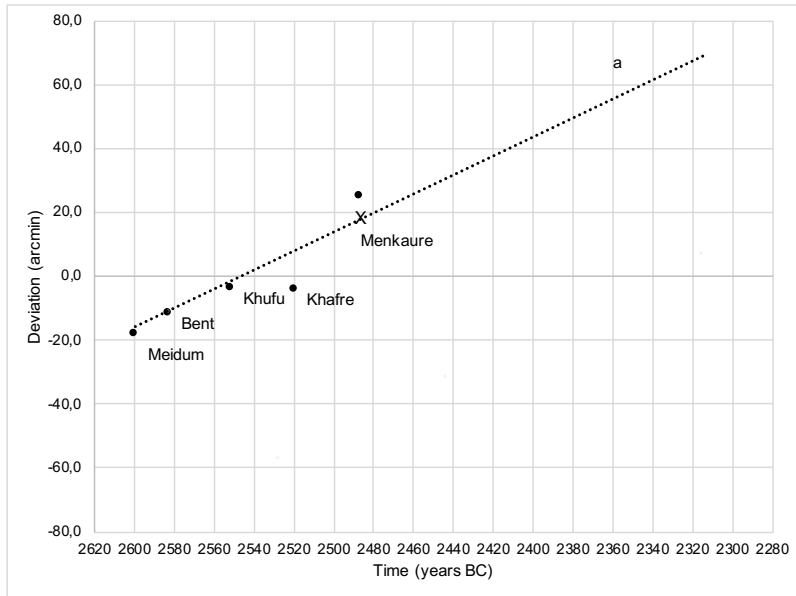


FIGURE 2. Deviations of pyramid orientations (west sides) from true north over time vs. azimuth of the lower vertical alignment of Kochab and ζ UMi (von Beckerath's chronology).

References

- [1] J. v. Beckerath, *Chronologie des pharaonischen Ägypten*, Mainz, von Zabern, 1997.
- [2] J. Malek, *The Old Kingdom*, in: *The Oxford History of Egypt*, I. Shaw (ed.), Oxford, Oxford Univ. Press, 89–117, 2000
- [3] E. Hornung, R. Krauss, and D. A. Warburton (eds), *Ancient Egyptian Chronology*, Leiden & Boston, Brill, 490–491, 2006.
- [4] R. Stadelmann, *Beiträge zur Geschichte des Alten Reiches. Die Länge der Regierung des Snofru*, MDAIK 43, 229–240, 1986.
- [5] S. Haack, *The Astronomical Orientation of the Egyptian pyramids*, *Archaeoastronomy* 7, 119–125, 1984.
- [6] K. Spence, *Ancient Egyptian chronology and the astronomical orientation of pyramids*, *Nature* 408, 320–324, 2000.
- [7] D. Rawlins, and K. Pickering, *Astronomical orientation of pyramids*, *Nature* 412, 699, 2001
- [8] J. A. Belmonte, *On the orientation of Old Kingdom Egyptian pyramids*, *Archaeoastronomy* 32(26), 1–20, 2001.

- [9] A. Puchkov, *Stretching of the Cord Ceremony for Astronomical Orientation of the Old Kingdom Pyramids*, 2019, revised 22 October 2020, available at <https://www.academia.edu/41240818>.
- [10] J. Vondrák, N. Capitaine, and P. Wallace, *New precession expressions, valid for long time intervals*, *Astronomy & Astrophysics* 534, 317–323, 2011.
- [11] R. O. Faulkner, *The King and the Star-Religion in the Pyramid Texts*, *Journal of Near Eastern studies* 25, 153–161, 1966.
- [12] D. Rawlins, *Greater Pyramid Misses Old Kingdom's Polestar & Giza Monumental Considerations*, *DIO* 13(1), 2–3, 2003.
- [13] M. Shaltout, J. A. Belmonte, and M. Fekri, *On the orientation of ancient Egyptian temples: (3): Key Points at lower Egypt and Siwa Oasis, Part II*, *Journal for the History of Astronomy* 38, 412–442, 2007.
- [14] G. Magli, *On the Relation between Archaeoastronomy and Exact Sciences: a Few Examples*, Proceedings of the SIA 2005 conference, Rome, SIA, 2005.
- [15] G. Magli, and J. A. Belmonte, *The stars and the pyramids: facts, conjectures, and starry tales*, in *In Search of Cosmic Order: Selected Essays on Egyptian Archaeoastronomy*, J. A. Belmonte and M. Shaltout (eds.), Cairo, Supreme Council of Antiquities Press, 2009.
- [16] I. Tupikova, *Astronomical orientation of the Pyramids and Stellar Alignments*, preprint MPIWG Berlin 511, 1–64, 2022, available at https://www.mpiwg-berlin.mpg.de/sites/default/files/P511_1.pdf
- [17] E. Nell, and C. Ruggles, *The orientation of the Giza Pyramids and Associated Structures*, *Journal for the History of Astronomy* 45 (3), 304–360, 2014.

Irina Tupikova
Lohrmann Observatory
Dresden University of Technology
Dresden, Germany
e-mail: irina.tupikova@googlemail.com

A natural riemannian metric on the space of Keplerian orbits based on the Hausdorff metric

Nikolay Vassiliev

Abstract. In this talk we consider the question about existence of a natural riemannian metric in the space of Keplerian orbits. In the works of the author and Kholshevnikov [1,2,3], a discussion of various issues of the geometry of the space of Keplerian orbits was initiated. In particular, we have proposed a whole class of natural metrics in this space. We also discussed the construction of riemannian metrics. Such a riemannian metric in the space of energetically bounded orbits was constructed in 2010 by J.Maruskin. [4]. However, his construction depends on the choice of a specific Keplerian element system. Here we propose an approach that is free from this disadvantage. Our approach is based on the Hausdorff distance between the Keplerian orbits. Finally we discuss a geodesic flow on the space of orbits generated by the riemannian metric we constructed in terms of classical orbital elements.

References

- [1] Vassiliev N. N., Determining of critical points of distance function between points of two Keplerian orbits, *Bull. Inst. Theor. Astron.* 14(5) (1978), Leningrad, 266–268 (in Russian).
- [2] Kholshevnikov K. V., Vassiliev N. N., On the Distance Function Between Two Keplerian Elliptic Orbits. *Celestial Mechanics and Dynamical Astronomy* 75, 75–83 (1999).
- [3] Kholshevnikov K. V., Vassiliev N. N., Natural metrics in the spaces of elliptic orbits, *Celest.Mech. Dyn. Astron.* 89(2), 119–125 (2004)
- [4] Maruskin, J.M., Distance in the space of energetically bounded Keplerian orbits, *Celest Mech Dyn Astr* 108, 265–274 (2010). <https://doi.org/10.1007/s10569-010-9300-8>

Nikolay Vassiliev
St. Petersburg Department of Steklov Institute of Mathematics,
191023, 27 Fontanka,
St.Petersburg, Russia
e-mail: vassiliev@pdmi.ras.ru

Lidov-Kozai mechanism in 3:2 and 1:1 resonances

Vinogradova T. A.

Abstract. In this paper the Lidov-Kozai mechanism was studied in 3:2 and 1:1 resonances. For this aim, asteroids in the region of the Hilda group and Jupiter Trojans were considered. These populations of asteroids move in corresponding mean motion resonances with Jupiter. The study was carried out using numerical integration of real asteroids' equations of motion. A simplified dynamical model was adopted. Perturbations from only Jupiter moving in a fixed elliptical orbit were taken into account. Classical secular perturbations were excluded from osculating elements at every print step and derived orbital inclinations and eccentricities were plotted versus a perihelion argument ω . As a result, it was found that usual positions of an eccentricity maximum and, accordingly, an inclination minimum ($\omega = 90^\circ, 270^\circ$) are shifted in these resonant regions. For Hildas the maximum of the eccentricity is achieved with perihelion argument values $\omega = 0^\circ, 180^\circ$. For L4 Trojans it is achieved with $\omega = 30^\circ, 210^\circ$, and for L5 Trojans - with $\omega = 150^\circ, 330^\circ$.

Vinogradova T. A.
Institute of Applied Astronomy
St. Petersburg, Russia
e-mail: vta@iaaras.ru

The ephemeris of the Moon in the framework of the numerical theory of Solar system bodies EPM, IAA RAS

Yagudina E.I. and Lebedeva M.A.

Abstract. Since 1969, the laser observations of the Moon (LLR) have been used to build support and improve the parameters of the Moon EPM ephemeris within the ERA7 system. The results of processing new LLR observations to obtain refined parameters of the Moon EPM2023a ephemeris within the framework of the modernized ERA8 system are considered. In order to ascertain the parameters of the Moon's ephemeris, 33602 observations of LLR (normal points - n.p., 1985-new) are used. About 100 parameters of the ephemeris of the Moon EPM2023a were improved and compared with some parameters of the ephemerides INPOP21a (France) and DE440 (USA). The values of individual parameters in different ephemerides are generally close. In some cases, discrepancies require a careful review of the list of parameters.

Introduction

The main attention will be paid to the problems of clarifying the parameters of the ephemeris of the Moon EPM2023a. Currently, there are 3 centers where accurate ephemerides of Solar System bodies are created and maintained: DE (USA), INPOP (France), and EPM (Russia). From 1989 till 2014 years, the ephemeris EPM-ERA was developed and supported on the basis of the model of the Moon's motion of Krasinsky G.A. and realized within the ERA-7 system [1]. From 2014, it was being developed a new version of the EPM ephemeris within the modernized ERA-8 system [2]. The geophysical and geodynamical parameters recommended by IERS were included. To obtain and refine the parameters of the Moon's ephemeris, EPM2023a uses 33602 observations of LLR n.p. About 100 parameters of the ephemeris of the Moon EPM2023a were improved and compared with some parameters of the ephemerides INPOP21a and DE440.

| Sations | Years | Normal points | Added |
|---------------------|------------------|---------------|-------------|
| Grasse, France (IR) | 2015-2023 | 8479 | 1632 |
| Matera , Italy | 2003-2023 | 460 | 13 |
| Apache Point, USA | 2006-2023 | 4126 | 225 |
| Wettzell, Germany | 2018-2023 | 329 | 115 |
| Total | 1969-2023 | 33602 | 1985 |

TABLE 1. LLR Observations 1969 - 2023

Model of the orbital-rotational motion of the Moon

When constructing the model of the orbital-rotational motion, the Moon is considered an elastic body with a rotating liquid core. The model in EPM2023a is constructed by joint numerical integration of the relativistic Einstein-Infeld-Hoffman equations using the extended Adams method in the inertial BCRS using the TDB dynamic scale, taking into account the compression of the Sun, additional disturbances from the largest asteroids (277), asteroid belts, TNO (30), and the TNO ring. The rotation of the Moon around the center of mass in the celestial coordinate system is given by Euler's three angles, which participate in numerical integration together with the position of the Moon's center. Changes of the model of the orbital-rotational motion of the Moon (in the ERA-8 system) are taken into account in the processing of LLR observations and obtaining new parameters of the ephemeris of the Moon. The i -th body (for example, Moon) in a rectangular and nonrotating coordinate system with the origin at the barycenter of the solar system at the epoch J2000 is as follows:

$$\begin{aligned}
\ddot{\mathbf{r}}_{i\text{point mass}} = & \sum_{j \neq i} \frac{\mu_j}{r_{ij}^3} (\mathbf{r}_j - \mathbf{r}_i) \left\{ 1 - \frac{2(\beta + \gamma)}{c^2} \sum_{k \neq i} \frac{\mu_k}{r_{ik}} - \frac{2\beta - 1}{c^2} \sum_{k \neq j} \frac{\mu_k}{r_{jk}} + \right. \\
& \gamma \left(\frac{|\dot{r}_i|}{c} \right)^2 + (1 + \gamma) \left(\frac{|\dot{r}_j|}{c} \right)^2 - \frac{2(1 + \gamma)}{c^2} \dot{\mathbf{r}}_i \dot{\mathbf{r}}_j - \frac{3}{2c^2} \left[\frac{(\mathbf{r}_i - \mathbf{r}_j) \times \dot{\mathbf{r}}_j}{r_{ij}} \right]^2 + \\
& \left. + \frac{\ddot{\mathbf{r}}_j}{2c^2} (\mathbf{r}_j - \mathbf{r}_i) \right\} + \frac{1}{c^2} \sum_{j \neq i} \frac{\mu_j}{r_{ij}^3} \{ [\mathbf{r}_i - \mathbf{r}_j] \times [(2 + 2\gamma)\dot{\mathbf{r}}_i - (1 + 2\gamma)\dot{\mathbf{r}}_j] \} \\
& (\dot{\mathbf{r}}_i - \dot{\mathbf{r}}_j) + \frac{(3 + 4\gamma)}{2c^2} \sum_{j \neq i} \frac{\mu_j \ddot{\mathbf{r}}_j}{r_{ij}}
\end{aligned} \tag{1}$$

It is also necessary to add terms containing the effect of the compression of the Sun:

$$C = 3J_2\mu_s \frac{R^2}{r_{is}^4} \left\{ \left[\frac{5}{2} \left(\frac{r_i - r_s}{r_{is}} \times \rho \right)^2 - \frac{1}{2} \right] \frac{r_i - r_s}{r_{is}} - \left(\frac{r_i - r_s}{r_{is}} \times \rho \right) \rho \right\} \tag{2}$$

as well as terms containing the Lense-Thirring acceleration:

$$D = \frac{2}{c^2} G S_{Sun} \frac{1}{r_{iS}^3} M_{Sun} \left(\dot{\mathbf{r}}_{iS} \times \mathbf{z} + 3 \frac{\mathbf{z} \times \mathbf{r}_{iS}}{r^2} \mathbf{r}_{iS} \times \dot{\mathbf{r}}_{iS} \right) \tag{3}$$

Lunar Laser Ranging observations (LLR)

The EPM2023a lunar ephemeris was produced using 33,602 LLR observations between 1969 and 2023. The parameters of the EPM2023a lunar ephemeris were

updated with a total of 1985 new LLR observations, which were added to the earlier ones. The number of added observations between 1969 and 2023 is shown in Table 1.

| Refl. | X_{DE440} | X_{EPM23} | Y_{DE440} | Y_{EPM23} | Z_{DE440} | Z_{EPM23} |
|-------|-------------|-------------|-------------|-------------|-------------|-------------|
| A11 | 1591967.049 | 1591966.865 | 690698.573 | 690699.163 | 21004.461 | 21003.740 |
| A14 | 1652689.369 | 1652689.637 | -520998.431 | -520997.770 | -109729.869 | -109730.550 |
| A15 | 1554678.104 | 1554678.476 | 98094.498 | 98095.267 | 765005.863 | 765005.253 |
| L1 | 1114291.452 | 1114292.318 | -781299.273 | -781298.603 | 1076059.049 | 1076058.727 |
| L2 | 1339363.598 | 1339363.663 | 801870.995 | 801871.636 | 756359.260 | 756358.713 |

TABLE 2. The coordinates of the reflectors in the ephemerides DE440 and EPM2023a (in meters)

Results of processing new observations

During the processing of LLR observations, the parameters (about 100) at the epoch JD 2446000.5 have been clarified. The new parameters of ephemeris EPM 2023a were compared with some parameters of the ephemerides DE440 and INPOP2021a (see Tables 2 and 3), and the results of processing LLR observations and comparison with parameters of the ephemeris EPM2022 are demonstrated in the Table 4.

| Parameter | INPOP 2021a | EPM2023a | INPOP21a – EPM2023a |
|--|-------------|-------------------------------|---------------------|
| f_c - core compression ratio | 2.8E-04 | $2.505E-04 \pm 0.018E-04$ | 0.295E-04 |
| C_{32} - moon potential parameter | 4.84501E-06 | $4.93236E-06 \pm 0.00044E-06$ | -0.08735E-06 |
| h_2 - Moon – Love number | 4.23E-02 | $4.47E-02 \pm 0.03E-02$ | -0.24E-02 |
| k_v/C_T - coefficient of friction between the core the crust | 1.62E-08 | $1.61E-08 \pm 0.01E-08$ | 0.01E-08 |
| τ_m - lunar tidal delay (days) | 9.6E-02 | $9.6E-02 \pm 0.1E-02$ | 0.00E-02 |
| Rotational delays of the earth tides τ_{R1} (days) | 8.02E-03 | $7.664E-03 \pm 0.019E-03$ | 0.356E-03 |
| Rotational delays of the earth tides τ_{R2} (days) | 2.82E-03 | $2.859E-03 \pm 0.002E-03$ | -0.039E-02 |

TABLE 3. Some parameters of the Earth-Moon system in INPOP21a and EPM2023a

Conclusion

1. The new values the parameters of ephemeris Moon EPM 2023a were obtained during processing of new LLR observations (1985 n.p.) on four 4 stations taking into account all past observations from 1969 till 2023.
2. There are next step for clarify parameters of ephemeris:
 - (a) It is necessary to continue to study cases of deviation of erroneous observations at various stations and introduce biases.
 - (b) In the papers [3, 4] based on mathematical modeling, it was shown that there are some ways to improve the parameters of lunar ephemeris: adding new observation stations (up to 12%); involvement of radar observations of the Moon (from 20% to 60%); as well as VLBI observations (at the LLR accuracy level).

| Station | EPM 2022a | | | | EPM 2023a | | | |
|------------|-----------|--------------------|-------|----------|-----------|--------------------|-------|----------|
| | Years | Normal points num. | Disc. | rms (cm) | Years | Normal points num. | Disc. | rms (cm) |
| McDonald | 1970-1985 | 3588 | 34 | 21.3 | 1970-1985 | 3588 | 34 | 21.7 |
| MLRS1 | 1983-1988 | 631 | 46 | 8.8 | 1983-1988 | 631 | 46 | 8.8 |
| MLRS2 | 1988-2015 | 3669 | 388 | 3.5 | 1988-2015 | 3669 | 388 | 3.6 |
| Haleakala | 1984-1990 | 770 | 22 | 5.1 | 1984-1990 | 770 | 22 | 5.3 |
| Cerga Ruby | 1984-1986 | 1112 | 3 | 16.7 | 1984-1986 | 1112 | 3 | 16.7 |
| Cerga YAG | 1987-2005 | 8316 | 39 | 2.3 | 1987-2005 | 8316 | 40 | 2.3 |
| Cerga MeO | 2009-2022 | 2097 | 0 | 1.5 | 2009-2022 | 2097 | 0 | 1.5 |
| Cerga IR | 2015-2022 | 6847 | 7 | 1.2 | 2015-2023 | 8479 | 4 | 1.4 |
| Apache | 2006-2022 | 3901 | 78 | 1.4 | 2006-2023 | 4126 | 78 | 1.5 |
| Matera | 2003-2022 | 421 | 2 | 3.2 | 2003-2023 | 460 | 28 | 3.4 |
| Wetzell | 2018-2022 | 212 | 0 | 1.5 | 2018-2023 | 329 | 3 | 1.6 |

TABLE 4. The comparison parameters of the ephemerides EPM2023a and EPM2022a

- (c) Regarding the use of lunar radar observations (LRR): there are already real observations [5], which were used to obtain selenocentric coordinates of the lander and other parameters (joint work with Chinese colleagues) - observations at the level of 1-3 mm [6].

References

- [1] Krasinsky G.A., Vasilyev M.V., *ERA-7 Knowledge base and programming system for dynamical astronomy*, Manual ERA-7. 2007.
- [2] Pavlov D.A., Skripnichenko V.I., *The first results of experimental operation of the cross-platform version of the ERA system*, Transactions of IAA RAS, Vol. 30, 2014.
- [3] Vasilyev M.V., Shuygina N.V., Yagudina E.I., *Expected Impact of the Lunar Lander VLBI Observations on the the Lunar Ephemeris Accuracy*, The 13th EVN Symposium & Users Meeting Proceedings, 2016.
- [4] Vasilyev M.V., Grishin E., Ivlev O.A. et al., *On the accuracy of the Moon's ephemerides using data from the projected Russian lunar laser rangefinder*, Astronomical Bulletin, vol. 50, No.5, 2016.
- [5] Li Chunlai, Liu Jianjun, Ren Xin, et al., *The Chang'e3 Mission Overview*, Space Science Reviews, vol. 190, 2015.
- [6] Marshalov D., Jinsong Ping, Wenxiao Li, et al., *3-way Lunar Radio Experiment on RT-32 Radio Telescope*, Latvian Journal of Physics and Technical Sciences, V. 57, I. 1-2, 2020.

Yagudina E.I. and Lebedeva M.A.
 Laboratory of Ephemeris Astronomy
 Institute of Applied Astronomy RAS
 Sankt-Petersburg, Russia
 e-mail: eiya@iaaras.ru, ma.lebedeva@iaaras.ru

K.V. Kholshevnikov and the Euler-Lambert problem of constructing the orbit of a body based on its two positions

V.V. Ivashkin

Abstract. In the report, the author first shares personal memories of Konstantin Vladislavovich Kholshevnikov as a person. Then the author describes a new method for solving the Euler-Lambert problem, which is one of the main problems of celestial mechanics and to which K.V. Kholshevnikov paid attention in one of his works.

In the first part of the presentation, first of all, the author expresses his deep respect to Professor K.V. Kholshevnikov. The author was lucky enough to meet with K.V. repeatedly, mainly at scientific events. K.V. was a wonderful person - with a constant smile, friendly to colleagues, the "soul" of the team, always created a warm, friendly "aura" around himself. And at the same time, he had encyclopedic knowledges, was a worthy scientist of high, international class. When analyzing complex problems of celestial mechanics, he was able to combine the construction of a clear mathematical statement of the problem and a rigorous mathematical approach to its solution, the ability to find simple methods for solving the problem.

- The second part of the presentation notes the analysis made by K.V. for two important celestial-mechanical problems. This is, firstly, an analysis of the "modern" mitigation problem of ensuring the asteroid-comet safety for the Earth. This analysis was presented by K.V. at a scientific conference together with T.N. Sannikova and a scientist of the M.V. Keldysh IAM Professor V.M. Chechetkin. In the presence of a controlled space influence on a dangerous celestial body, the equations of motion for the body become complex, difficult to analyze them. The authors average these equations, simplify them, and then analyze the multi-revolutions motion of a dangerous body, obtaining a number of results important for practice.

- The second problem is a classic problem that is stated in the 18th century by the great L. Euler. This is the task of determining the orbit of a celestial body by its two positions $\mathbf{r}_1, \mathbf{r}_2$ at given times t_1, t_2 . A separate paragraph of chapter 4

The study is supported by Russian Scientific Foundation, Grant No. 22-79-10206.

"Determining orbits" of the book "The Problem of two Bodies" [1], published in 2007 as a textbook by K.V. Kholshchevnikov together with a colleague V.B. Titov and presented to me in October 2017. The solution to this classic problem given in this book is interesting in two ways. First, the authors, following to I. Kepler and I.K.F. Gauss, are shown the "physics" of the solution, and then given a mathematical algorithm of the solution of the problem. At the end of this iterative algorithm, the authors analytically show (this is very rarely doing) that the solution exists and is the only one (for the considered special case, at a flight angle of $0 < \varphi < \pi$). The specified Euler-Lambert problem is important for astronomy and classical celestial mechanics for preliminary (without taking into account perturbations) determination of the orbits of natural celestial bodies (asteroids, comets), as well as for astronautics, space flight mechanics – for preliminary design construction of the orbit of a spacecraft during flight on a time interval (t_1, t_2) from the orbit of one celestial body to orbit another celestial body [2-4].

- Due to the importance of this problem, many methods have been developed to solve it. A comparative analysis of some methods is given, for example, in the works of M.F. Subbotin, P. Escobar [5-6]. Most of the developed methods for solving the problem are usually based on the fact that the set of flight orbits between two points in the central field forms a one-parameter family of orbits with flight between specified points in some time $(t'_2 - t_1)$. Depending on the choice of the parameter of this family, we obtain different methods for solving this Euler-Lambert problem. V.A. Egorov, apparently, for the first time drew attention to the fact that the results of D.E. Okhotsimsky on the analysis of ballistic flights can be used to construct a simple and very visual, new method for solving the Euler-Lambert problem. Therefore, this method is often called the Okhotsimsky D.E.-Egorov V.A. method. In the Okhotsimsky – Egorov method, the angle of inclination θ_1 of the initial velocity to the initial transversal is taken as a parameter of the specified family [2-4]. Knowing the angle of flight in the plane of the orbit, as well as the initial and final distances to the center of gravity $\mathbf{r}_1, \mathbf{r}_2$, allows us to determine the value of the initial flight velocity of the body V_1 and all the parameters of the orbit, including the flight time Δt . Iteratively, we select the initial angle of inclination of the speed so that the flight time is equal to the specified time. Analysis has shown that this method has good convergence characteristics and solutions to the Euler-Lambert problem.

The author is grateful to A.V. Ivanyukhin and A.V. Koroleva for the help in preparing the paper.

References

- [1] Kholshchevnikov K.V., Titov V.B., *The problem of two bodies*. St. Petersburg State University. A study guide. 2007. 180 p.
- [2] Ivashkin V.V., *The Euler-Lambert problem and its solution using the Okhotsimsky-Egorov method*. XIII All-Russian Congress on Fundamental problems of theoretical and Applied Mechanics: St. Petersburg, August 21-25, 2023 Collection

- of abstracts in 4 volumes. Vol. 1. General and Applied Mechanics-St. Petersburg: Polytechnic University PRESS. 2023. 668 p. ISBN 978-5-7422-8280-8 (vol.1). <https://ruscongrmech2023.ru/program/>. C. 588-590. doi:10.18720/SPBPU/2/id23-627.
- [3] Ivashkin V.V. , *On the application of the Okhotsimsky–Egorov method to solve the Euler–Lambert problem* , RAS reports. Physics. Technical Sciences, 2024, vol. 514, pp. 58-62.
 - [4] Ivanyukhin A.V., Ivashkin V.V., *Solving the Euler–Lambert problem based on the Okhotsimsky–Egorov ballistic approach* , Astronomical Bulletin. Exploration of the Solar system. 2024, vol. 58, No. 6, (in print).
 - [5] Subbotin M.F., *Introduction to theoretical astronomy* Nauka publishing house. 1968. 800 p. (in Russian)
 - [6] Escobal P.R., *Methods of Orbit Determination* John Wiley and Sons, New York-London-Sydney, 1965

V.V. Ivashkin
Keldysh Institute of Applied Mathematics, RAS
Moscow, 125047, Miusskaya Sq., 4
Moscow, Russia
e-mail: v.v.ivashkin@mail.ru

Professor Konstantin Kholshchevnikov as the historian of science

Elena N. Polyakhova, Andrey A. Vasilyev, Denis V. Mikryukov, Igor I. Nikiforov and Boris B. Eskin

Abstract. To memory of Prof. K. V. Kholshchevnikov we outline his contribution to the History of Astronomy and other exact sciences, particularly Celestial Mechanics. His activity concerned from Enlightenment century epoch of Science up to Educational aspects of modern teaching. He was interested in scientific biographies of outstanding scientists: Leonhard Euler, Joseph Louis Lagrange, Pierre Simon Laplace, Michael Ostrogradsky, Henri Poincaré, Alexander Lyapunov, Pafnuty Chebyshev, Sofia Kovalevskaya and many others persons. He used the history of science in his educational process of humanitarian lecture course "Natural Science Concepts" widely presenting the modern level of Natural History in frame of several centuries of its development. Kholshchevnikov was the author of several popular textbooks, he took part in edition of Encyclopedia "Russia's Astronomers" written both in Russian and English, in the book "History of Astronomy in Russia (the chapter "Celestial Mechanics")" he took a lot of effort to outline the main principles and fundamental of Celestial Mechanics in frame of Soviet and Russian History. He had done the wide exposition of the three-body problem development in XIX and XX century in Russia up to our days.

Elena N. Polyakhova
Dept. of Celestial Mechanics
Saint-Petersburg State University
Saint-Petersburg, Russia
e-mail: pol@astro.spbu.ru

Andrey A. Vasilyev
Laboratory of Observational Astrophysics
Saint-Petersburg State University
Saint-Petersburg, Russia
e-mail: andrey.vasilyev@spbu.ru

Elena N. Polyakhova, Andrey A. Vasilyev, Denis V. Mikryukov, Igor I. Nikiforov and Boris B. Eskin

Denis V. Mikryukov
Dept. of Celestial Mechanincs
Saint-Petersburg State University
Saint-Petersburg, Russia
e-mail: denastron@yandex.ru

Igor I. Nikiforov
Dept. of Celestial Mechanincs
Saint-Petersburg State University
Saint-Petersburg, Russia
e-mail: i.nikiforov@spbu.ru

Boris B. Eskin
Dept. of Celestial Mechanincs
Saint-Petersburg State University
Saint-Petersburg, Russia
e-mail: esk@astro.spbu.ru